

## **Factors Affecting Catheter Contact in the Human Left Atrium, its Impact on the Electrogram and Radiofrequency Ablation.**

Ullah, Waqas

The copyright of this thesis rests with the author and no quotation from it or information derived from it may be published without the prior written consent of the author.

For additional information about this publication click this link.

<http://qmro.qmul.ac.uk/jspui/handle/123456789/9020>

Information about this research object was correct at the time of download; we occasionally make corrections to records, please therefore check the published record when citing. For more information contact [scholarlycommunications@qmul.ac.uk](mailto:scholarlycommunications@qmul.ac.uk)

# Factors Affecting Catheter Contact in the Human Left Atrium, its Impact on the Electrogram and Radiofrequency Ablation

---

Waqas Ullah

Submitted in fulfillment of the requirements of the  
Degree of  
Doctor of Philosophy

University of London  
2015

## Statement of Originality

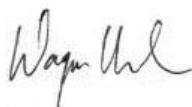
I, Waqas Ullah, confirm that the research included within this thesis is my own work or that where it has been carried out in collaboration with, or supported by others, that this is duly acknowledged below and my contribution indicated. Previously published material is also acknowledged below.

I attest that I have exercised reasonable care to ensure that the work is original, and does not to the best of my knowledge break any UK law, infringe any third party's copyright or other Intellectual Property Right, or contain any confidential material.

I accept that the College has the right to use plagiarism detection software to check the electronic version of the thesis.

I confirm that this thesis has not been previously submitted for the award of a degree by this or any other university.

The copyright of this thesis rests with the author and no quotation from it or information derived from it may be published without the prior written consent of the author.

Signature: 

Date: 23<sup>rd</sup> February 2015

## Abstract

The interaction between the mapping/ablation catheter and left atrial (LA) myocardium potentially affects the LA electrical and mechanical properties and impacts on ablation efficacy. Using catheters able to provide real-time contact force (CF) measurement, it has become possible to explore these relationships *in vivo*.

In 60 persistent atrial fibrillation (AF) patients, ablation CF was higher in the right than left wide area circumferential (WACA) lines and where steerable transseptal sheaths were used. Differences were also apparent in the burden of WACA segment reconnection but did not just reflect differences in ablation CFs, suggesting factors other than CF contribute to ablation efficacy.

Relationships between ablation force time integral (FTI), impedance drop and electrogram attenuation were assessed in 15 persistent AF patients. FTI significantly correlated with electrogram attenuation and impedance drop from ablation. The relationship was stronger for the former but in both cases plateaued at 500g.s, suggesting no ablation efficacy gains beyond this.

Factors further affecting CF and ablation efficacy, the latter judged by impedance drop, were assessed in 30 patients. The variability of the CF waveform and catheter locational stability were both affected by factors including atrial rhythm and catheter delivery mode. Greater CF variability, catheter drift and perpendicular catheter contact were associated with reduced ablation efficacy.

The relationship between CF and the electrogram was assessed in 30 patients. The size of the electrogram complexes was affected by CF increases but only where initial CF was <10g. This was also the case for electrogram fractionation measurements. Increasing CF was associated with an increasing incidence of atrial

ectopics during sinus rhythm. Spectral parameters (dominant frequency and organisation index) were unaffected by CF.

Various factors affect the contact between the catheter and LA myocardium. In turn, catheter contact significantly affects the electrogram during LA mapping and the efficacy of clinical radiofrequency ablation.

# Table of Contents

Statement of Originality .....	1
Abstract .....	2
Table of Contents .....	4
List of Tables.....	7
List of Figures .....	8
Acknowledgements .....	10
Publications .....	12
Chapter 3: The Impact of Catheter Contact Force on Human Left Atrial Electrogram Characteristics in Sinus Rhythm and Atrial Fibrillation .....	12
Abstracts & presentations at learned societies .....	12
Chapter 4: Target indices for clinical ablation in atrial fibrillation: insights from contact force, electrogram, and biophysical parameter analysis.....	13
Manuscript .....	13
Abstracts & presentations at learned societies .....	13
Chapter 5: Factors Affecting Catheter Contact in the Human Left Atrium and their Impact on Ablation Efficacy .....	14
Manuscript .....	14
Abstracts & presentations at learned societies .....	14
Chapter 6: Impact of Steerable Sheaths on Contact Forces and Reconnection Sites in Ablation for Persistent Atrial Fibrillation .....	14
Manuscript .....	14
Abstracts & presentations at learned societies .....	15
1. Introduction .....	16
1.1 Abbreviations .....	16
1.2 Atrial Fibrillation - Background.....	18
1.3 Management of Atrial Fibrillation .....	19
1.4 Atrial remodelling in Atrial Fibrillation.....	22
1.5 Left Atrial Compliance .....	24
1.6 Mechanisms of Atrial Fibrillation.....	27
1.7 Atrial Fibrillation Electrograms .....	29
1.7.1 Fractionated Atrial Electrograms .....	29
1.7.2 Spectral Analysis of Electrograms .....	33
1.8 Mechanoelectric Coupling .....	35
1.8.1 Atrial Mechanoelectric Coupling.....	35
1.8.2 Localised Mechanoelectric Coupling.....	39
1.8.3 Localised, Catheter-Mediated, Stretch in vivo.....	41
1.9 Steerable Sheath Technology .....	42
1.10 Contact Force Sensing Technologies .....	44
1.10.1 Sheath-Based Technology.....	44
1.10.2 Catheter-Based Technology .....	44
1.11 Biophysics of Ablation.....	46
1.11.1 Contact Force and Ablation .....	48
1.12 Ablation Efficacy .....	52
1.14 Conclusions and formulation of current studies .....	56
2. Methods.....	61
2.1 Study Institutions and Personnel.....	61
2.2 Patients .....	62

2.3 Cardiac Catheter Laboratory Setup .....	62
2.4 Electroanatomic Navigation System .....	64
2.5 Electrogram Recording System .....	68
2.6 Co-ordinating Electroanatomic Mapping and Electrogram Recording Systems ..	69
Results .....	70
Conclusion .....	71
2.7 Data Analysis .....	71
3. The Impact of Catheter Contact Force on Human Left Atrial Electrogram	
Characteristics in Sinus Rhythm and Atrial Fibrillation .....	77
3.1 Abstract .....	77
3.2 Introduction .....	78
3.3 Methods.....	79
3.3.1 Statistics .....	83
3.4 Results .....	83
3.4.1 Contact Force and the Electrogram.....	84
3.4.2 Contact Force and CFAE .....	88
3.4.3 Contact Force and Dominant Frequency.....	89
3.4.4 Catheter Orientation .....	91
3.5 Discussion .....	91
3.5.1 Catheter contact and the electrogram.....	91
3.5.2 Catheter contact and CFAE parameters .....	94
3.5.3 Catheter contact and Spectral Analysis Parameters .....	95
3.6 Conclusions .....	96
4. Target indices for clinical ablation in atrial fibrillation: insights from contact force,	
electrogram and biophysical parameter analysis.....	97
4.1 Abstract .....	97
4.2 Introduction .....	98
4.3 Methods.....	99
4.3.1 Statistics .....	103
4.4 Results .....	103
4.4.1 The electrogram and ablation.....	106
4.5 Discussion .....	107
4.5.1 Limitations .....	112
4.6 Conclusions .....	112
5. Catheter contact characteristics and ablation efficacy in the human left atrium....	114
5.1 Abstract .....	114
5.2 Introduction .....	115
5.3 Methods.....	116
5.3.1 Statistics .....	120
5.4 Results .....	121
5.4.1 Mapping Results .....	122
5.4.2 Ablation Results .....	123
5.5 Discussion .....	127
5.5.1 Limitations .....	133
5.6 Conclusions .....	133
6. Contact Force and Pulmonary Vein Reconnection in Persistent Atrial Fibrillation	
Ablation: Impact of Steerable Sheaths .....	135
6.1 Abstract .....	135
6.2 Introduction .....	136
6.3 Methods.....	137

6.3.1 Statistical Methods .....	140
6.4 Results .....	141
6.4.1 Procedural Mean Contact Forces .....	142
6.4.2 WACA Segmental Contact Forces .....	142
6.4.3 Reconnections .....	145
6.5 Discussion .....	147
6.5.1 Limitations .....	151
6.6 Conclusions .....	151
7. Conclusions and Future Directions .....	153
8. References .....	162



## List of Tables

1.1 Clinical studies assessing ablation efficacy with respect to catheter contact force	p53
2.1 Part of a Carto3 contact force data export for a point	p64
2.2 Part of a Carto3 location data export for a point	p66
2.3 Part of a Carto3 ablation biophysical data export	p66
3.1 Study Population Characteristics	p90
3.2 Change in mean complex size by atrial rhythm, initial CF and increase in CF between pairs of measurements at a location	p92
3.3 Change in CFAE and spectral analysis measurements at a location by initial CF and increase in CF between pairs of measurements at a location	p94
3.4 The change in electrogram properties with a change in catheter orientation between measurements taken at the same location	p96
4.1 Study Population Baseline Characteristics	p109
5.1 Study Population Baseline Characteristics	p127
5.2 Multivariate analysis of factors affecting contact force variability	p128
5.3 Multivariate analysis of factors affecting the impedance drop with ablation	p132
6.1 Study Population Baseline Characteristics	p147
6.2 Contact Force and Wide Area Circumferential Ablation Segment Reconnection	p151

## List of Figures

1.1 Agilis NxT manual Steerable Trans-septal Sheath	p48
1.2 The Sensei Robotic Navigation System Control Console at St Bartholomew's Hospital	p49
1.3 The Thermocool SmartTouch catheter	p50
1.4 The Display of Contact Force Data Measured by the SmartTouch Catheter on the Carto3 Screen	p51
2.1 Cardiac Catheter Laboratory Control Room at St Bartholomew's Hospital	p69
2.2 Cardiac Catheter Laboratory at St Bartholomew's Hospital	p69
2.3 Comparison of timestamps of Carto3 and LabSystem Pro for simultaneously acquired points	p76
2.4 Trapezoid integration of a contact force waveform	p78
2.5 Impedance waveform	p79
2.6 Incremental FTI analysis	p80
2.7 Electrogram analysis	p81
3.1 Electrogram analysis	p86
3.2 Histogram of the rising or falling angle for all of the complexes identified	p87
3.3 Histogram of mean CF of the study points	p90
3.4 Complex size versus left atrial location	p91
3.5 Percentage of 8s SR electrograms with $\geq 1$ atrial ectopic observed versus mean CF	p93
4.1 Maximum Percentage Impedance Drop versus Incremental Force Time Integral	p110

4.2 Influence of Mean Contact Force and Ablation Duration on Impedance Drop at a Target Force Time Integral	p111
4.3 Force Time Integral versus Percentage Change in Electrogram Complex Size	p112
5.1 Catheter stability and orientation analysis	p124
5.2 Contact Force Versus Contact Force Variability	p127
5.3 Catheter drift by navigation mode and atrial rhythm	p129
5.4 Factors affecting impedance drop during ablation	p130
5.5 Factors affecting impedance drop during ablation	p131
6.1 Clock face scheme for assigning ablation location in wide area circumferential ablation lines	p144
6.2 Mean contact force during ablation	p148
6.3 Distribution of contact force in the right and left WACA	p149
6.4 Percentage of wide area circumferential ablation segments reconnecting	p150
6.5 WACA reconnection plots	p152

## Acknowledgements

There are many people who need thanking for their contributions to this thesis. The most important are the patients who very generously consented to participate in this research.

Several industry representatives answered my questions regarding the inner workings of their clinical systems (and how I could maximise their usage for my work). I'm sure it was a frustrating process for them but their help was invaluable. Chief among those who helped me were Mike Berry and Miz Rashid from Biosense Webster and Helen Clements and Kathryn Foskett from Bard.

The electrophysiology laboratory team at St Bartholomew's Hospital were exceptionally helpful during my research cases and maintained their enthusiasm to a surprising degree. Troy Watts among them provided important insights into the usages of the various systems and helped optimise the protocols. The staff at St Bartholomew's Hospital are very accommodating to research cases and remain a core reason for the academic effectiveness of the unit.

Among the clinicians, Drs Mark Early, Mehul Dhinoja, Ling Liang-han and Simon Sporton helped focus my ideas and writing to try and bring to the fore findings of clinical interest and patiently helped with the collection of the data. The research nurses Victoria Baker and Ailsa McLean both provided vital input into the manuscripts. Victoria Baker also provided invaluable advice in managing the studies, including the ethics applications.

My supervisors Drs Ross Hunter and Professor Richard Schilling have been an inspirational source of support during this research. They've given me the freedom to explore different ideas, encouragement when some of those ideas did not work out and saved me from straying down several blind alleys. Dr Hunter's advice regarding the statistical analyses conducted was especially appreciated.

Lastly, and most importantly, my mother and brothers and my wife and children have maintained patience with me during this period and allowed me to focus all my energies on the work in this thesis.

## **Publications**

The publications detailed below are based on the work presented in this thesis.

### ***Chapter 3: The Impact of Catheter Contact Force on Human Left Atrial Electrogram Characteristics in Sinus Rhythm and Atrial Fibrillation***

#### **Abstracts & presentations at learned societies**

*Ullah W, Hunter RJ, Baker V, Liang-han L, Dhinoja MB, Sporton S, Earley MJ, Schilling RJ. , Catheter Contact Force and Human Left Atrial Electrogram Parameters in Sinus Rhythm and Atrial Fibrillation*

#### **Poster Presentation Heart Rhythm Congress 2014.**

*Ullah W, Hunter RJ, Baker V, Liang-han L, Dhinoja MB, Sporton S, Earley MJ, Schilling RJ. , Catheter Contact Force and Human Left Atrial Electrogram Parameters in Sinus Rhythm and Atrial Fibrillation*

#### **Poster Presentation ECAS 2015.**

*Ullah W, Hunter RJ, Baker V, Liang-han L, Dhinoja MB, Sporton S, Earley MJ, Schilling RJ. , Catheter Contact Force and Human Left Atrial Electrogram Parameters in Sinus Rhythm and Atrial Fibrillation*

#### **Poster Presentation Heart Rhythm Society 2015.**

***Chapter 4: Target indices for clinical ablation in atrial fibrillation: insights from contact force, electrogram, and biophysical parameter analysis***

**Manuscript**

*Ullah W, Hunter RJ, Baker V, Dhinoja MB, Sporton S, Earley MJ, Schilling RJ* Target indices for clinical ablation in atrial fibrillation: insights from contact force, electrogram, and biophysical parameter analysis

**Circ Arrhythm Electrophysiol.** 2014 Feb 1;7(1):63-8

**Abstracts & presentations at learned societies**

*Ullah W, Hunter RJ, Baker V, Dhinoja MB, Sporton S, Earley MJ, Schilling RJ* Target indices for ablation in atrial fibrillation: insights from contact force, electrogram and biophysical parameter analysis

**Oral Presentation Heart Rhythm Congress 2013.**

*Ullah W, Hunter RJ, Baker V, Dhinoja MB, Sporton S, Earley MJ, Schilling RJ,* Contact Force During Ablation of Persistent Atrial Fibrillation and Electrogram Attenuation

**Poster Presentation European Society of Cardiology 2013.**

## ***Chapter 5: Factors Affecting Catheter Contact in the Human Left Atrium and their Impact on Ablation Efficacy***

### **Manuscript**

*Ullah W, Hunter RJ, Baker V, Dhinoja MB, Sporton S, Earley MJ, Schilling RJ. Factors Affecting Catheter Contact in the Human Left Atrium and their Impact on Ablation Efficacy. J. Cardiovasc. Electrophysiol. 2014, September 12.*

### **Abstracts & presentations at learned societies**

*Ullah W, Hunter RJ, Baker V, Dhinoja MB, Sporton S, Earley MJ, Schilling RJ. , Factors affecting contact force variability and catheter drift in the left atrium*

**Poster presentation at Heart Rhythm Society 2014.**

*Ullah W, Hunter RJ, Baker V, Dhinoja MB, Sporton S, Earley MJ, Schilling RJ. ,*

*Factors affecting catheter contact in the human left atrium and their impact on ablation efficacy*

**Moderated Poster Presentation Heart Rhythm Congress 2014.**

## ***Chapter 6: Impact of Steerable Sheaths on Contact Forces and Reconnection Sites in Ablation for Persistent Atrial Fibrillation***

### **Manuscript**

*Ullah W, Hunter RJ, Mclean A, Dhinoja M, Earley MJ, Sporton S, Schilling RJ. Impact of Steerable Sheaths on Contact Forces and Reconnection Sites in Ablation for Persistent Atrial Fibrillation. J. Cardiovasc. Electrophysiol. 2014, October 27*



## **Abstracts & presentations at learned societies**

*Ullah W, Hunter RJ, Mclean A, Dhinoja M, Earley MJ, Sporton S, Schilling*

RJ Distribution of Contact Forces during Persistent Atrial Fibrillation Ablation and

Pulmonary Vein Reconnection – Impact of Remote Robotic Navigation and a Steerable

Trans-Septal Sheath

**Oral presentation and Finalist for the Young Investigator Award at Heart Rhythm Congress 2013.**

*Ullah W, Hunter RJ, Mclean A, Dhinoja M, Earley MJ, Sporton S, Schilling RJ, Contact*

Force and Pulmonary Vein Reconnection Distribution in Persistent Atrial Fibrillation

Ablation - Impact of Steerable Sheaths

**Poster presentation at Heart Rhythm Society 2014.**

# 1. Introduction

## 1.1 Abbreviations

ADC: Analogue-to-digital converter

AF: Atrial fibrillation

AFCL: Atrial fibrillation cycle length

AFFIRM: Atrial Fibrillation Follow-Up Investigation of Rhythm Management

AV: Atrioventricular

ACI: Average complex interval

CFAE: Complex fractionated atrial electrograms

CF: Contact Force

CFV: Contact Force Variability

DE-MRI: Delayed enhancement MRI

DF: Dominant frequency

ERP: Effective refractory period

ETI: Electrode Tissue Interface

FFT: Fast Fourier transform

FTI: Force Time Integral

ICL: Interval confidence level

LAA: Left atrial appendage

LA: Left atrium

OI: Organisation index

PAF: Paroxysmal AF

PV: Pulmonary Vein

PVI: Pulmonary vein isolation

QoL: Quality of life

RACE: Rate Control and Rhythm Control in Patients With Recurrent Persistent Atrial Fibrillation

RRN: Remote Robotic Navigation

SCI: Shortest complex interval

SAECG-P: Signal averaged ECG p-wave analysis

SR: Sinus Rhythm

SAC: Stretch Activated Channels

WACA: Wide area circumferential ablation

## **1.2 Atrial Fibrillation - Background**

Atrial fibrillation (AF) is characterised by chaotic electrical activation of the left atrium leading to discordant mechanical contraction, manifesting on the electrocardiogram as a loss of the normal sinus p-wave. In the presence of intact atrio-ventricular conduction, an irregularly irregular pulse is noted. Different types of AF have been defined according to international consensus<sup>1</sup>:

- Paroxysmal AF (PAF) - recurrent  $\geq 2$  episodes of AF terminating spontaneously within 7 days (or episodes  $\leq 48$  hours that are cardioverted).
- Persistent AF - continuous AF sustained beyond 7 days and those episodes cardioverted between 48 hours and 7 days into an episode.
- Longstanding persistent AF – continuous AF for  $>12$  months.
- Permanent AF – if a patient is in persistent AF and there is an acceptance that the patient will remain in this rhythm.

AF is associated with a significantly increased mortality, with a risk factor–adjusted odds ratio for death of between 1.5 and 1.9 in the Framingham Heart Study population<sup>2</sup>. AF also confers an almost five-fold increased risk of suffering a stroke<sup>3</sup> and increases the risk of heart failure admissions<sup>4</sup>. Common symptoms due to AF include dyspnoea, palpitations and fatigue, with only around 15% of patients in one registry being asymptomatic<sup>5</sup>. In a study of 152 consecutive arrhythmia clinic outpatients, both general and disease specific quality of life (QoL) scores were significantly worse compared for AF patients compared with healthy controls, with similar scores these patients as for those with heart failure, or post-infarction or angioplasty<sup>6</sup>. From a psychological viewpoint, around one-third of patients with AF were found in one study to have persistently elevated levels of depression and anxiety<sup>7</sup>.

AF therefore poses serious risks in the longer term as well as having a more immediate impact on sufferers' quality of life.

In a large general practice research database in England and Wales, the incidence of this arrhythmia was just over 1%, increasing with age up to over 10% in those over 85 years old<sup>8</sup>. With our aging population, one would expect the prevalence of this condition to increase with time, but in addition to such a rise, an increase in prevalence independent of age has also been observed<sup>8</sup>. In 2000, the direct cost of AF was between 0.9-2.4% of overall health care expenditure in the UK, almost double the level it had been in 1995<sup>9</sup>. AF therefore represents a health problem with serious consequences, which is becoming increasingly common and is therefore a growing burden on the health service.

### **1.3 Management of Atrial Fibrillation**

Presently, the principal intervention with proven prognostic benefit is anticoagulation. Compared with placebo, warfarin leads to a 62% relative (3.1% absolute) risk reduction for stroke<sup>10</sup>. Patients are started on anticoagulation based on their risk of stroke using scores such as the CHA<sub>2</sub>DS<sub>2</sub>-VASc score<sup>11</sup> which take into account their clinical profile to assign them to an overall stroke risk category. Warfarin has been the most widely used anticoagulant in AF but now newer agents have become available which may offer advantages over this established drug<sup>12,13</sup>. An alternative strategy to anticoagulation to reduce the risk of stroke is the use of left atrial appendage occlusion devices<sup>14</sup>.

Beyond stroke risk reduction, the management of AF generally involves commitment to either a rate or rhythm control strategy. In the case of the former, this involves accepting the patient is in AF but aiming to regulate the ventricular response

rate. Strategies for achieving this involve utilising rate-controlling medications, permanent pacemaker implantation and atrioventricular node ablation. Conversely, a rhythm control strategy aims to maintain patients in sinus rhythm and this is achieved by using antiarrhythmic drugs, cardioversion and catheter-based ablation. Comparison of the benefit of these strategies has been the subject of several studies<sup>15-17</sup>, and on meta-analysis, no significant difference with regard to mortality or morbidity<sup>18-20</sup>, has been demonstrated. On grouping the thromboembolic stroke and mortality end point, a significant increase in those undergoing rhythm control has been observed<sup>19</sup>. No difference has been demonstrated in QoL scores between patients randomised to either strategy, regardless of their rhythm<sup>21</sup>. The underperformance of the rhythm control arm in these studies has been subjected to further analysis: the rhythm control strategy has been mainly pharmacological, only 14 of the 4060 patients in the largest study, the Atrial Fibrillation Follow-Up Investigation of Rhythm Management (AFFIRM) trial had an ablation for AF (or atrial flutter)<sup>16</sup>. Antiarrhythmic drugs were associated with more drug intolerances and by the third year there was a 37.5% actuarial cross-over rate from the rhythm to the rate control arm due to ineffectuality and intolerance of these drugs in AFFIRM<sup>16</sup>. In the Rate Control and Rhythm Control in Patients With Recurrent Persistent Atrial Fibrillation (RACE) trial of persistent AF patients, only 39% of patients in the rhythm control arm were in sinus rhythm at the end of follow-up and again there were more adverse drug effects<sup>15</sup>. In an on-treatment analysis of the AFFIRM study, sinus rhythm *per se* was associated with a lower risk of death while a higher risk of death was associated with rhythm-control drug use<sup>22</sup>.

Whether a therapy that is better able to maintain sinus rhythm without requiring the use of potentially toxic anti-arrhythmic drugs has benefit is unclear, but catheter ablation shows promise in this regard. A retrospective epidemiological study of 37,908

patients has suggested that patients who have had ablation for AF have a lesser risk of dementia, stroke and death compared to those who do not have an ablation of AF, although differences in the study population demographics do make this harder to interpret<sup>23</sup>. A further registry study comparing 1273 ablated patients with medically managed and control, non-AF patients suggested that freedom from AF was significantly associated with a reduction in the risk of stroke and death compared to medically managed AF patients, and no difference compared to the control non-AF population<sup>24</sup>.

These results suggest the prognostic benefit of achieving sinus rhythm through ablation, and the NHLBI sponsored trial **Catheter Ablation Versus Antiarrhythmic Drug Therapy for Atrial fibrillation (CABANA)**, Clinicaltrial.gov registration: NCT00911508, is currently underway to prospectively compare medical management with catheter ablation.

From the point of view of quality of life, a prospective study of 133 ablated patients showed that QoL scores improved after an ablation and that successful ablation caused a significantly greater improvement than unsuccessful ablation, with benefits maintained at four years<sup>25</sup>.

A 2005 world-wide survey of over 9000 patients having undergone catheter ablation suggested an overall success rate of 75.9% (of whom 53% were no longer on anti-arrhythmic drugs)<sup>26</sup>. Almost a quarter of the patients required a second ablation procedure and there was around a 6% major complication rate which included deaths and strokes<sup>26</sup>. This survey included patients with persistent AF and PAF, as well as ablations done in by a variety of methods at varying stages after the introduction of AF ablation. More recent data from a single centre demonstrates an 86% long-term rate of freedom from PAF and 68% rate for persistent AF; the former patients requiring a mean

of 1.7 procedures and the latter a mean of 2<sup>27</sup>. The major complication rate in this analysis was 3.1%<sup>27</sup>. In a multicentre registry, the rates of freedom from AF (off drugs) post-ablation were 76% for PAF and 60% Persistent AF, with over half the patients needing more than one ablation procedure<sup>24</sup>. A further prospective registry of 1410 patients demonstrated a single procedure success rate of 40.7% for AF ablation at one year, with a 2.5% adverse event rate during follow-up<sup>28</sup>.

From the above it will have been noted that ablation of AF is a procedure with some risk. Generally, patients require repeat procedures to improve success rates and this further subjects them to risk. Combined with the modest success rates for the procedure in persistent AF, this suggests that there remains scope to improve the efficacy of the procedure.

#### ***1.4 Atrial remodelling in Atrial Fibrillation***

Atrial fibrillation results in electrical remodelling of the atrium. Recurrent AF induced by atrial pacing results in an increase in the length of the induced episodes until after around two weeks the AF becomes persistent<sup>29</sup>. With the increasing length of these episodes, the rate of the AF increases and the atrial electrogram becomes more fragmented<sup>29</sup>. The duration of the action potential also reduces in pacing induced animal models<sup>30</sup>. There is also an associated reduction in the atrial ERP and these changes take a week to normalise following reversion to sinus rhythm<sup>29</sup>. Therefore, AF is associated with progressive electrical remodelling of the atrium and this persists beyond restoration of sinus rhythm. This remodelling has been studied at a subcellular level.

At an ion channel level, sustained AF was found in dogs to cause a reduction in outward currents, calcium currents<sup>30</sup> and sodium currents<sup>31</sup>.



Gap junctions are responsible for ion conduction between cells and therefore facilitate transmission of the electrical impulse. These structures are formed of connexions, and connexin 40 is specific to the atrium and conducting system. Mice with the gene for this protein knocked out spontaneously develop AF<sup>32</sup> and have a 30% reduction in atrial conduction velocity<sup>33</sup>. In a model of persistent AF, as the AF became more persistent, the distribution of connexin 40 became more heterogeneous and its levels reduced<sup>34</sup>. In a porcine model with AF induced by recurrent burst atrial pacing, burst pacing was associated with a reduction in the time in sinus rhythm, reduced atrial conduction velocity and reduced expression of connexin 43 and 40<sup>35</sup>. Gene transfer of either connexin 40 or 43 prevented the reduction in the expression of these proteins with burst pacing and prevented the reduction in atrial conduction velocity and protected against the development of AF in the model<sup>35</sup>.

In patients with longstanding AF, there is a redistribution of intercellular gap junctions. At the tissue level, there is decrease in the amount of connexin 43 and 40, with increased heterogeneity in the distribution of the latter<sup>36</sup>.

A canine sustained AF model demonstrates fibre disarray and early hypertrophy with AF<sup>37</sup>. In a goat model, changes in myocytes including myolysis and glycogen accumulations have been observed secondary to sustained AF<sup>38</sup>. Myocytes from patients with AF demonstrate increased contraction bands and in addition, in patients with persistent AF there are an increased number of hibernating (myolytic) cells, and the latter increase with the duration of AF<sup>39</sup>. Further investigation of atrial tissue from patients with chronic AF has demonstrated that the myolytic cells observed are in a dedifferentiated state with characteristics of embryonic muscle cells<sup>40</sup>. Thick layers of fibrosis between myocytes forming collagenous septa have been observed in the atria of

patients with long standing AF<sup>40</sup> and significantly more collagen type I is seen in the atria of these patients compared to patients without AF<sup>36,41</sup>.

Atrial fibrillation therefore leads to electrical remodelling of the atrium in association with changes to myocytes at the cellular and subcellular level as well as remodelling of the extracellular matrix.

### **1.5 Left Atrial Compliance**

Stress ( $\sigma$ ) is defined as the force per unit area exerted on a material, while strain is the deformation caused by this stress, and is the change in length per unit length ( $\epsilon$ ). The ratio of stress to strain for a material is the elastic modulus (E), known as Young's Modulus and is measured in Pascals ( $\text{N/m}^2$ ). This is a measure of the resistance of the material to deformative force, the elasticity or stiffness. A stiffer material has a higher elastic modulus (for a given stress, the strain is small). Compliance is the inverse of stiffness, with units of  $\text{m}^2/\text{N}$ , and a more compliant material has a lower elastic modulus (for a given stress, the strain is large). The elastic modulus applies while the ratio between stress and strain is constant – while the material obeys Hooke's Law. Beyond the elastic limit, the relationship is no longer linear and plastic behaviour (where a material does not return to its baseline shape on removal of the stress) can be observed.

The left atrium (LA) makes several important contributions to cardiovascular function: in sinus rhythm, the LA contracts immediately prior to LV systole, therefore elevating the LV end diastolic pressure; the LA also has a reservoir function for pulmonary venous return during ventricular systole and isovolumic relaxation, and it also functions as a conduit that empties blood down a pressure gradient into the left ventricle on opening of the mitral valve<sup>42</sup>. A loss of coordinated atrial contraction (as

occurs with AF) results in a reduction in the ventricular stroke volume, with a greater effect at higher heart rates<sup>43</sup>.

In response to increasing LA pressure, a greater change in the atrial volume is noted in non-hypertensive than hypertensive rats and greater stiffness is also observed in left atrial tissue strips taken from the latter rats<sup>44</sup>. From canine studies, a regional difference in the compliance of the left atrium has been observed, with the appendage having a lower elastic modulus (higher compliance) than the left atrium<sup>45,46</sup> and following appendectomy, or ligation of the appendage, the stiffness of the left atrial chamber is increased<sup>46,47</sup>. The relationship between the left atrial pressure and volume has also been found to be different depending on whether the left atrial pressure is increasing or decreasing, being greater if the pressure was falling than rising<sup>47</sup>.

Left atrial compliance can be determined invasively at cardiac catheterisation, where the systolic rise in the left atrial pressure is divided into the stroke volume<sup>48</sup>. Comparison of the dynamic echocardiographic left atrial area, as determined by an automated boundary detection application, with the invasively determined left atrial pressure has also been used to determine compliance<sup>49</sup>. Using echocardiographic assessment of transmitral velocity profiles, it is possible to determine the net atrioventricular compliance<sup>50</sup> and in the presence of normal left ventricular compliance, this compliance has been taken as a surrogate of left atrial compliance, and correlates with peak pulmonary systolic and diastolic flow velocity as well as the pulmonary artery systolic pressure<sup>51</sup>. An acoustic microscope has also been used in a post-mortem human tissue study, and found that the speed of sound through left atrial tissue specimens increased with increasing subject age, this increase was felt to reflect an increase in the elasticity of the tissue with ageing<sup>52</sup>.

There is a suggestion of a relationship between the left atrial compliance and AF: in a canine study, the increase in left atrial dimensions for a given rise in left atrial pressure was larger in the LA before it was induced to fibrillate, reflecting a reduced compliance during AF acutely<sup>53</sup>. Similarly, in a porcine study, the induction of AF resulted in a smaller end systolic LA volume, larger end diastolic volume and a reduction in the compliance of both atria<sup>54</sup>. In contrast to these findings though, in patients with mitral stenosis undergoing echocardiographic left atrial compliance assessment, no difference was found in the left atrial compliance comparing those who were in AF to those who were not<sup>51</sup>. In another study though, using echocardiography and invasive left atrial pressure measurement, left atrial stiffness was higher for patients with atrial fibrillation compared to control patients<sup>55</sup>, findings more in keeping with the preclinical studies described above.

Compliance has been postulated to be lower during AF acutely for a number of reasons<sup>54</sup>: unsynchronised myofibre contractions, greater myocardial turgor due to increased blood flow in the atrial myocardium during AF<sup>56</sup> or due to increased cytosolic calcium concentrations. Further to this, one would also expect a contribution secondary to the structural remodelling discussed above secondary to sustained AF.

In AF, the LA loses its contractile contribution to cardiac output. An increase in the stiffness of the left atrium, certainly acutely, may be an important response to this loss as it results in an elevation in the left atrial pressure, allowing for increased blood flow down the higher pressure gradient into the left ventricle and so reduces the decline in stroke volume from the loss of atrial systole<sup>54</sup>.

## **1.6 Mechanisms of Atrial Fibrillation**

The underlying electrical mechanism of AF is the subject of several theories. Support for an ectopic focus as a source of AF came from the experiments by Scherf et al., in which aconitine applied to the atria resulted in AF or atrial flutter, but removal of the aconitine exposed area by excision, cooling or clamping would terminate the arrhythmia<sup>57,58</sup>. Interestingly, whether AF or atrial flutter was induced depended on the atrial firing rate induced by the aconitine. Above a certain threshold, the atrium was unable to conduct in a 1:1 manner and conduction degenerated, a phenomena known as fibrillatory conduction. Such fibrillatory conduction was experimentally demonstrated in an isolated sheep right atrial preparation where pacing Bachman's Bundle above a threshold frequency led to a breakdown of uniform conduction<sup>59</sup>. Support for a focal source of AF in humans was provided in 1998 by Haïssaguerre et al who reported the initiation of paroxysms of AF by ectopics, most commonly from the pulmonary veins<sup>60</sup>.

An alternative theory for the cause of AF was proposed by Moe and Abildskov<sup>61</sup>, with the theory tested by computer modelling<sup>62</sup>. This was called the multiple re-entrant wavelet hypothesis and suggested that AF was the result of multiple wandering wavelets across the atrium independent of their initiating event. AF becoming sustained was postulated to be dependent on the number of such wavelets within the atrium at a single moment (to prevent the rhythm organising through wavelet fusion and termination). The number of wavelets supported by the atrium depended on the mass of atrial tissue, its refractory period and conduction velocity. Support for the multiple wavelet hypothesis can be found in humans during epicardial mapping studies of electrically induced AF where multiple re-entrant wavelets, displaying random re-entry and leading circle re-entry have been observed<sup>63</sup>.

In an isolated canine right atrial model, where extrastimuli were added at decreasing coupling intervals with increasing acetylcholine levels, it was observed that during repetitive firing there were increasing numbers of re-entrant wavelets. This was concordant with predictions from the multiple wavelet hypothesis. Interestingly though, when stable AF was induced, a small stable re-entrant circuit supervened<sup>64</sup>. Such activity, termed a rotor, was also observed in a Langendorff-perfused sheep heart model, and was one of the mechanisms for spatiotemporal periodicity seen in the left atrium<sup>65</sup>.

A computational mapping approach to human AF has suggested the presence of stable sources within the atria, both rotors and focal sources, with persistent AF patients having more such sources<sup>66</sup>. Conduction from these sources degenerates to become fibrillatory. This therefore suggests that AF is the result of stable sources driving the atria with fibrillation ensuing through a breakdown of 1:1 conduction.

One would postulate that a combination of mechanisms therefore underlies AF. It may be that a focal source generates impulses that undergo fibrillatory conduction with an increasing number of wavelets generated and establishment of rotors that then maintain AF, with or without continuing firing from the focal source. The transition from PAF to persistent AF may be related to the atrial tissue having negatively remodelled such that these rotors are more likely to be generated and have increased stability (either individually or as a group through increased numbers of rotors in persistent AF guarding against the effects of rotor extinction), or simply from the presence of more focal sources.

Based on the finding of pulmonary vein-based ectopics, pulmonary vein isolation (PVI) has become the cornerstone of AF ablation and is recommended by current guidelines as the strategy for PAF ablation<sup>1</sup>. In patients with persistent AF

though, such an approach in isolation is associated with lower success rates<sup>67,68</sup> and therefore more extensive ablation is undertaken such as the additional ablation of CFAE<sup>68,69</sup> or linear lesions<sup>70</sup>.

## **1.7 Atrial Fibrillation Electrograms**

### **1.7.1 Fractionated Atrial Electrograms**

In patients undergoing surgical resection of accessory pathways, Konings et al studied electrically-induced AF using a 244 pole electrode applied to the epicardial surface of the right atrium<sup>71</sup>. They specifically correlated the unipolar signals observed at each pole with the underlying fibrillation wave activity and found that fragmented signals occurred with high specificity at points of slow conduction and wavefront pivoting, and postulated the former were important in AF to allow shortening of the fibrillation wavelength and so accommodate more wavelets, while the latter would prevent wavelet extinction by increasing their propagation pathway. In this study, collision of wavefronts did not cause fractionated unipolar signals, causing instead long double potentials.

Bipolar signals were used in another study, in a canine model of persistent AF induced by prolonged atrial pacing to identify areas of complex fractionated atrial electrograms (CFAE), with the wavefront activity underlying these signals subsequently investigated by non-contact mapping<sup>72</sup>. In this case, the fractionated signals seen were found to relate to the centre of re-entrant wavefronts, at collision of wavefronts and during conduction through channels with wavebreak. Contrary to this, in an optical mapping murine monolayer model of AF, the centre of a rotor was not found to show fractionation (unless two pseudo bipoles were recorded and the signals combined),

whereas the presence of a meandering rotor or sites of wavebreak or collision were associated with fractionation of pseudo-bipolar signals<sup>73</sup>.

Studies of PAF patients in AF have demonstrated that CFAE genesis is preceded by an acceleration in the AF rate<sup>74,75</sup>. The transition to fractionation has been noted to be associated with a re-entry pattern around a line of functional block and activation breakthrough across a line of slow conduction<sup>74</sup>. The increase in rate responsible for these changes has been suggested to be secondary to a wandering rotor or change in the rate of a remote source<sup>74</sup>, though in a minority of cases, there was a suggestion of local complex activation or reentry<sup>75</sup>. The relationship with a remote source is further suggested by optical mapping studies in explanted sheep hearts which have suggested that fractionation occurs at the edge of a domain of high dominant frequency with fractionation due to increased beat to beat variation in the direction and conduction velocity of AF waves<sup>76</sup>.

As well as the pulmonary veins, regions of CFAE have also been shown in patients with AF to produce spontaneous discharges initiating AF<sup>77,78</sup>. Such spontaneous discharges, whether from the pulmonary veins or CFAE regions, result in an increase in left atrial activation time and initiate AF if at a short enough coupling interval to impair conduction in regions of CFAE allowing a meandering re-entrant wave to become established<sup>78</sup>. Once initiated, these regions then maintain AF through slow conduction and pivoting of waves leading to wave break and fusion<sup>77</sup>.

CFAE therefore reflect a variety of underlying wavefront mechanisms and CFAE are likely to represent areas responsible for both the initiation and maintenance of AF.

While the wavefront activity underlying CFAE, and the potential causes of fractionation have been studied, their importance to the maintenance and initiation of



AF, as evidenced by the response to ablation is less certain. The initial published trial where CFAE were ablated as a sole strategy resulted in a highly impressive 91% (110 out of 121 patients) freedom from arrhythmia and symptoms at one year<sup>79</sup>. In this trial, CFAE were defined as either electrograms with a very short cycle length ( $\leq 120$ ms) averaged over a ten second recording period or atrial electrograms that had fractionated electrograms composed of two deflections or more, and/or perturbation of the baseline with continuous deflection of a prolonged activation complex over the same recording period<sup>79</sup>. However, subsequent trials of CFAE ablation either alone<sup>80-82</sup> or in combination with PVI<sup>81-86</sup> have met with varying success. On meta-analysis though, the combination of PVI with CFAE ablation leads to significantly improved outcomes in the ablation of persistent AF (though not PAF)<sup>87</sup>.

CFAE have been shown to have a reasonable degree of temporal and spatial stability with 73-78% concordance between different maps during the same<sup>88,89</sup> and different<sup>90</sup> episodes of AF. Common sites of CFAE include the base of the left atrial appendage and the pulmonary vein antra<sup>88,89</sup>. In a study of patients undergoing PAF ablation where AF was induced, comparison of bipolar contact mapped points with non-contact mapping of wavefront propagation suggested that different patterns of bipolar CFAE related to different underlying wavefront activity<sup>91</sup>. Rapid repetitive bipolar CFAE (cycle length under 120ms, separated by isoelectric interval) were predominantly due to either arrhythmogenic sites or pivot points, whereas fragmented bipolar CFAE (continuous fractionated activity) was mainly caused by passive activation and slow conduction<sup>91</sup>.

While these studies demonstrate that CFAE are a reasonably stable phenomenon they also tell us that not all CFAE are equally important to the AF process: some are purely passive epiphenomena. Further evidence for this is the finding that PVI results

in a reduction in CFAE burden<sup>92,93</sup> as does linear ablation<sup>93</sup>, with a reduction even at regions distant to the ablation. It may be that these passive CFAE are secondary to wave collision or other causes such as activation of overlying structures<sup>94</sup>. Certainly, a mapping study comparing monophasic action potentials to local bipolar signals found that the CFAE seen with the latter in 67% of cases represented farfield signals (with other mechanisms seen in other cases including rapid localised organised AF activity, possibly consistent with AF drivers and acceleration related changes)<sup>95</sup>.

Therefore, as CFAE can be caused by a variety of active and passive phenomena, an understanding of the mechanism underlying a particular CFAE signal would help focus ablation efforts. The above studies suggest that such identification may be possible on morphological grounds. To this end, the definition of a CFAE becomes very important. An epicardial mapping study found that CFAE defined by an atrial fibrillation cycle length (AFCL) of <120ms and those defined by continuous/multicomponent activity have different distributions, with the area under the receiver operator curve for the former predicting a site of the latter being only 0.59<sup>96</sup>. Takahashi et al found that ablation at signals displaying continuous fractionation for  $\geq 70\%$  of the time in a 4 second sample or a temporal gradient of activation across bipoles was associated with significantly more AFCL prolongation or AF termination<sup>97</sup>. Using a visual fractionation scale to grade signals from 1 to 5 where grade 1 are the most fractionated signals and grade 5 normal<sup>98</sup>, Hunter et al studied the effect of ablating different CFAE grades<sup>99</sup>. Of note grade 1 and 2 signals in this scheme are those with fractionation for  $\geq 70\%$  of the 10 second sample. Following PVI, the remaining CFAE were on average less fractionated<sup>99</sup> (a mean increase in CFAE). Ablating more fractionated CFAE signals first was found to reduce the incidence of less fractionated signals (grade 3 and 4) whereas the converse was not true. There was also

a differential effect on the AFCL from ablating different grades of CFAE, with grade 1, 2 and 4 having a significant effect while grade 3 had no effect<sup>99</sup>.

These studies therefore suggest that certain types of CFAE are actively involved in driving AF, whereas others are passive phenomena, and highlight the importance of the electrogram in guiding ablation of AF.

### **1.7.2 Spectral Analysis of Electrograms**

The use of spectral analysis represents an attempt to study in more detail the multiplicity of signals forming the fibrillatory electrogram. This method allows the frequency of the superimposed components of an AF electrogram to be analysed separately and the relative contribution of each to the final electrogram weighted, resulting in the establishment of a dominant frequency (DF) for the complex electrogram.

In AF, a DF gradient from the left to right atrium has been observed in an isolated sheep heart AF model and also in patients with PAF<sup>100,101</sup> and persistent AF<sup>101</sup>, (though not in persistent AF patients in one study<sup>100</sup>). Spectral analysis has shown that the overall DF is higher in patients with persistent AF than PAF and that DF sites (sites with a 20% higher DF than surrounding atrial tissue with a 20% frequency gradient from them) are more often situated in the atrium itself rather than the pulmonary vein region in persistent AF atria<sup>101</sup>; moreover, the sites with maximal DF were less likely localised to the pulmonary vein in persistent AF: these findings are consistent with a more advanced atrial substrate in persistent AF maintaining the arrhythmia.

In terms of the change in DF in response to ablation, in one study the DF measured at single points in the LA, CS and RA were significantly reduced by PVI in PAF but not persistent AF patients<sup>100</sup>, whereas in another study, PVI reduced the mean

DF in persistent AF patients as well<sup>102</sup>. In patients with PAF, isolation of pulmonary veins harbouring DF sites leads to a reduction in AFCL or termination of AF, whereas this is not the case in pulmonary veins without DF sites<sup>101</sup>. Spectral analysis of PAF patients in sinus rhythm has demonstrated that the majority of high DF sites are at the pulmonary veins with patients with larger left atria having more non-pulmonary vein high DF sites<sup>103</sup>. Patients with high DF sites outside the pulmonary vein regions were more likely to remain inducible following PVI, with further substrate ablation required to reduce this inducibility<sup>103</sup>. Two main patterns of DF distribution have been seen in persistent AF patients: in one there is a large gradient (>20% compared to average LA DF) between the sites of maximal DF and the surrounding atrial tissue, and in the other there is less of a gradient<sup>104</sup>. Patients with the latter pattern had a lower proportion of termination to sinus rhythm during the procedure and a greater AF recurrence rate<sup>104</sup>.

It is therefore postulated that regions of higher dominant frequency are drivers of AF, representing rotors. One source of variability in the literature though is the definition of a high DF site. Some investigators have counted this as those sites with DF values 20% higher than neighbouring sites<sup>101</sup> (though clearly what constitutes a neighbouring site is affected by the density of the map collected) and others have taken those values as 20% higher than the mean DF for the LA map<sup>104</sup> and in a prospective DF-guided ablation study, sites with a DF higher than the mean for the LA map were targeted<sup>105</sup>.

CFAE ablation has been found to reduce the mean DF in both persistent AF and PAF patients<sup>102</sup>. Lin et al studied the interaction of CFAE and DF in patients with persistent AF<sup>104</sup>. The most fractionated signals were found in the centre or at the boundary of the maximal DF sites, with the most temporal and regional CFAE consistency found at these sites<sup>104</sup>. In an epicardial mapping study, it was found that

CFAE defined as continuous/multicomponent electrograms localised to DF sites in around 20% of cases, while in around 80% of cases these electrograms were found in the boundary regions of the DF sites (CFAE defined purely on the basis of cycle length <120ms were found to poorly localise to DF sites)<sup>96</sup>. An endocardial study also found similar results, with there being poor point-by point correlation of CFAE and high DF sites but a high incidence (80%) of DF sites within 10mm of CFAE areas<sup>106</sup>. The finding of CFAE in the boundary regions of high DF sites seems a more common observation than finding CFAE at DF sites themselves and correlates with previous optical mapping studies in explanted sheep hearts<sup>76</sup>.

CFAE and DF measurements may therefore be of use in delineating regions actively involved in driving AF. Any factors which can affect the electrogram could therefore impact on the efficacy of targeting driver regions based on the above types of analyses in a proposed ablation strategy. Nothing is known regarding how catheter contact may affect CFAE or spectral analysis measurements *per se* and knowledge of the mechanoelectric relationship of these signals may further our understanding of them.

## **1.8 Mechanoelectric Coupling**

### **1.8.1 Atrial Mechanoelectric Coupling**

Cardiac tissue demonstrates electromechanical coupling whereby electrical impulses are converted into mechanical responses to allow the heart to contract. There is also the reverse relationship whereby mechanical inputs such as stretch and compression have electrical consequences.

Historical studies suggested that mechanoelectric coupling may be present in man. Ventricular repolarisation was noted to lengthen in patients undergoing balloon valvuloplasty for pulmonary vein stenosis as the right ventricular systolic pressure

dropped, and as the pressure in the right ventricle was increased by blocking of the right ventricular outflow tract, monophasic action potentials shortened and early after depolarisations developed<sup>107</sup>. Similarly, in patients being weaned off bypass, as the ventricle is increasingly stretched, the monophasic action potential has been observed to shorten<sup>108</sup>.

In a canine study, increases in the intraventricular volume caused changes in the duration of the epicardial monophasic action potential, with a shortening earlier in repolarisation and a lengthening due to early after depolarisations later in repolarisation<sup>109</sup>. Another group did not demonstrate such a relationship though<sup>110</sup>, and another only observed changes epicardially (lengthening of the monophasic action potential) and not endocardially in response to stretch<sup>111</sup>. A stretch-related reduction in the monophasic action potential amplitude has also been noted<sup>109,112</sup>. Acute stretch can cause ventricular ectopics to be generated, with the probability of an ectopic correlating positively with the rate of rise of volume and the peak volume of a pulse administered to the chamber<sup>109,112</sup>.

The ventricle is a thicker walled and morphologically more complex structure than the atrium. Using a Langendorff-perfused rabbit heart preparation, Ravelli and Allesie investigated the effect of stretch on the electrical properties of the atrium<sup>113</sup>. The model involved biatrial dilation with the interatrial septum perforated to ensure equalisation of pressures and the atrioventricular node ablated with the ventricle paced into ventricular fibrillation to control for any atrial pressure changes caused by ventricular activity. Premature stimulated beats were used to gauge the vulnerability of the atrium to arrhythmia – at baseline, no arrhythmia could be induced. With increasing intra-atrial pressure and consequent increasing stretch, abnormal electrical activity, ranging from repetitive firing to atrial flutter to AF, was induced. There was a

significant relationship between rising intra-atrial pressure and the incidence of AF, with termination of the arrhythmia by release of the pressure. Electrically, an increase in pressure led to a shortening of the refractory periods of both atria, taking around 3 minutes of sustained pressure to reach steady state. The change in refractory period correlated with a shortening of the action potential. The latter was mainly due to an increase in the rate of early repolarisation, and loss of the plateau phase of the action potential<sup>113</sup>.

In an isolated guinea pig heart model, different parts of the action potential were differentially affected by a stretching stimulus, with a decrease in the action potential duration at 50% repolarisation and an increase at 90% repolarisation<sup>114</sup>, similar to the findings in the canine ventricle<sup>109</sup>. With increasing stretch, increasing spontaneous premature atrial beats were also noted in the guinea pig model<sup>114</sup>. A decrease in the monophasic action potential amplitude with increasing stretch has also been observed in the atria<sup>113,114</sup>. These results contrast with the findings in an isolated rat right atrial model where no change in the action potential duration was seen but there was an increase in action potential amplitude and atrial conduction velocity with stretch<sup>115</sup>. In the latter study, atrial stretch was found to increase the incidence of delayed afterdepolarisations and ectopics<sup>115</sup>.

Globally, acute atrial stretch reduces atrial conduction velocity and increases the number of areas of slow conduction and conduction block<sup>116</sup>. This spatial heterogeneity is felt to be due to the differential distribution of stretch within the atrium in response to increased intra-atrial pressure. Stretch has also been found to increase the atrial effective refractory period (ERP) and, interestingly, this increase is greater in the thinner walled parts of the atria which are subject to greater stretch by an increase in global pressure<sup>117</sup>. Therefore an increase in intra-atrial pressure leads to an exaggeration of the

ERP differences already present at different parts of the atrium. This increasing dispersion of atrial refractoriness is felt to contribute to the increased propensity for AF in the stretched atrium.

In humans, increasing the right atrial pressure through atrioventricular (AV) pacing results in a reduction of the right atrial ERP and an increased propensity for AF, with the latter correlating with the increase in right atrial pressure<sup>118</sup>. Note that different studies have suggested that atrial stretch has different effects on the atrial ERP, with an increase in some cases<sup>117,119</sup> and a reduction<sup>113,118,120,121</sup> in others. One explanation put forward for this disparity is that ERP may depict the action potential duration at different stages of repolarisation depending on the stimulus strength<sup>121</sup>, and as stretch has different effects on the action potential depending on the stage of repolarisation<sup>109,114</sup>, this would have a significant impact. It is not difficult to propose that a shortening of the ERP could facilitate the maintenance of AF by allowing the atrium to support more wavelets. A direct relationship between the shortening of the atrial ERP in response to stretch and the inducibility of AF has been observed<sup>113</sup>.

Aside from changes in ERP, synchronously AV paced patients demonstrate a slowing of atrial conduction velocity and a higher incidence of slow conduction and intra-atrial conduction block sites<sup>122</sup>. These changes are also associated with an increased incidence of AF.

In man, at the junction between the left atrium and the pulmonary veins, increasing stretch leads to an increase in the dominant frequency significantly more than at the left anterior free wall<sup>123</sup>. Moreover the number of spatio-temporally periodic wavefronts increases with the increasing intra-atrial pressure<sup>123</sup>. In patients undergoing ablation for AF, the intra-atrial pressure is higher in those with persistent AF rather than



PAF and the mean dominant frequency of the left atrium has been found to correlate with the observed left atrial pressure<sup>124</sup>.

The mechanoelectric properties of the pulmonary veins have also been investigated. Isolated pulmonary veins demonstrate increased spontaneous firing in response to mechanical stretch as well as a reduction in action potential amplitude and duration with an increase in delayed and early afterdepolarisations<sup>125</sup>.

Based on the above discussion, mechanoelectric coupling can be implicated in both the genesis and maintenance of AF.

### **1.8.2 Localised Mechanoelectric Coupling**

The experiments discussed above have investigated the effect of increasing the pressure within cardiac chambers and looked at the electrical response. While increased intracavitary pressure does lead to mechanical deformation, it is an indirect, and at the organ level inhomogeneous, means of achieving this. To examine in more detail the influence of stretch *per se* requires study at a more localised level. In the *in situ* pig heart, local stretch of the right atrium using a tripodal suction device causes shortening of the action potential, early afterdepolarisations and atrial tachyarrhythmias<sup>126</sup>. In a study investigating an explanted rat atrial tissue preparation, stretch led to differential effects on the action potential, with a shortening mid-way through and a lengthening at the end of repolarisation, and beyond a threshold, premature atrial beats were induced<sup>127</sup>. These findings are similar to those seen with global stretch of the atrium<sup>114</sup> and ventricle<sup>109</sup>.

The study of mechanoelectric coupling at the cellular level has presented great methodological difficulties, with the aim being to mechanically manipulate cells without damaging them<sup>128</sup>.

Myocytes isolated from rats<sup>129,130</sup>, guinea pigs<sup>130</sup> and man<sup>130</sup> (but not frogs<sup>131</sup>) demonstrate stretch-induced cell depolarisation, with the possibility of causing extrasystoles if beyond a threshold. In guinea pig and human myocytes, stretch accelerated repolarisation in the first part of the action potential and lengthened it in the second phase, leading to an overall increase in the action potential duration<sup>129,130</sup>. In rat myocytes, an increase in the action potential duration is also observed with lengthening of the mid and late parts of the action potential<sup>129</sup>. Stretch was associated with an inward current, mainly carried by sodium ions, and this current was maintained during the stretch without inactivation or adaptation and stopped when the stretch stimulus ended<sup>129,130</sup>.

Interestingly, the orientation of mechanical deformation relative to the axis of a cell has been found to exert different effects on myocytes<sup>132</sup>. Compression of cells along their long axis causes them to depolarise and compression perpendicular to this causes them to hyperpolarise. These changes in the membrane potential from compression are potassium mediated (rather than sodium mediated as in the case of stretch induced changes)<sup>132</sup>.

Myocytes are not the only cells which have mechanosensitive properties. In fibroblasts, stretch has been found to hyperpolarise the zero current potential by reducing membrane conductance while compression depolarises the holding current potential by increasing membrane conductance<sup>133</sup>. In isolated right atrial and cultured cell preparations, fibroblasts and myocytes have been shown to display electrotonic and capacitive coupling<sup>134</sup>. Fibroblasts have demonstrated in cell culture experiments to be capable of transmitting electrical impulses over short (a few cells)<sup>135</sup> and long (up to 300µm)<sup>136</sup> distances (albeit with conduction delay) mediated by connexin43<sup>136</sup>. In the sinus node, mathematical modelling has suggested that stretching these electrically

passive cells may exert an effect on myocyte function by affecting the spontaneous depolarisation of pacemaker cells<sup>134</sup>. The contribution of the mechanosensitivity of fibroblasts to cardiac electrical properties *in situ* has not yet been clearly defined.

### **1.8.3 Localised, Catheter-Mediated, Stretch in vivo**

As can be seen from the above, myocardial stretch, and even the orientation of stretch relative to a myocyte, has a significant impact on electrical behaviour. In humans, there is iatrogenic exposure to localised myocardial stretch at the time of an electrophysiological procedure such as an ablation for AF. In this circumstance, the stretch stimulus is mediated by the contact force from the catheter placed within the heart. Electrogram amplitude has been shown to correlate with increasing contact force in canine atria<sup>137,138</sup> but not ventricles<sup>139</sup>. In clinical studies, the bipolar and unipolar electrogram amplitude has been shown to be higher at increasing contact forces in the ventricle (though there is a threshold beyond which higher contact forces are not associated with a change in the electrogram), and more ventricular late potentials are seen at higher contact forces<sup>140</sup>. The reason for a change in electrogram properties with increasing contact may simply represent better transmission of electrical signals to the electrode, or it could be that the catheter is actively affecting the electrical properties of the myocardium by the mechanisms discussed above.

During bipolar recordings, atrial electrograms have been found to vary with electrode orientation both prior to and following ablation within porcine atria in sinus rhythm<sup>141</sup>. Such a relationship is predictable from the nature of bipolar recordings, and in conjunction with catheter contact could have a significant bearing on the electrograms recorded from fibrillating human myocardium.

The effect of localised stretch, including its orientation, on the human atrium has not been studied. This effect may be especially of relevance to any drivers of AF that are present as one would postulate that changing their electrical behaviour could have wide ranging effects on the fibrillating atrium. In this context, the effect of contact force on CFAE merits further investigation. If contact force affects the expression of CFAE, then this would be of significance for clinical ablation. It may be the case that contact parameters are contributory to the variation seen in CFAE maps<sup>88-90</sup> and even the outcomes from strategies incorporating CFAE ablation in persistent AF<sup>79-87</sup>.

### **1.9 Steerable Sheath Technology**

Two types of steerable sheath technology are currently available: manual steerable sheaths (Figure 1.1) and remote robotic navigation systems. In a case-control study of 105 patients ablated using a steerable sheath were matched to 245 control



**Figure 1.1 Agilis NxT manual Steerable Trans-septal Sheath**

patients ablated with a conventional manual non-steerable sheath: the rate of sustained atrial tachyarrhythmia was significantly reduced in those in the former group at six months follow up<sup>142</sup>. These results were then expanded upon in a prospective randomised study of 130 patients which again found a significant benefit from the use of steerable sheaths at 6 months follow up in terms of success rates, as well as a significantly lower fluoroscopy time during the procedure<sup>143</sup>. The advantages of steerable sheath technology are felt to relate to the improved access and contact to ablation target sites, improving the efficacy of lesion delivery.

Another system using steerable trans-septal sheath technology is the Sensei<sup>®</sup> Robotic Catheter System from Hansen Medical Inc. (Mountain View, California, USA). This system obtained its CE mark in 2007. The system incorporates an inner and outer sheath, each containing pull wires enabling deflection of the sheaths and a conventional catheter is passed through the inner sheath. This system has the advantage of having the controls placed outside of the radiation field (remote from the patient, Figure 1.2), and is used with the operator seated. The movements of the catheter are controlled using a 3D joystick (Figure 1.2).

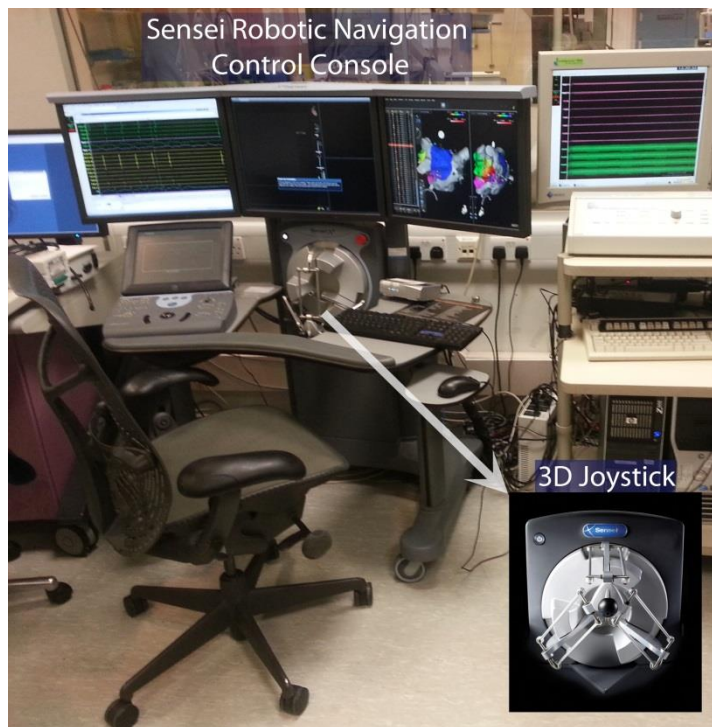


**Figure 1.2 The Sensei Robotic Navigation System Control Console at St Bartholomew's Hospital.** The console is placed outside of the radiation field and is therefore used without radiation protection equipment (and with the operator seated). The 3D joystick which is used to control the deflection of the steerable robotic trans-septal sheath is highlighted.

Two randomised trials comparing manual to robotic ablation have been published<sup>144,145</sup>. These data plus registry studies suggest a benefit from RRN use in terms of fluoroscopy time<sup>144-149</sup>, catheter stability<sup>145,148,150</sup> and more rapid and greater electrogram attenuation<sup>151,152</sup> without an impact on success rates<sup>144,145,147,148</sup>.

## 1.10 Contact Force Sensing Technologies

### 1.10.1 Sheath-Based Technology

The longest established contact force sensing technology is incorporated in the Sensei<sup>®</sup> Robotic Catheter System. The force sensing system incorporated in this robotic system is known as IntelliSense<sup>®</sup>. This pulses the catheter at 4Hz proximally and extrapolates the catheter contact force (CF) with the myocardium by the resistance to motion of the catheter in response to this proximal pulsation.

### 1.10.2 Catheter-Based Technology



**Figure 1.3 The Thermocool SmartTouch catheter.** On the left side of the image is a cartoon representation of the distal end of the catheter and on the right side, a photograph of a catheter. The spring element is annotated.

The first of the catheter-based technologies to obtain a CE mark (2009) was the TactiCath<sup>®</sup> from Endosense (Geneva, Switzerland). This catheter uses three optical fibres between the second and third electrodes of the catheter and an elastic polymer catheter tip<sup>153</sup>. The latter undergoes microdeformations in response to contact which changes the wavelength of reflected infrared light transmitted by the optical fibres: from the wavelength of reflected light at the three fibres, the orientation and magnitude of

contact force is derived<sup>153</sup>. In so doing, information regarding catheter tip contact force and the orientation of this is derived.

The most recently CE marked of the contact force sensing technologies is the ThermoCool® SmartTouch™ Catheter from Biosense Webster (Diamond Bar, CA, USA). Here the catheter the tip electrode is mounted on a precision spring permitting a

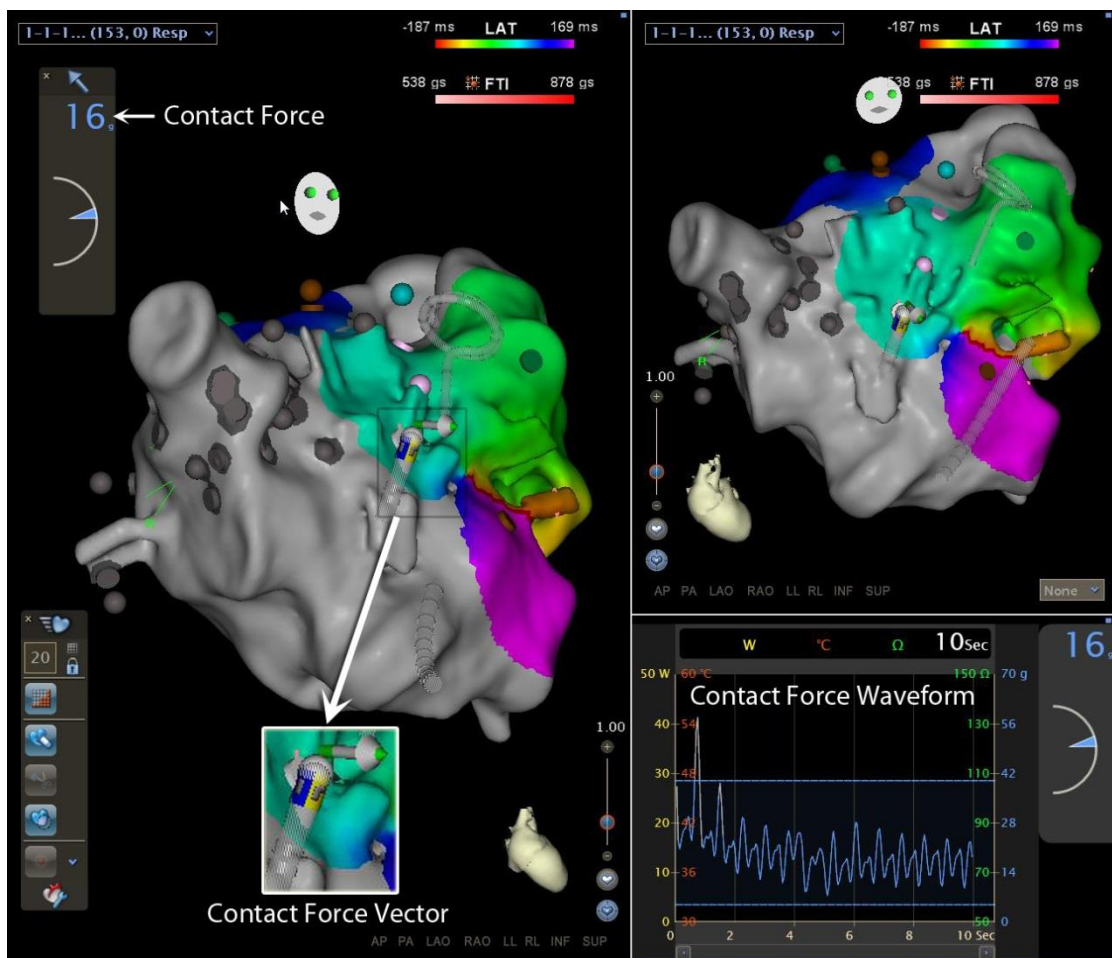


**Figure 1.4 The Display of Contact Force Data Measured by the SmartTouch Catheter on the Carto3 Screen.** Displayed is a left atrial geometry created using the Carto3 electroanatomic navigation system. Highlighted are the contact force, contact force vector and the contact force waveform for the contact between the catheter and the myocardium.

small amount of electrode deflection (Figure 1.3). By measuring this deflection using location sensor coils at the proximal end of the spring, the system can calculate the force being exerted (and its orientation) using the known characteristics of the spring. The

SmartTouch catheter integrates with the Carto3 platform. During a case, the magnitude of contact force and its vector are displayed in real-time on the Carto3 display screen as well as the contact force waveform (Figure 1.4).

For the SmartTouch catheter, the reported sensitivities reported by the manufacturer is less than 1g of contact force. Data has been published for the Tacticath, where a comparison has been made between the measurements made by the catheter and a calibrated balance: this demonstrated the measurements by the catheter were highly sensitive and accurate (mean error  $\leq 1\text{g}$ )<sup>153</sup>.

### **1.11 Biophysics of Ablation**

Catheter-based radiofrequency ablation utilises alternating electrical current to create a tissue lesion through resistive heating (which occurs at the electrode-tissue interface (ETI)), and conductive heating spreading away from this latter zone. One method of increasing efficacy is to produce larger volume lesions during ablation. This ensures continuity and transmuralty of lesions to make reliable lines of block.

Initial studies demonstrated that lesion size correlates positively with catheter tip temperature<sup>154,155</sup>. The threshold temperature for tissue viability has been calculated to be between 46.6 and 48.9°C, with tissue temperature being inversely related to the distance from the electrode<sup>154,156</sup>. If the temperature at the ETI exceeds 100°C then blood boils and a coating of coagulum and char on the electrode forms which electrically insulates the electrode and causes a rise in impedance<sup>157</sup>, preventing further delivery of energy to the tissue.

Cooling the catheter tip through irrigation prevents the formation of coagulum and char by reducing the temperature at the ETI, and allows for greater power delivery, resulting in larger lesions compared with non-irrigated catheters<sup>158</sup>. The degree of



cooling, as dictated by the rate of irrigation flow, also affects lesion size, with a very high rate associated with a reduced lesion width<sup>159</sup>. A by-product of catheter tip irrigation though is that temperatures deeper in the tissue can rise to the extent that superheating occurs with a sudden explosion of steam (which can be heard as a pop) associated with crater formation and an impedance rise<sup>158</sup>.

As one would expect, cooling the catheter tip changes the relationship between the catheter-tip temperature and lesion size: from animal models, there is no correlation between the ETI temperature or the electrode temperature and the lesion depth or maximal temperature in irrigated ablation, while the converse is true in non-irrigated ablation<sup>158</sup>.

The diameter of the catheter also makes a difference: with non-irrigated catheters, larger lesions are caused by catheters with a larger diameter<sup>156</sup>, while the converse is true with irrigated catheters<sup>160</sup>.

The duration of ablation also affects lesion size. A monoexponential increase in lesion size with time at a target electrode temperature has been noted with non-irrigated catheters, with a plateau when a steady state of tissue temperature is reached after around sixty seconds<sup>161</sup>. With irrigated catheters, the temperature at deeper levels continues to rise at sixty seconds, with a suggestion that lesion size may also follow this trend<sup>158</sup>.

Electrode orientation also affects lesion size<sup>162,163</sup>, with a vertical orientation increasing, and a horizontal orientation reducing lesion sizes with irrigated catheters<sup>162,163</sup> and the converse the case with non-irrigated catheters *in vitro*<sup>163</sup>.

### 1.11.1 Contact Force and Ablation

Aside from the variables detailed above, another important factor is the degree of contact between the catheter and the tissue. Earlier *in vitro* work with non-irrigated catheters in temperature-controlled ablation demonstrated a linear relationship between contact force and lesion size, with the largest difference between no contact and being in contact with tissue<sup>161</sup>. Over a wide range of contact forces (0-400N), there was only a small increase in lesion size with increasing contact force (as long as the electrode tip temperature was maintained at the pre-set value and contact was maintained)<sup>161</sup>. The modest nature of this relationship in this setting was further highlighted by a study comparing 10g to 20g of contact, and in this narrow range no difference in lesion size was found<sup>162</sup>. With non-irrigated catheters and temperature controlled ablation, as the power output during ablation can be titrated to achieve target temperatures, the effect of degrees of contact will be reduced. Poorer contact entails more power output to reach the same temperatures<sup>161</sup> and since lesion size relates to temperature at the electrode tip<sup>154</sup>, similar lesion sizes are therefore produced.

An *in vivo* study of epicardial ablation compared good with bad contact (the latter defined as light or no contact) with power-controlled ablation and found that lesion size correlated with the degree of contact<sup>164</sup>. In this case, there were more pops and impedance rises with greater contact at higher powers and these were associated with rapid, excessive electrode temperature rises. The importance of contact force in irrigated catheters has been studied *in vitro* with lesion size significantly greater at a force of 30g compared to 10g in one study<sup>165</sup>, and another finding that 0.5N of force (but only with a perpendicular orientation) created significantly deeper lesions than lesser contact forces, but with also a higher incidence of pops<sup>159</sup>. In another study examining temperature controlled power limited ablation in excised porcine ventricle,

where fluid flow external to the catheter was utilised to cool the catheter tip, lesion size increased with catheter contact before a plateau was attained<sup>166</sup>.

The above studies of catheter contact force during ablation extrapolated the force at the catheter tip from the force loaded onto the catheter, with for example a dynamometer. Such a method could not be used in the endocardial clinical *in vivo* setting. Electrical impedance has been used as an *in vivo* marker of contact. Impedance is the opposition to flow of a current through a circuit in response to a voltage. Impedance has been suggested to fall during ablation as a rise in temperature is felt to increase the conductivity of cardiac tissue<sup>166</sup>. Impedance at baseline has been observed to be higher in the pulmonary veins than the body of the atrium<sup>167</sup>. Impedance falls with ablation, and this fall correlates with the temperature at the catheter tip<sup>164,167</sup>, with a steeper relationship in the pulmonary veins than the left atrium<sup>167</sup>. Greater contact force between the ablation catheter and tissue results in a greater impedance drop<sup>164,166</sup> and later plateau of this fall with ablation in animal studies, with an excessive drop ( $>20\Omega$ ) associated with tissue overheating, a subsequent rapid rise in impedance and tissue explosions<sup>164</sup>. The impedance drop has also been found to correlate with lesion depth<sup>166</sup>. These studies have examined impedance during non-irrigated ablation. Animal studies have also looked at this measure during irrigated ablation. There is a small but significant increase in the impedance with the start of irrigation and the baseline impedance is higher when the catheter is in contact with tissue rather than in the blood pool<sup>168</sup>. With irrigated ablation, the magnitude of the impedance drop is not predictive of pops but a greater drop is predictive of thrombus formation<sup>168</sup>.

In a study of 394 ablation points in 35 patients undergoing AF ablation, the maximum impedance drop with ablation was found to correlate with the CF during

ablation, and a more perpendicular catheter contact orientation was associated with a lesser impedance fall (but also lesser CF) than a more parallel contact orientation<sup>169</sup>.

Bipolar voltage amplitude significantly correlates with increasing contact: while this cannot differentiate between consistent contact and tenting, there is a significant difference between no contact, minimal contact and consistent contact<sup>137</sup>.

Studies using sheath-based force sensors *in vivo* have shown increased CF is associated with larger and more transmural lesions<sup>137</sup> but also more pops<sup>170</sup>. Irrigated tip force-sensing catheters have further examined the impact of different levels of contact force on lesion size and also the interplay of this variable with the ablation power. Increased contact force is associated with increased tissue temperature at 3 and 7 mm away from the ETI, and is associated with increased lesion size at a given level of CF, as is increasing ablation power<sup>153</sup>. Increasing CF is also associated with an increased incidence of thrombus formation at the electrode edge, especially with increasing power, and a similar relationship is also apparent for steam pops<sup>153,168</sup>.

Within the beating heart, even within the fibrillating atrium, it would be expected that contact will be dynamic rather than static. Such dynamic contact has been simulated in an *in vitro* setting where constant (static) contact has been found to produce the largest lesions while variable and intermittent contact produce progressively smaller lesions<sup>171</sup>. Therefore the dynamic quality of the contact between electrode and tissue is also of great importance in the efficacy of lesion formation. In addition to motion from the beating heart, respiratory motion also affects the contact force from the catheter, with apnoea, as expected, leading to higher average contact force and force time integral during ablation<sup>172</sup>.

Better electrode-tissue contact results in a greater proportion of the delivered power contributing to the resistive heating of the tissue, rather than wasted in the blood

stream. Consequently, this can lead to larger, more likely transmural lesions but also increases the risk of complications through excessive tissue heating.

The LA is not a uniform structure: there is a normal variation in its wall thickness and texture<sup>173</sup>. During electrical isolation of the pulmonary veins, areas which are more frequently resistant to electrical isolation have been identified<sup>174</sup>. Moreover there is also a preferential distribution of sites of acute and chronic reconnection<sup>175</sup>. The intervenous ridges and pulmonary vein-left atrial appendage ridge are important areas in this respect<sup>174,175</sup>. The reason for this locational variation in the efficacy of ablation may relate to variations in wall thickness making transmural lesions harder to produce, epicardial connections or difficulties achieving optimal contact in those regions. A significant variation of the contact forces exerted within the atrium during ablation has in fact been observed: for example the left anterior inferior ridge area has lower catheter contact<sup>176</sup>. Contact force during ablation also predicts acute reconnection in patients with PAF, with sites of pulmonary vein reconnection having a lower average contact force<sup>172,177</sup> and force time integral during ablation<sup>172</sup>. At 3 months' follow up, segments within a wide area circumferential ablation (WACA) line ablated with a minimum force time integral (FTI: the area under the force-time curve) below 400g.s had a greater chance of reconnection among PAF patients<sup>178</sup>. At 12 months of follow up, the average contact force, force time integral and incidence of low contact force during ablation are predictive of procedural success in PAF patients<sup>179</sup>.

The use of CF sensing catheters, in small non-randomised studies, has been found to be associated with a reduction in fluoroscopy<sup>180,181</sup>, procedure<sup>180-182</sup> and ablation times<sup>180,181</sup>, as well as AF recurrence rates at 12 months in some studies<sup>180,183</sup>, but not in another<sup>181</sup>. In these studies, generally a minimum average CF during ablation of 10g was targeted. The FTI achieved during ablation also has a bearing on procedural

parameters: in one study an average ablation FTI of under 543g.s was found to be associated with longer procedure and fluoroscopy times<sup>184</sup>.

In an *ex vivo* porcine heart study, a force of  $417 \pm 167$ g could perforate un-ablated left atrium, while ablation reduced the force needed to perforate<sup>185</sup>. A further study of *in vivo* porcine hearts found that the lowest contact force recorded to cause perforation was 77g, with a force of  $158.4 \pm 55.4$  needed to perforate unablated left atrium<sup>186</sup>. A study in patients undergoing AF ablation demonstrated that the actual contact forces exerted on the myocardium vary significantly among operators during mapping and ablation when they were asked to maintain what they perceive (without CF-sensing technology) to be 'good contact'<sup>176</sup>. This included multiple high force events defined as the contact force exceeded 100g for 200ms, with six of the thirty four patients having over 40 such instances<sup>176</sup>. These episodes occurred during catheter manipulation as well as ablation. Therefore, knowledge of the CF even while not actively ablating may be important from the point of view of safety.

## **1.12 Ablation Efficacy**

The aim of a radiofrequency application during AF ablation is the generation of a transmural lesion. This results in a persistent barrier to electrical conduction or the elimination of a driver. At a procedural level, this is best reflected by an improvement in the single procedure success rate for the ablation. Clearly, this is the most relevant outcome measure clinically. CF parameters have been compared between cases with and without a recurrence of symptoms by Reddy et al.,<sup>179</sup> (Table 1.1), with higher CFs during ablation observed in those without recurrence. An improvement in success rates may not necessarily mean that the ablation procedure has been more efficient: this would be reflected by a reduction in the procedure length, for example. In order to

make procedures more efficient, the aim should be for every radiofrequency application to be contributory to the success of the procedure. This would lead to shorter procedures and potentially less risk. Moreover, suboptimal applications may lead to short term procedural success but long-term failure – by causing tissue oedema and an incomplete transmural lesion. Consequently, it is useful to be able to assess the efficacy of individual radiofrequency applications.

**Table 1.1 Clinical studies assessing ablation efficacy with respect to catheter contact force: methods used to assess efficacy and cut off values for effective ablation**

Author	Number of Patients	AF Subtype	Method to judge ablation efficacy	Suboptimal Ablation	Effective Ablation
Reddy <sup>179</sup>	32	PAF	12 months recurrence of symptoms	CF <10g; FTI <500g.s	CF >20g FTI >1000g.s
Halдар <sup>177</sup>	40	35% PAF	Acute PV reconnection in a 7 segment model per PV pair	CF 14.5g	CF 19.6g
Kumar <sup>172</sup>	12	PAF	Acute PV reconnection in a 5 segment model per PV pair	LPV: CF 9g, FTI 173g.s RPV: CF 11g, FTI 282g.s	LPV: CF 20g, FTI 436g.s RPV: CF 24g, FTI 609g.s
Kumar <sup>187</sup>	20	PAF	EGM criteria for transmurality <sup>141</sup>		CF >16g, FTI >404g.s
Neuzil <sup>178</sup>	40	PAF	PV reconnection at 3 month protocol-driven restudy in a 5 segment model per PV pair	CF 15.5g Minimum CF 3.6g Minimum FTI 118g.s	FTI >400g.s CF 19.5g Minimum CF 8.1g Minimum FTI 232g.s
Sohns <sup>188</sup>	6	PAF	MRI-defined scar in 5mm <sup>2</sup> zone		>1,200g.s

In preclinical studies, the efficacy of an individual ablation is relatively straightforward to judge as histological lesion dimensions are available<sup>158,161</sup>. Lesion histology is not available for clinical studies though and therefore alternative measures of the effect of ablation are used.

Classically, the attenuation of the electrogram has been used to judge the efficacy of an individual ablation. Unipolar atrial electrogram attenuation has been found to be associated with transmuralty of ablative lesions<sup>189</sup>. Significantly more amplitude reduction in the bipolar signal during sinus rhythm and AF with transmural lesions is seen *in vitro*, with a reduction of  $\geq 60\%$  having a high specificity for lesion transmuralty<sup>190</sup>. In clinical studies, an  $\geq 80\%$  reduction in electrogram amplitude has been targeted<sup>175,191</sup>. The location of the lesion, whether in smooth or trabeculated atrial tissue affects the ability to attain target reductions in electrogram amplitude, likely due to the non-uniformity of electrode contact in the latter regions<sup>192</sup>.

Changes in electrogram morphology have also been shown to be predictive of transmuralty of ablation lesions in a porcine model by Otomo et al.,<sup>141</sup>. This approach is limited clinically in that it has been validated only in sinus rhythm cases. One group have used these criteria for bipolar signals to judge ablation efficacy<sup>187</sup>.

The most commonly employed model for assessing ablation efficacy is reconnection of the pulmonary vein isolation (PVI) lines which are used to isolate the pulmonary veins from the left atrium<sup>172,177,178</sup> (Table 1.1). In this approach, the ipsilateral paired PVI line is divided into five to seven segments and efficacy is based on whether that segment reconnects or not. The disadvantage here is that target parameters for individual radiofrequency applications are being assessed based on the response of a region, quite often with overlapping ablations, to ablation. In all but one of these studies, operators were blinded to CF measurements (in the other study, the operators were blinded in only half the cases). This blinding serves to exaggerate the differences between ineffective and effective ablations as a lack of knowledge of CF allow for a greater range of CF to be applied and therefore makes it difficult to establish where the actual threshold for effective ablation lies. Based on these studies, a mean



ablation CF of at least 15g and FTI of >400g would appear to be associated with a reduced risk of an ablation being in a reconnecting segment.

While histological lesion parameters are not available for clinical cases, work has been done using cardiac MRI to attempt to image ablation lesions. McGann et al., described a methodology for imaging LA scar using delayed enhancement MRI (DE-MRI) following pulmonary vein isolation, and the burden of LA scar they observed correlated with arrhythmia recurrence<sup>193</sup>. This group went on further to demonstrate that areas of DE-MRI enhancement correlate with areas of electrical scar ( $R^2=0.57$ ) and that DE-MRI imaging could be used to identify breaks in the pulmonary vein isolation lines<sup>194</sup>. In a blinded analysis using pre- and post-ablation MRI images, another group found that investigators were able to identify ablated LA myocardium in only 60% of cases, with a poor ability to distinguish ostial from circumferential ablation lesions<sup>195</sup>. This contrasts with another report in which ablated myocardium could be identified in 100% of cases on DE-MRI<sup>196</sup>. These findings suggest MRI may be useful in determining the sites of ablation lesions but the difference in the reported reliabilities may relate to the signal intensity thresholds being used to assign scar on MRI. To address this, recent work has correlated macroscopic scar volumes with DE-MRI imaging scar volumes in the right atria of 8 swine: based on this, DE-MRI signal intensity thresholds have been proposed which allow the best approximation of the macroscopic scar volume<sup>197</sup>.

Contact force parameters have been compared with MRI-imaged atrial scar by Sohns et al.<sup>188</sup>, Table 1.1. In this study of six patients, the FTI of ablation was correlated with DE-MRI scar. In order for this comparison to occur though, the FTI was not examined from the perspective of a single radiofrequency application, but in a subdivision of 1cm zones. Increasing FTI above 1,200g.s was associated with a

significant increase in the proportion of a 5mm<sup>2</sup> region of myocardium exhibiting DE-MRI scar (below this FTI value, the increase in the scar burden in that zone with an increase in FTI was small). This study therefore raises the possibility of using cardiac MRI to assess ablation efficacy clinically. The drawback here though is that the efficacy is being assessed at a MRI-zone level (albeit a small zone) rather than an individual radiofrequency application. This therefore relies on extremely accurate registration of each radiofrequency application between the electroanatomic navigation system and the MRI being used to judge scar. Moreover, this method is unable to account for any overlap in applications (for example through catheter drift even during a putative static application). It may be for these reasons that the threshold for effective ablation is much higher in this study compared with the other work presented in Table 1.1.

### **1.14 Conclusions and formulation of current studies**

The human left atrium is an important structure and the disruption of its normal function through the onset of the chaotic electrical activity associated with AF has important symptomatic and prognostic implications, and is becoming increasingly common at a population level. With the advent of contact force sensing catheter technology, as well as the detailed information available from electroanatomic mapping systems, it is possible to increase our knowledge of *in vivo* human left atrial mechanical and electrical behaviour. Moreover, catheter contact has been found to be an important determinant of radiofrequency ablation efficacy in preclinical studies<sup>161,164</sup>. The use of CF sensing catheters also allows us to assess the importance of catheter contact to clinical ablation. The initial goal of this thesis is to explore the effect catheter contact on the electrogram. Following on from this, it is hoped to investigate factors affecting

the contact between the catheter and the atrial myocardium, to examine the nature of catheter contact in more detail. The effects of catheter contact on ablation will also be studied..

The interaction between the catheter and myocardium results in a stretch stimulus and this may affect the measured electrical properties of the tissue as suggested by previous work<sup>122,130</sup>. Such an effect could impact on the targets identified for an ablation such as fractionated electrograms or regions with high dominant frequency. Aside from CF, an important component of catheter contact is the catheter's orientation, especially for bipolar electrograms<sup>141</sup>. Therefore, in Chapter 3, the impact of catheter contact on the electrogram is studied. The hypothesis for this experiment is that catheter CF (and the contact orientation) significantly affects the electrogram, including CFAE and spectral parameters. In the first instance, knowledge of the relationship between the atrial electrogram and CF has direct clinical utility as the data can be used to assess whether CF-sensing technology is necessary, or whether electrogram characteristics can be used as a surrogate for this. Whether the degree of contact between the catheter and myocardium causes clinically relevant changes in the fibrillatory electrogram is also assessed, based on the effect on automated CFAE analysis scores and the DF of the electrogram. In sinus rhythm, the relationship between catheter contact and the incidence of atrial ectopics is investigated.

In Chapter 6, the effects of different catheter delivery mechanism on catheter contact during ablation are examined. The hypothesis here is that as the mechanical properties of the technologies differ (principally the stiffness), this would affect the CF. The experiment also investigates CF distribution in different areas of the WACA lines, to characterise the interaction between the CF delivered, the technology used to deliver the catheter and the left atrial location. This regional assessment is further extended by

examining sites of immediate and delayed reconnection in the WACA lines. The aim here is to observe differences in the sites of reconnection between transseptal sheath technologies and to then compare this with differences in CF during ablation. With these data one would also hope to gain further insight into thresholds of CF necessary during ablation to reduce the risk of reconnection (in other words, give an indication of how to improve ablation efficacy).

While sites of reconnection in a WACA line and the CF delivered during the initial ablation of those sites can give important information regarding targets for ablation, the difficulty here is that the ability to correlate a site of reconnection with a particular ablation is limited. This is mainly because ablations in regions are generally overlapping, and it is challenging to know at what exact location a reconnection is present within an ablation line. In experiment 4, a different approach to this question is adopted. Here, rather than assessing the efficacy of ablation based on regional reconnections relating to regional ablations, other consequences of ablation are studied for individual, non-overlapping, static ablations: in this case the attenuation of the electrogram and the impedance drop from ablation. These indices are known to correlate with histological lesion parameters in preclinical studies<sup>166,189,190</sup> and so are used as surrogates for lesion parameters to gauge ablation efficacy. The hypothesis for this chapter is therefore that CF is a significant determinant of clinical ablation efficacy as judged by biophysical and electrogram parameters. Secondly, on the basis that a plateau in the change of the latter lesion surrogates with increasing levels of CF during ablation represents a plateau in lesion maturation, it is hypothesised that if such a plateau is observed, it is possible to establish target CF parameters for ablation.

The contact between the ablation catheter and myocardium can be described in terms of its magnitude but also its duration: both of these measures are incorporated in

the FTI and this would seem the optimum descriptor of catheter contact during ablation. An important question explored in Chapter 4 is whether the constituent parts of the FTI or the actual FTI achieved itself are more important to the efficacy of ablation. Previous work suggested 10g of contact force was necessary for effective ablation<sup>179</sup>: therefore the hypothesis here is that the mean CF is a significant determinant of the efficacy of ablation (more so than the FTI).

Chapter 5 builds on the work of the preceding chapters. The first part of the chapter examines the factors affecting the catheter's contact with the myocardium. Specifically this is an examination of the stability of contact in terms of CF and catheter location. These factors are studied not just in terms of the catheter delivery technology but also the atrial rhythm, LA location and catheter orientation. The interaction between the catheter and different parts of the atrium also gives important indicators as to the mechanical properties of the underlying atrial tissue.

In the second portion of Chapter 5, the impact of differences in catheter contact on the efficacy of ablation is assessed using the impedance drop with ablation as a surrogate of lesion parameters. As with Chapter 5, the assessment is at the single ablation level using static, non-overlapping ablations. The hypothesis explored here is that the efficacy of ablation would be affected more than just by the FTI but also other factors affecting the contact between the catheter and myocardium such as the atrial rhythm and location.

The overarching aim of the thesis is to explore the effect of catheter contact on left atrial electrical and mechanical properties as well as on the efficacy of ablation. The general hypothesis is that such relationships exist and are significant. If this is proven to be the case, then understanding the relationships may assist in the establishment of optimal target parameters for left atrial ablation and mapping. In so

doing, the aim is the optimisation of clinical AF ablation procedures in order to improve procedural success rates and safety.

## **2. Methods**

The specific methods used vary for each chapter are presented in detail separately. Prior to such discussion, points of commonality in the methods will be discussed.

### ***2.1 Study Institutions and Personnel***

In the case of all of the chapters other than Chapter 4, patients were exclusively recruited from St Bartholomew's Hospital, part of Bart Health NHS Trust, which serves a population of 2.5 million. For Chapter 6, patients who had procedures at a further two hospitals: London Bridge Hospital and the London Independent Hospital were also included. These two hospitals are private London hospitals, though the operators whose patients were included in the study are those based at St Bartholomew's Hospital. There are differences in the ethical approval under which the work in the different chapters was conducted.

- Chapter 3 involved assessment of the impact of changes in contact force on electrogram parameters in patients undergoing AF ablation. The study was approved by the institutional Cardiac Peer Review Committee and by National Research Ethics Committee London – West London (reference 11/LO/1861). The sponsor for the study was the Barts NHS Foundation Trust.
- Chapter 4 assessed ablation outcomes from an electrogram and impedance drop perspective with respect to the contact force during ablation for persistent AF. The work in this chapter was covered by the same ethics application as Chapter 3.

- Chapter 5 involved a detailed assessment of contact force characteristics in the left atrium and their impact on ablation efficacy. This work was also covered by the same ethics application as Chapter 3.
- Chapter 6 was a retrospective analysis of the effect of steerable sheath technology on the quality of ablation catheter contact during persistent AF ablation, as well as how this impacted on reconnection sites in pulmonary vein isolation lines acutely and at the time of repeat ablation procedures. As this was a retrospective analysis of anonymised data, formal ethical approval was not required.

All of the studies were conceived and designed by the author and Professor Richard Schilling. Co-investigators for the work were Drs Ross Hunter, Simon Sporton, Mehul Dhinoja Ling Liang-han and Mark Earley.

## **2.2 Patients**

The patients enrolled in the study all had their AF ablations performed on clinical grounds. In most cases this would mean they had failed at least one anti-arrhythmic drug. The exclusion criteria for enrolment in the research conducted were as follows:

- Inability or unwillingness to consent to enrolment
- Age <18 years
- Contraindication to anticoagulation or transoesophageal echocardiography
- Contraindications to AF ablation such as unresolved intracardiac thrombus

## **2.3 Cardiac Catheter Laboratory Setup**



Multiple systems are incorporated into the setup for AF ablation. During the procedure, the patient's vital signs are monitored (oxygen saturations through pulse oximetry and non-invasive blood pressure). Two different forms of anatomic visualisation system are



**Figure 2.1 Cardiac Catheter Laboratory Control Room at St Bartholomew's Hospital.** The haemodynamic monitoring system allows non-invasive systemic blood pressure and invasive pressures to be monitored. The electroanatomic mapping system (Carto3) and fluoroscopy screens as well as the electrogram recording system (LabSystem Pro) can all be monitored from the control room.

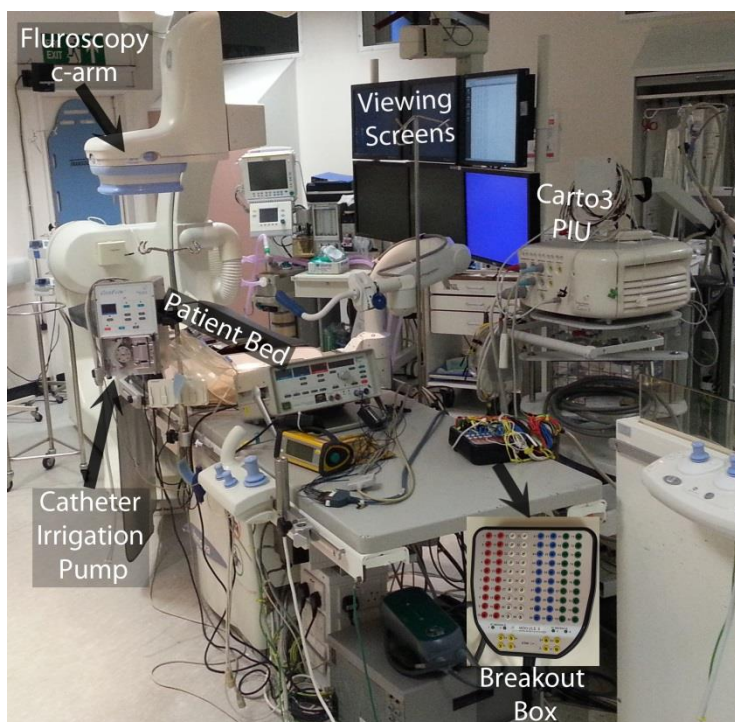


**Figure 2.2 Cardiac Catheter Laboratory at St Bartholomew's Hospital.** During a case, the viewing screens display the fluoroscopy, electroanatomic mapping, haemodynamic and electrogram data for the operator. The intracardiac electrical signals from the patient pass through the Carto3 Patient Information Unit (PIU) and are fed into the breakout box connector for LabSystem Pro.

utilised: fluoroscopic for radiographic visualisation (mainly to guide placement of the coronary sinus catheter and trans-septal puncture), and electroanatomic navigation systems for non-fluoroscopic visualisation (used to guide catheter manipulation during mapping and ablation). The surface ECG and intracardiac electrograms are recorded using an electrogram recording system. To allow for pacing and ablation, stimulator and ablation units are also included in the setup. Figures 2.1 and 2.2 illustrate the set up in the cardiac catheter laboratory control room and in the laboratory itself respectively at St Bartholomew’s Hospital.

## **2.4 Electroanatomic Navigation System**

In the case of all of the procedures in this thesis, the SmartTouch contact force sensing ablation catheter from Biosense Webster Inc. was used. This has been described in the introduction and incorporates with the Carto 3 electroanatomic navigation system from the same company.

**Table 2.1 Part of a Carto3 contact force data export for a point.** Index here refers to the measurement number for a point (so for contact force measurements which were sampled over a 10 second window at 20Hz, there would be 200 measurements).

Index	Reference time (ms)	Time (ms)	Force Value (g)	(Contact) Axial Angle (°)	(Contact) Lateral Angle (°)
1	-7485	4051675	11.5813	-175	68
2	-7435	4051725	14.2221	-179	65
3	-7385	4051775	15.133	-178	66
4	-7335	4051825	15.2849	-174	66
5	-7285	4051875	15.0851	-177	73
6	-7235	4051925	14.9851	-174	74
7	-7185	4051975	15.3761	-172	69
8	-7135	4052025	14.4308	-174	79
9	-7085	4052075	15.0131	-173	69
10	-7035	4052125	15.4966	-172	64

The Carto3 system uses a hybrid of magnetic location technology and current-based visualisation to localise catheters within the heart. The magnetic component uses a miniature passive magnetic field sensor which is incorporated in the distal element of the ablation catheter. A locator pad is placed beneath the patient and produces ultralow magnetic fields from three coils<sup>198</sup>. These fields decay with distance from the source. Based on the strength of each of these fields at the location of the sensor, the distance from each source coil in the location pad can be determined. Assessment of the *in vitro* and *in vivo* accuracy of the magnetic localisation has demonstrated that location measurements are highly reproducible with very little measurement error<sup>198</sup>. For current-based visualisation, two sets of reference patches are affixed to the front and back of the patient's thorax. The magnetic technology is complementary to the current-based technology, as the former is used to calibrate the latter, minimising distortions at the peripheries of electrical field<sup>199</sup>. The system generates a small current which goes from the electrodes of the catheters and is localised to the surface patches. Each electrode emits a different frequency of current which means they can be distinguished from one another. The strength of the current is measured for each electrode at each patch and using this information a current-ratio is produced for each electrode location, and by indexing this to the magnetic location data, the locations of the electrodes in three dimensional space are determined<sup>199</sup>.

The Carto3 system is capable of generating a data export file including the geometries collected, electrode locations, CF, electrogram and ablation biophysical data. The export consists of separate text files for each element for each point: typically over 3,500 separate files constitute each export. The CF data (magnitude and vector), is collected at 20Hz. For a mapping point the window of recording is 10 seconds (9.5

seconds retrospective to a point being acquired and 0.5 seconds prospective), while during ablation, CF data is stored throughout (Table 2.1).

In addition to this data, it is also possible to export location data for each

**Table 2.2 Part of a Carto3 location data export for a point.** The X, Y and Z co-ordinates for the position of the mapping catheter magnetic location sensor at each time point are given. Here the sensor number refers to the location sensor for the catheter.

Sensor#	Time (ms)	X	Y	Z
1	5	21.1298	25.9182	95.933
1	22	21.1636	25.8995	95.9143
1	39	21.1937	25.8778	95.8934
1	55	21.2396	25.8583	95.869
1	72	21.271	25.8464	95.8522
1	89	21.3109	25.8325	95.818
1	105	21.3504	25.814	95.7924
1	122	21.383	25.8042	95.772
1	139	21.4126	25.7965	95.7406

electrode as well as the passive magnetic sensors. This export is limited to 2.5 seconds (2 seconds retrospective to a point being acquired, 0.5 seconds prospective) and in this case the sampling rate is 60Hz (Table 2.2).

During ablation, as well as the CF data, the system also records biophysical data

**Table 2.3 Part of a Carto3 ablation biophysical data export.**

AblTime (ms)	Power (W)	Impedance ( $\Omega$ )	Distal Temperature ( $^{\circ}\text{C}$ )	Proximal Temperature ( $^{\circ}\text{C}$ )
8215324	0	164	37	0
8215418	2	163	37	0
8215518	2	166	37	0
8215618	2	167	37	0
8215718	2	166	37	0
8215818	2	167	37	0
8215918	2	168	37	0
8216018	2	169	37	0
8216118	4	168	36	0

including the catheter tip temperature, ablation power and the impedance - all sampled at 10Hz (Table 2.3).

The Carto3 system is also able to record electrogram data. Incorporated in this is an automated CFAE grading system. The basis for this system is the identification of deflections in the fibrillatory electrogram and certain criteria are set for a deflection to fulfil, otherwise it is discounted as noise. To be counted as a deflection, its width must fall within a certain range (15-30ms are default settings). There is also a range of deflection amplitudes that must be fulfilled (0.05-0.15mV by default). Based on the identified deflections, the system then generates three different scores:

- The interval confidence level (ICL) counts the number of intervals between deflections falling within a range (70-120ms is suggested).
- The average complex interval (ACI) is the mean time interval between deflections (within a specified range).
- The shortest complex interval (SCI) is the shortest interval between deflections falling within the specified range.

The automated CFAE analysis scores are not part of the general Carto3 data export and therefore had to be taken from the point log for each study. This was performed by acquiring image files for each point log manually and then using optical character recognition software (ABBYY FineReader 11, ABBYY, Moscow, Russia), the data from the image files were then extracted for further analysis.

## **2.5 Electrogram Recording System**

A limitation of the Carto3 electrogram recordings is that the recording window is limited to 2.5 seconds. Therefore, the electrogram data used in the current study were taken from LabSystem Pro (Bard Electrophysiology Division). This system continuously records the electrograms and allows the required data to be manually exported for analysis. For each contact force mapping point therefore, the corresponding electrogram data were exported from LabSystem Pro (the Carto3 electrogram export was not used in view of the 2.5 second limitation in its duration).

The LabSystem Pro electrogram export values are exported in a raw unit-less decimal number representing a signed 16-bit analogue-to-digital converter (ADC) value where the iso-electric point or zero potential is “0”.

The numeric limits of the 16-bit value are: 32,767 to -32,768. As the Clearsign ADC hardware that is part of the system measures to the saturation point, the full binary value in the positive range is 32,768. Therefore, the equation for the conversion to millivolts used was:

$$[\text{mV}] = [\text{ADC value}] * [\text{Range in mV}] / 32768$$

Here the “Range” value represents the positive range of the amplifier and was given as part of the LabSystem Pro electrogram output for each point.

In order to be able to export the required electrogram duration for a point, the LabSystem Pro Registry file had to be edited to adjust the export window. Each electrogram was manually exported and the data in the resulting text files subsequently converted to mV using the above equation.

## ***2.6 Co-ordinating Electroanatomic Mapping and Electrogram Recording Systems***

For the purposes of Chapters 4-6, it was necessary to acquire data from Carto3 and LabSystem Pro simultaneously. This was either to be able to compare contact force and electrogram data (Chapter 6) or post-ablation and pre-ablation mapping point electrogram data (Chapters 4 and 5). For a minority of the cases, the LabLink data interface (Bard Electrophysiology Division) was available. This allows automated, simultaneous, acquisition of data by both systems. Where this system was not available though, a methodology was sought to co-ordinate the two systems. As all of the data collected by both systems has a time stamp, one possibility was to co-ordinate based on the system time stamps.

To assess the reliability of the co-ordination between the time logs of the two systems, in 3 patients the time stamps for points simultaneously acquired manually (by a single researcher pressing the acquisition buttons on both systems) were compared. As a further comparison, the time stamps were compared for a further 4 patients for points simultaneously acquired using the LabLink interface. The hypothesis here was that if the time stamps between the two systems remained comparable throughout the case, then any difference between the two systems' time stamps at baseline should remain constant throughout the procedure. Therefore in all cases, the gap between timestamps was also referenced to the difference in time at baseline.

## Results

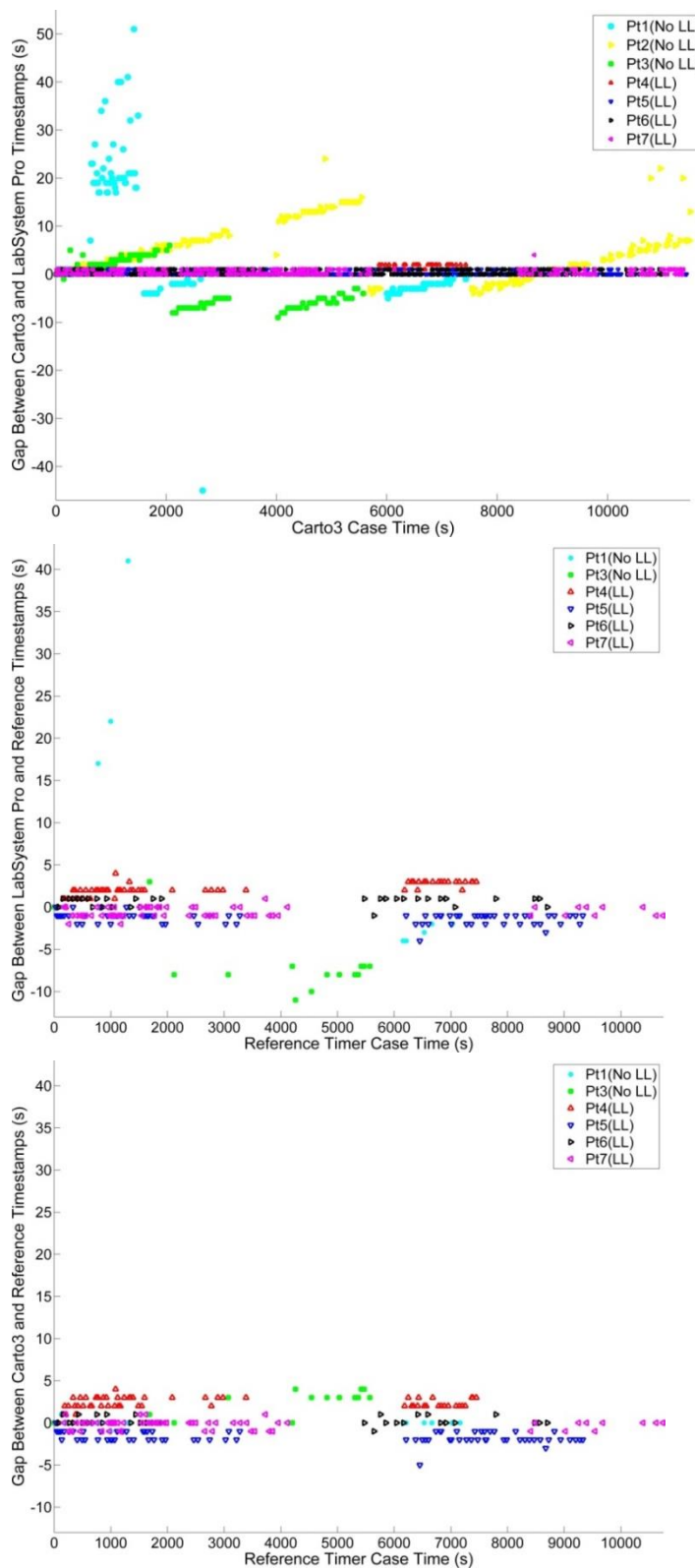


**Figure 2.3 Comparison of timestamps of Carto3 and LabSystem Pro for simultaneously acquired points.**

Top – the gap between the timestamps for the two systems varies over the course of each procedure in the non-LabLink cases.

Middle – Comparing the gap between the time stamps for LabSystem Pro against a reference timer, one can see that the gap varies without LabLink but varies very little when LabLink is used.

Bottom – When the Carto3 timestamps are compared to the reference timer, there is very little variation in the time logs, regardless of LabLink use.

LL=LabLink



The results of this analysis are presented in Figure 2.3 (upper panel). As can be seen, during the course of a procedure there is a varying gap between the two time stamps, with a greater difference for the non-LabLink rather than LabLink cases (median(range): 2 (-45-51)s versus 0(0-4)s respectively,  $p < 0.0005$ ).

Based on these data, it was unclear whether the problem was with the time log for either or both systems, and consequently in which system the LabLink interface was improving the timestamp consistency. Therefore in 6 of the cases, an external reference timer was used and the time on this recorded when points were taken on the two systems. As can be seen in Figure 2.3 (middle panel), this analysis suggests the issue is with the LabSystem Pro internal timer drifting during the procedure and that the addition of the LabLink software rectifies this problem (-4(-11 41)s versus 0(-4-4)s respectively,  $p < 0.0005$ ). The Carto3 timestamp was unaffected by the presence or absence of the LabLink interface (Figure 2.3, lower panel).

## **Conclusion**

The LabSystem Pro timer drifts during the case unless used with LabLink. These findings were confirmed by the manufacturer of LabSystem Pro and are under investigation. For the purposes of the experiments in this these, where LabLink was not available, synchronicity of the two systems was ensured by manually acquiring study data points simultaneously in both systems (as the time-logs from the two systems could not be relied upon to do this).

## **2.7 Data Analysis**

The analysis of the data in all of the studies was performed using custom written scripts in the Matlab (MathWorks, MA, USA) programming environment. These scripts were

written for the purposes of this research from the ground up by the thesis author.

Aspects of this analysis that were shared between experiments are explained in more detail here, while analyses used which were unique to a particular experiment are detailed in the relevant chapters.

In the case of all of the experiments, CF data were processed in order to determine the mean contact force and FTI. The latter is the area under the force/time curve. This was determined by the process of dividing the waveform into a series of trapezoids, establishing the area of each of these and then summing them to give the

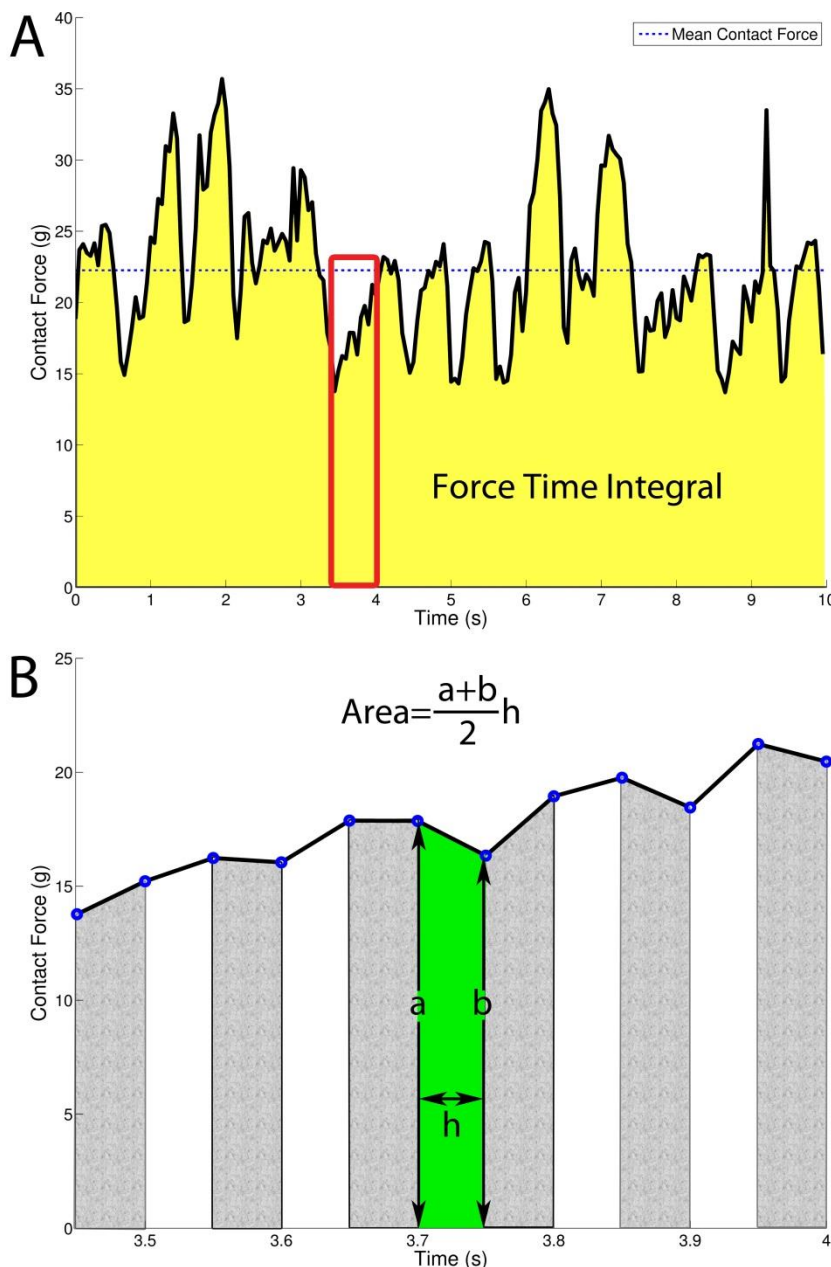


**Figure 2.4 Trapezoid integration of a contact force waveform.** (A) Contact force waveform over 10 seconds (black solid line) with mean contact force displayed as a dotted line. The shaded area under the curve is the force time integral. The portion of the waveform boxed in red is shown in more detail in (B). In (B), each contact force measurement is displayed as a blue circle. The trapezoids making up the waveform area are highlighted. The formula to establish the area of one trapezoid is displayed. Summating the areas for each of the trapezoids under the curve will give the area under the curve which is the force time integral.

FTI for the waveform (trapezoidal integration, Figure 2.4). The advantage to this approach is that it only uses the data collected (essentially a series of trapezoids) and makes no assumptions regarding the nature of the waveform between measurements.

Experiments 4 and 5 analysed impedance drop over the course of static ablations. Impedance was sampled at 10Hz and the waveforms produced were found to suffer from a lot of noise. In order to remove this noise, to appreciate better the change in impedance over the course of the ablation, the waveform was filtered using a Savitzky-Golay filter (Figure 2.5). This is a digital least squares smoothing filter, described by Savitzky and Golay in 1964<sup>200</sup>, applied with the intention of increasing the signal-to-noise ratio without excessively distorting the waveform.

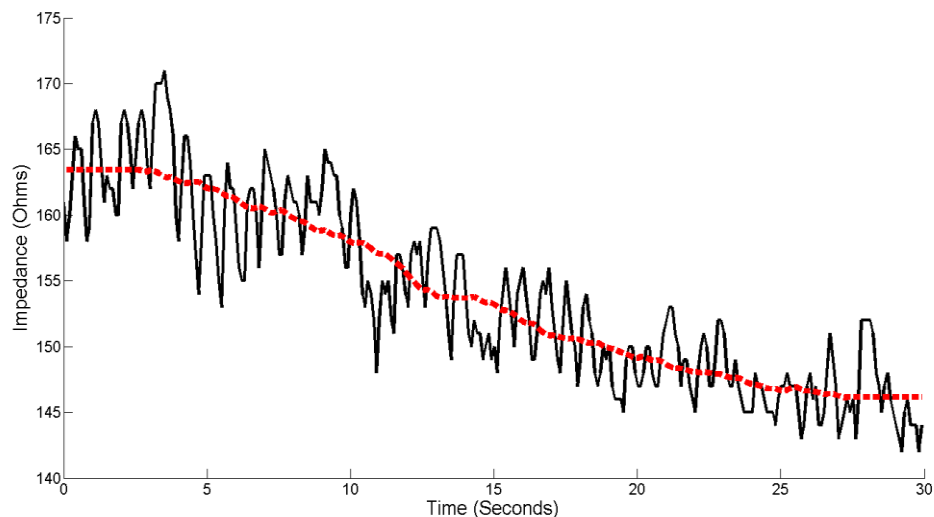


**Figure 2.5 Impedance waveform.** Impedance measurements sampled at 10Hz, recorded for a 30 second ablation. The black line is the original data while the broken red line is the filtered waveform.

To assess the effect of the FTI of ablation on the impedance, an incremental analysis was performed in experiments 4 and 5 (Figure 2.6). All ablations were divided into consecutive, cumulative, 10g.s FTI intervals. Using the filtered impedance waveforms, the maximum impedance drop was then compared with the initial impedance at the ablation's start. Consequently, a 600g.s ablation yielded 60

incremental measurements, with the maximum impedance drop assessed from 0-10g.s, 0-20g.s and so on up to 0-600g.s.

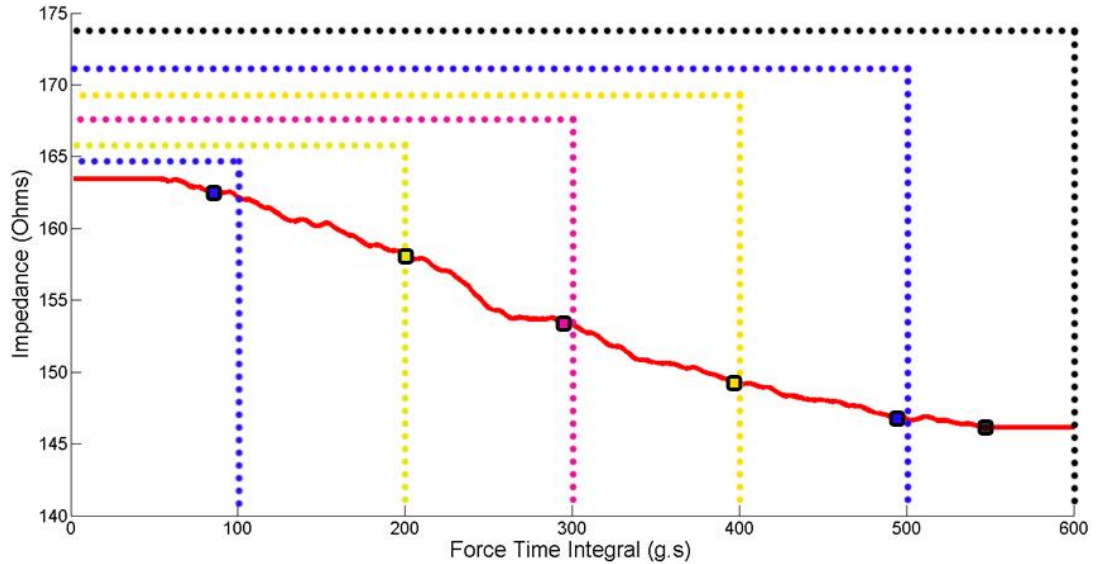


**Figure 2.6 Incremental FTI analysis.** The impedance curve for a single static ablation is presented with the ablation FTI rather than time on the x-axis. The ablation is then split into FTI segments. Here a 100g.s increment is used. The different coloured dotted lines highlight the area within which the impedance curve is being analysed for each increment, the first (blue) is 0-100g.s while the last (black) is 0-600g.s. Within each subdivision, the minimum impedance value is then found (highlighted by the coloured squares). The percentage impedance drop is then derived for each increment to allow comparisons to be drawn regarding the change in impedance over the course of the ablation.

Where mapping points were acquired (in the experiments in chapters 3 and 5), 8 seconds of data were analysed. This was despite the catheter being held at a location for 10 seconds. The reason for this was that the first and last second of the latter period were discarded to ensure the catheter was stable for the data collection.

For the experiments detailed in chapters 3 to 6, the requirement was for scripts that were capable of identifying and measuring complexes within an electrogram.

The first step was converting the raw ADC electrogram data exported by LabSystem Pro into mV, using the equation detailed in the previous section. The

electrograms analysed in this study were bipolar electrograms (set up between the distal adjacent electrodes on the ablation catheter). Signals in the electrogram recording system were recorded at a low cut-off of 30Hz and a high cut-off of 250Hz. The peaks and troughs in the signal were identified using a 70ms cut off prevent double counting of complexes<sup>98</sup>. Complexes less than 0.05mV (peak to trough) were assigned as noise<sup>201</sup>.

The angles of the rising and falling signal were determined for the dominant peak or trough in a complex, from a point at one-third of the complex size from the peak or trough of the signal. A correction factor for angle measurements was used to make the signal equivalent to that displayed on LabSystem Pro at a sweep speed of 100mm/s and a 32x scale. The reason a correction factor was needed is because the sharpness of the waveform is affected by the ratio of the two axes displayed. Therefore if the y-axis

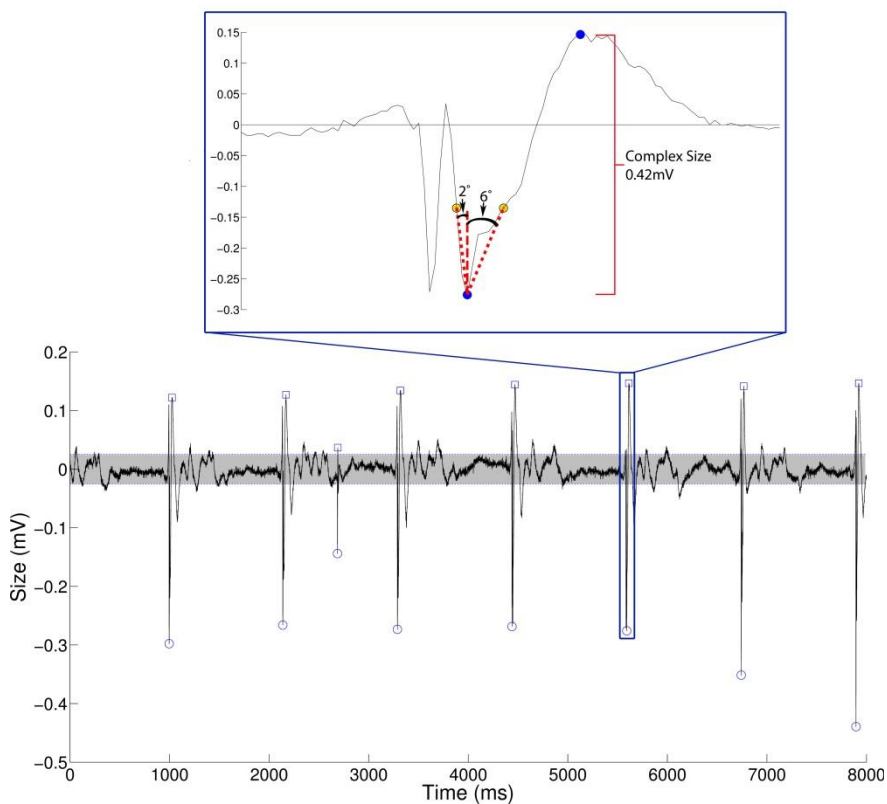


**Figure 2.7 Electrogram analysis.** Shaded area is 0.05mV noise window. Empty circles are dominant deflections in the complex, empty squares are the opposite extent of the measured complex. Inset figure is a zoomed in view of the complex highlighted in blue. Shaded circles here are points between which the complex size is measured. Angles shown are the falling and rising angles to the points 1/3 the height of the complex from the dominant deflection (yellow circles).

was kept unchanged but half as much of the x-axis displayed on the same screen, the

electrograms would be stretched out and appear less sharp. This is analogous to increasing the sweep speed of the electrograms displayed. Similarly, increasing the scale of the signal also affects the displayed signal sharpness. As judgements regarding the sharpness of signals are based on assessing the signals at a fixed sweep speed and fixed scale, a correction factor was needed to make the results of the angle analysis analogous to what is observed clinically.

The complex size was measured from the dominant peak to trough of a complex. The electrogram amplitude was then defined as the mean amplitude of these complexes (Figure 2.7).

# 3. The Impact of Catheter Contact Force on Human Left Atrial Electrogram Characteristics in Sinus Rhythm and Atrial Fibrillation

## 3.1 Abstract

**Background:** During LA mapping, optimal contact parameters minimizing variation secondary to catheter contact are not established.

**Methods and Results:** Across 30 patients undergoing first-time ablation for AF, 1,965 stable mapping points (1,409 AF, 556 SR), comprising 8s of CF and bipolar electrogram data were analysed. Points were taken in groups at locations with CF or catheter orientation actively changed between acquisitions. There was no correlation between CF and electrogram complex size (Spearman's rho  $p > 0.3$ , both rhythms). Complexes were less positive at higher CF (Pearson's correlation  $-0.2$ ,  $p < 0.005$ , both rhythms). Increasing CF at a location significantly increased complex size, but only where the initial CF was  $< 10\text{g}$ , and if the change was  $\geq 4.5\text{g}$  in SR and  $\geq 8\text{g}$  in AF ( $p < 0.0005$ , both). Atrial ectopics during SR were observed more frequently when CF was  $\geq 10\text{g}$  ( $p < 0.0005$ ). Increasing CF at a location was associated with an increase in the CFAE interval confidence level score, but only if the initial CF was  $< 10\text{g}$  and CF increased  $\geq 8\text{g}$  ( $p = 0.003$ ). The DF and organisation index (OI) were unaffected by CF ( $p > 0.1$  for both). Changing the catheter orientation from perpendicular to parallel was associated with smaller, more positive complexes ( $p = 0.001$  for both), but no change in CFAE scores, DF or OI ( $p > 0.08$  for each).

**Conclusions:** During LA mapping, including CFAE but not spectral parameter mapping, CF and catheter orientation influence results: consequently, mapping CFs should be  $\geq 10\text{g}$  to negate the influence of CF.

### **3.2 Introduction**

Global atrial stretch alters the electrical properties of the human atrium<sup>122,202</sup>, and human ventricular myocytes *in vitro* demonstrate stretch-induced depolarisations and extrasystoles<sup>130</sup>. During mapping of the atrium, the CF applied by the mapping catheter may affect the measured electrical properties of the LA by affecting the physical relationship between the electrodes and tissue (affecting electrogram measurement) and by applying a local stretch stimulus to the myocardium (affecting the underlying substrate). In this context, the optimal contact characteristics minimizing such effects, if apparent, are undetermined.

As part of the ablation procedure for persistent AF, CFAE have been targeted with varying success<sup>79,203</sup>. Assessment of the electrogram is clearly a pivotal part of CFAE ablation but, until recently, data regarding CF have not been available and hence the impact of this on CFAE parameters unexplored. Data from spectral analysis of electrograms to guide ablation<sup>101,204</sup> may also be of utility, but the effect of catheter contact on these measurements is similarly unknown. In man, a higher CF is weakly correlated with increasing electrogram amplitude in the LA<sup>187,205</sup> and left ventricle<sup>140</sup>. In porcine studies, the orientation of the catheter also impacts on the bipolar electrogram morphology observed<sup>141</sup>. The effect of changing catheter contact on electrogram parameters at a fixed location has not previously been investigated.

In this study we investigated the relationship between a change in CF and catheter orientation on LA electrogram characteristics, atrial ectopic burden, CFAE and spectral analysis parameters in SR and AF, to try to determine if there is an optimal CF for mapping to minimise any evident changes.



### **3.3 Methods**

All participants gave informed consent to participate in the study. The study had ethical approval from the UK National Research Ethics Service. Consecutive patients with persistent AF or PAF undergoing their first ablation were enrolled. Procedures were performed with patients under moderate ('conscious') sedation. CF was measured at 20Hz using a Thermocool SmartTouch catheter (Biosense Webster Inc., Diamond Bar, CA, USA).

Mapping points were prospectively taken at evenly spaced LA locations. No ablation was performed in these regions until mapping was completed. At each location, three to four 8s recordings of CF and electrograms were taken with the catheter in a stable location, with a minimum CF of 1g. At alternate locations, the CF was deliberately changed by the operator for the second two readings (data being collected once the catheter was stable at the new CF). In a subset of locations, the orientation of the catheter (the catheter itself rather than the contact orientation) was changed from perpendicular to parallel and a further two 8s readings taken.

The Carto3 electroanatomic mapping system (Biosense Webster Inc.) recorded CF and location data. Electrograms were recorded simultaneously using LabSystem Pro (Bard Electrophysiology Division, Lowell, MA, USA). Synchronicity between CF and electrogram measurements was ensured by manually taking points at the same time or through the LabLink LabSystem Pro module (Bard Electrophysiology Division), which synchronizes the two systems.

Catheter tip and electrode location data were recorded over a 2.5s window for each point, sampled at 60Hz. Catheter tip displacement was referenced to the averaged location of the 20 electrode poles of a circular PV catheter, positioned in a PV (to account for movement secondary to respiration). Displacement >7mm (over twice the

length of the catheter tip electrode) between points excluded that pair from the paired analysis, as did the presence of more than a single atrial ectopic in SR.

Electrograms analysed were bipolar and filtered at 30-250Hz. In SR, the incidence of atrial ectopics was determined for each 8s electrogram on visual review of the surface ECG and intracardiac bipolar and unipolar (referenced to an indifferent electrode in the inferior vena cava) signals.

Electrogram data were processed and analysed using custom written Matlab

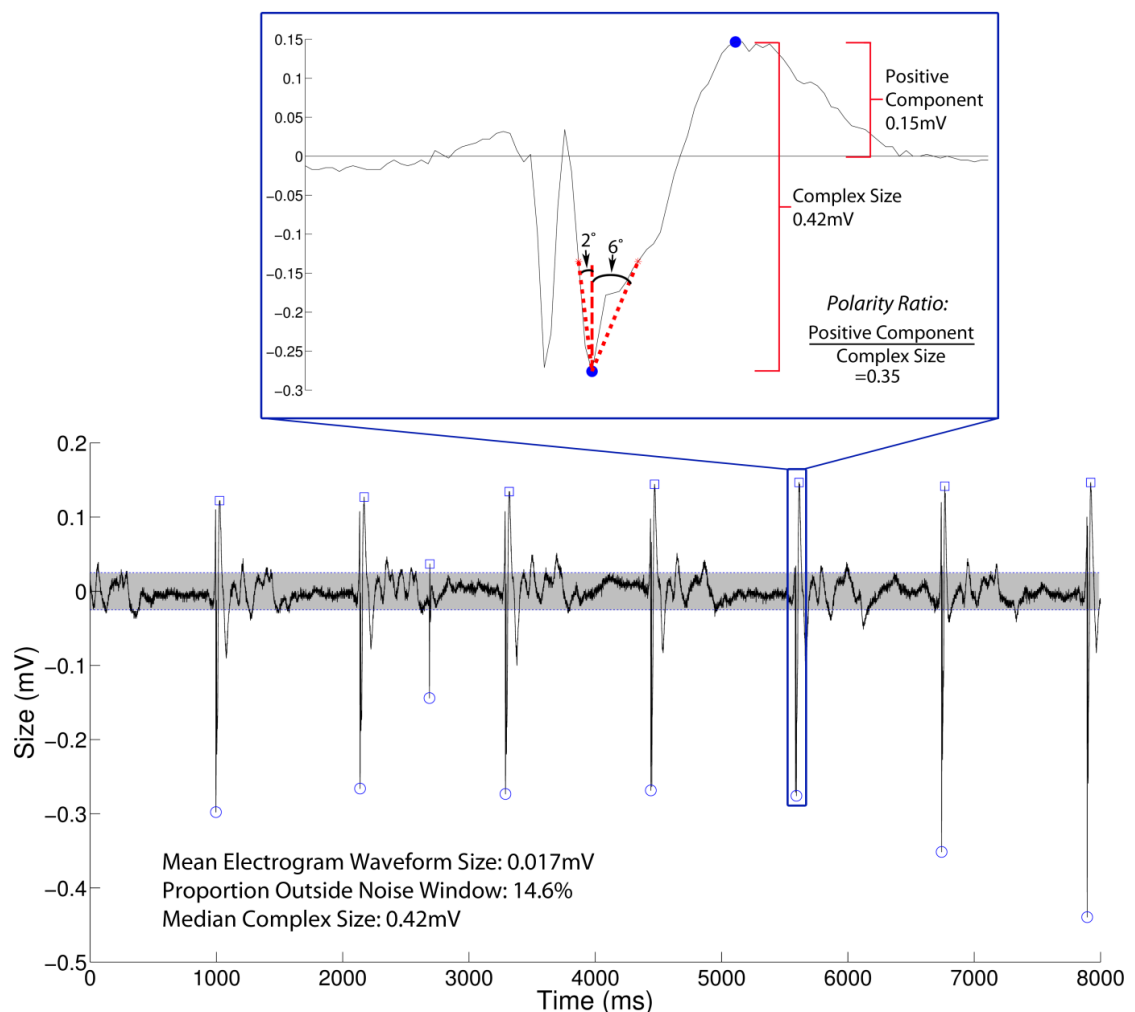


**Figure 3.1 Electrogram analysis.** Shaded area is 0.05mV noise window. Empty circles are dominant deflections in the complex, empty squares are the opposite extent of the measured complex. Inset figure is a zoomed in view of the complex highlighted in blue. Shaded circles here are points between which the complex size is measured. Angles shown are the falling and rising angles to the points 1/3 the height of the complex from the dominant deflection (red broken lines). *Modified from Figure 2.7, page 81.*

scripts (MathWorks, Natick, MA, USA).

The peaks and troughs in the signal were identified using a 70ms cut off to prevent double counting of complexes<sup>98</sup>. Electrogram complex size was measured from the dominant peak to trough of a complex using previously described methods<sup>206</sup>, and averaged for the signal, Figure 3.1.

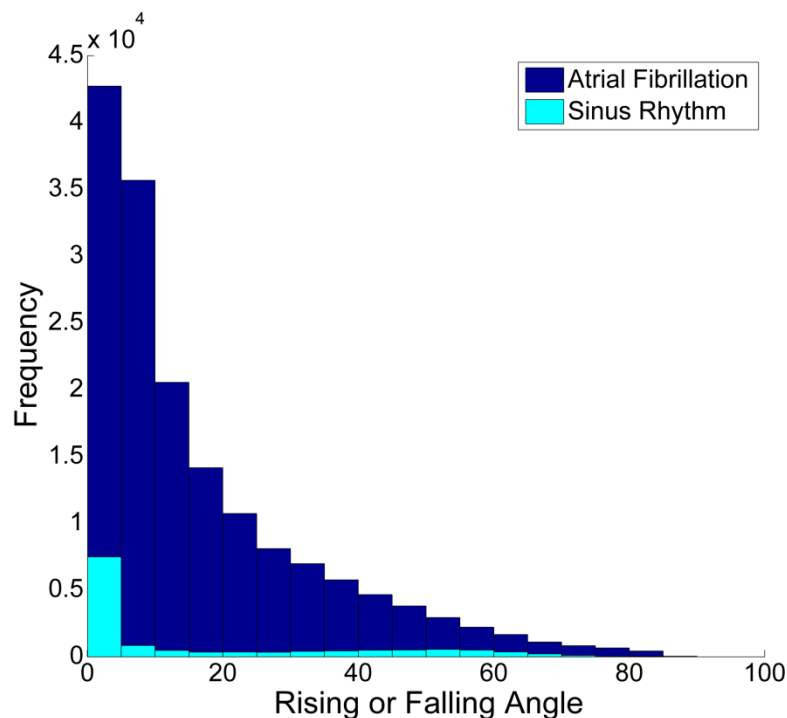


**Figure 3.2 Histogram of the rising or falling angle for all of the complexes identified** (based on deflection size and activation time criteria). The x-axis here is the rising or falling angle of the dominant deflection in a complex – the former where the dominant deflection is positive and *vice versa*. The y-axis is the number of such dominant deflection angles observed. A greater number of complexes were identified in the atrial fibrillation cases, hence the larger numbers in the atrial fibrillation chart.

Complexes  $<0.05\text{mV}$  (peak to trough) were assigned as noise<sup>201</sup>. The angles of the rising and falling signal were determined for the dominant deflection in a complex, from a point at one-third of the complex size from the dominant peak or trough. A correction factor for angle measurements was used to make the signal equivalent to that displayed on LabSystem Pro at a sweep speed of 100mm/s at 32x scale. A total of

89,105 complexes were identified based on the complex size and 70ms double counting cut off. Histograms constructed demonstrated the majority of complexes had a rising or falling angle  $\leq 15^\circ$  (with the difference more pronounced in the SR signals), Figure 3.2. For the data as a whole, 60% of the rising or falling angles in the complexes were  $\leq 15^\circ$ . This value was taken as the farfield cut off: complexes with a rising or falling angle  $> 15^\circ$  were therefore excluded. Points with no identifiable complexes based on the above criteria were excluded from further analysis (other than the automated CFAE score analysis).

The polarity ratio was determined by the ratio of the positive deflection in a complex to the total complex size. These values were then averaged for a signal to give the mean polarity ratio. To determine the non-noise level in the signal, the proportion of the total waveform outside a 0.05mV window centred at 0mV was determined.

DF analysis was performed for the AF points using previously described methods to pre-process the electrograms<sup>95,207</sup>: the signal was bandpass filtered at 40-250Hz, rectified and lowpass filtered at 20Hz. A Hanning window was then applied to the signal. Following this, an 8,192 point fast Fourier transform (FFT) was performed on the signal and the DF determined as the largest peak from 3 to 15 Hz<sup>101</sup>. The organization index (OI) was determined from the ratio of the area under the DF peak and its (up to 3) harmonic peaks compared with the area under the power spectrum<sup>204,207</sup>. A 4,096 point FFT was performed over a 4 second sliding window every second on the processed 8s signal<sup>208</sup>. The OI for each 8s signal was then derived from the mean of the values for each window. High DF points were taken as those where the DF was  $\geq 20\%$  the mean DF for that patient<sup>104</sup>.

Automated CFAE analysis was performed at each point for the persistent AF patients using the Carto3 system with intervals of interest between deflections specified

as a minimum of 70ms, maximum of 120ms and voltage thresholds left at factory settings (0.05- 0.15mV)<sup>98</sup>. In this analysis, the SCI is the shortest interval between electrogram deflections falling within this range, the ACI is the average duration of all intervals falling within this range, and the ICL is the number of intervals within this range. High-grade CFAE were designated as those with an ICL  $\geq 7$  based on previous validation work comparing automated CFAE measurements with the degree of visually assessed fractionation of the electrogram<sup>98</sup>. As the CFAE analysis is conducted over a 2.5s window, where CF was compared with CFAE scores, the CF data for the same 2.5s period (rather than the whole 8s of data collected at a point) was used.

### **3.3.1 Statistics**

Statistical analysis was performed using SPSS (IBM SPSS Statistics, Version 20 IBM Corp, Armonk, NY, USA) and Matlab V7.12 with Statistics Toolbox V7.5. A p-value of  $<0.05$  was taken to indicate statistical significance. Correlations were assessed using a Pearson's correlation where the relationship appeared linear and a Spearman's rank correlation otherwise. Point-Biserial correlation was used to correlate continuous with binary variables. Normally-distributed data were analysed using a t-test or ANOVA and non-normally-distributed data analysed using a Mann-Whitney U test or Kruskal-Wallis test. Paired data were analysed using a paired t-test or Wilcoxon signed-rank test. Data are presented as mean $\pm$ standard deviation or median [interquartile range].

## **3.4 Results**

The baseline characteristics of the study patients are presented in Table 3.1.

**Table 3.1 Study Population Baseline Characteristics**

Number of Patients	30
Age, mean±SD	61±8 years
Gender	21 Male (70%)
Persistent AF	15 (50%)
Duration of Persistent AF	20±12 months
CHA <sub>2</sub> DS <sub>2</sub> -VAsc Score, mean±SD	1.4±1.0
Left Atrial Diameter, mean±SD	4.4±0.6cm
Severe Left Ventricular Impairment (Ejection Fraction<35%)	2 (7%)

### 3.4.1 Contact Force and the Electrogram

1,945 data points were collected (1,396 in AF, 549 in SR), and the spread of CFs is shown in Figure 3.3.

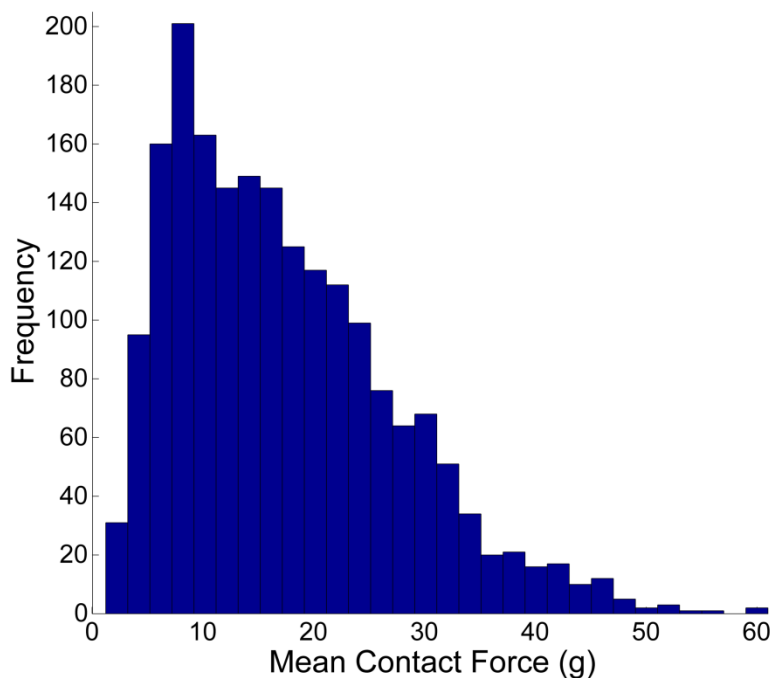


**Figure 3.3 Histogram of mean CF of the study points.**

For both SR and AF points, there was a weak correlation between the CF and mean electrogram waveform amplitude (Spearman's  $\rho$  0.19 and 0.13 respectively,  $p < 0.005$  for both) as well as the amount of the waveform outside the 0.05mV noise

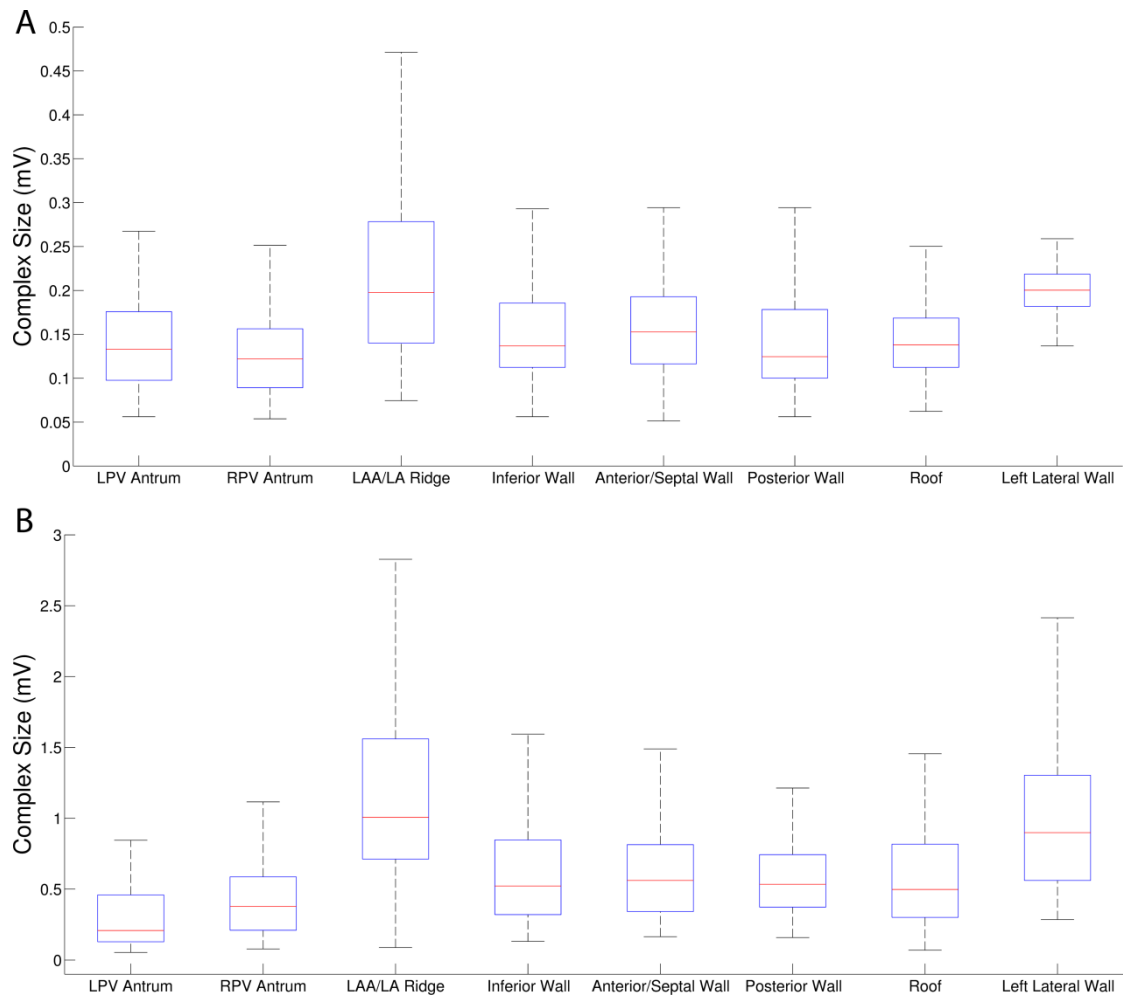


**Figure 3.4 Complex size versus left atrial location in (A) AF and (B) SR.**  
 LPV=Left pulmonary vein; RPV=Right pulmonary vein; LAA=Left atrial appendage

window (Spearman's  $\rho$  0.21 and 0.18 respectively,  $p < 0.005$  for both). To determine if the size of the complexes in the waveform (rather than just the waveform as a whole) was related to the CF, the individual complexes in the signals were identified and measured using automated analysis. 44,888 complexes were analysed across all the data points: there were a median of 29 [18-41] complexes per 8s data point in AF and 8

[7-9] in SR. In this case, there was no significant correlation between the CF and electrogram complex size in either rhythm (Spearman's  $\rho$   $p > 0.2$  for both).

There was a significant difference by location for both AF and SR points in complex size ( $p < 0.005$  for each, Figure 3.4). There was a correlation between the polarity ratio of the complexes observed and the CF in AF and SR (Pearson's correlation  $-0.2$ ,  $p < 0.005$  for both), such that the complexes became proportionately less positive at higher CF.

To assess whether changing the CF at a location was associated with a change in electrogram parameters, the data were analysed in pairs for points taken at the same location. There were 2,515 pairs of CF/electrogram readings (2,117 in AF, 398 in SR).

As shown in Table 3.2, if the starting CF was  $< 10g$ , the difference between a

**Table 3.2 Change in mean complex size by atrial rhythm, initial CF and increase in CF between pairs of measurements at a location.**

Rhythm	Initial CF in a pair	Increase in CF between paired measurements							
		$< 4.5g$ SR and $< 8g$ AF				$\geq 4.5g$ SR and $\geq 8g$ AF			
		Change in Mean CF (g)	Median Change in complex size (%)	Number of pairs	p	Change in Mean CF (g)	Median Change in complex size (%)	Number of pairs	p
SR	1-10g	0.8 [0.4-3.1]	6 [-8 – 34]	81	0.06	10.9 [7.1-16.8]*	13 [-16 – 60]	181	$< 0.005$
	$\geq 10g$	1.7 [0.8-3.1]	3 [-8 – 22]	51	0.28	10.8 [7.8-15.3]*	-0.3 [-29 – 26]	85	0.43
AF	1-10g	1.8 [0.7-4.4]	0 [-12 – 16]	466	0.28	14.3 [10.9-21.7]~	6 [-11 – 41]	223	$< 0.005$
	$\geq 10g$	2.1 [0.9-4.5]	2 [-13 – 18]	965	0.09	13.2 [10-19.4]~	0 [-16 – 24]	463	0.12

pair of electrograms was only significant if the increase in CF between measurements was  $> 4.5g$  in SR, but not if the change in CF was below this. If the starting CF was  $\geq 10g$ , there was no significant change between pairs, even if the change in CF was  $> 4.5g$ . In AF, a similar relationship was found, though in this case, the electrogram



only changed significantly at a location when the initial CF was <10g and the change in CF was >8g and not if the change in CF was below this. In the case of both rhythms, the difference in the response to an increase in CF when the initial CF was <10g rather than  $\geq 10$ g was not explained by a lesser overall increase in the CF in the latter group between measurements as the increase in CF was not significantly different between groups – in other words, there was a similar increment in the CF between measurements in the <10g and >10g initial CF groups.

The likelihood of observing at least one atrial ectopic in SR during the 8s electrogram window significantly increased with the mean CF, Figure 3.5, with a

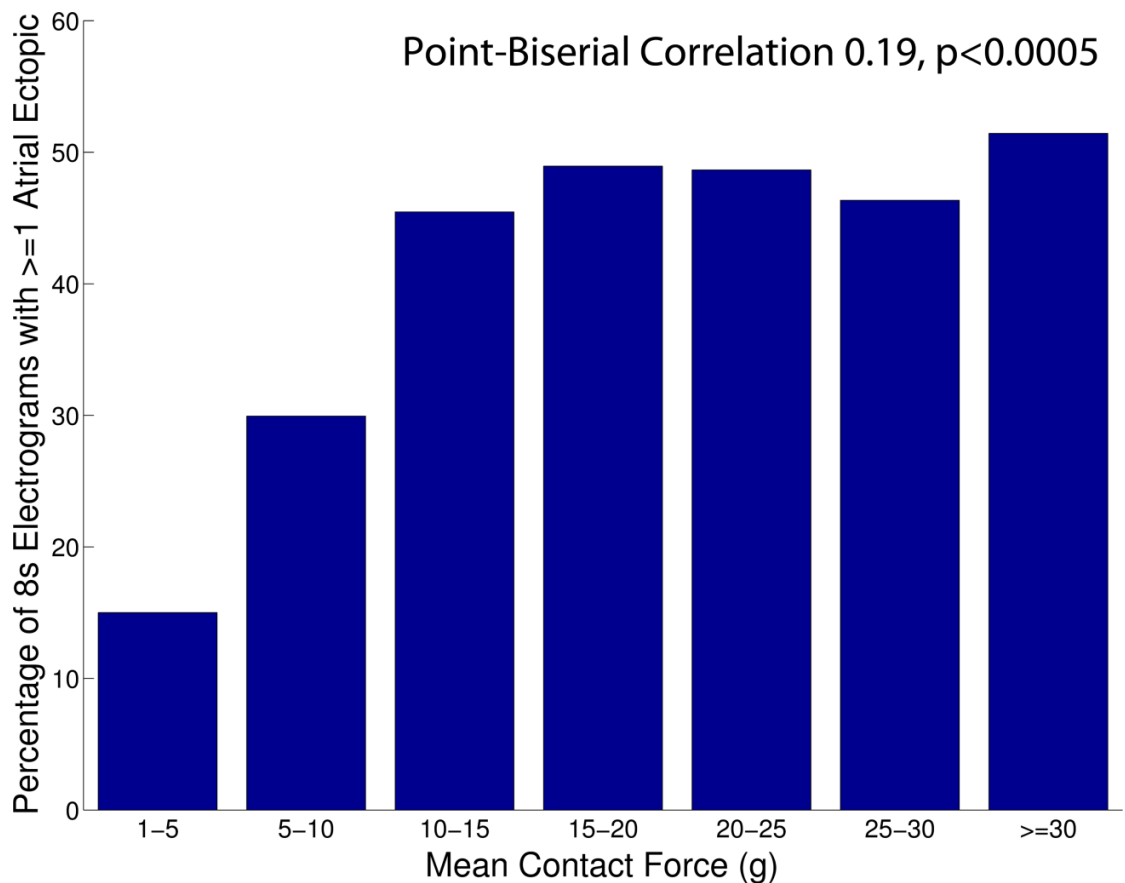


**Figure 3.5 Percentage of 8s SR electrograms with  $\geq 1$  atrial ectopic observed versus mean CF.**

significantly higher incidence of at least one ectopic if the CF was  $\geq 10$ g compared with <10g ( $p < 0.0005$ ). On sub-analysis by location, the correlation between the CF and

observation of at least one atrial ectopic was strongest at the inferior LA (Point-Biserial correlation 0.35,  $p=0.006$ ).

There was a weak positive correlation between the change in CF between points at a location and the change in the number of complexes observed in AF, but only if the starting CF was  $<10g$  (Spearman's  $\rho$  0.11  $p=0.003$ ), and not if it was  $\geq 10g$  (Spearman's  $\rho$   $p=0.05$ ).

### 3.4.2 Contact Force and CFAE

**Table 3.3 Change in CFAE and spectral analysis measurements at a location by initial CF and increase in CF between pairs of measurements at a location.**

Measure	Initial CF in a pair	Increase in CF between paired measurements							
		$<8g$				$\geq 8g$			
		Initial Value	Repeat Value	Number of pairs	p	Initial Value	Repeat Value	Number of pairs	p
ICL	1-10g	5 [3-7]	5 [3-7]	573	0.83	4 [2-6]	5 [3-7]	256	0.003
	$\geq 10g$	5 [3-7]	5 [3-7]	945	0.62	5 [2-7]	5 [3-7]	488	0.4
SCI	1-10g	77 [73-87]	76 [72-86]	573	0.3	78 [73-88]	76 [72-85]	256	0.16
	$\geq 10g$	76 [72-84]	75 [72-83]	945	0.57	76 [72-83]	76 [72-84]	488	0.2
ACI	1-10g	93 [88-100]	92 [87-99]	573	0.43	93 [88-101]	93 [88-99]	256	0.42
	$\geq 10g$	92 [87-98]	92 [85-98]	945	0.65	91 [85-98]	92 [87-98]	488	0.16
DF	1-10g	6 [5.5-6.6] Hz	6 [5.5-6.7] Hz	466	0.88	6 [5.4-6.6] Hz	6 [5.5-6.7] Hz	223	0.11
	$\geq 10g$	6 [5.4-6.7] Hz	6 [5.2-6.6] Hz	965	0.14	5.6 [5-6.5] Hz	5.7 [5-6.3] Hz	463	0.83
OI	1-10g	0.17 [0.15-0.2]	0.17 [0.15-0.2]	466	0.44	0.18 [0.15-0.2]	0.18 [0.15-0.21]	223	0.13
	$\geq 10g$	0.17 [0.15-0.2]	0.17 [0.15-0.2]	965	0.71	0.17 [0.15-0.21]	0.17 [0.15-0.21]	463	0.75

1,549 AF points had automated CFAE parameters recorded. There was a very weak negative correlation between the CF at a point and the SCI (Spearman's  $\rho$  -0.08,

p=0.002) and ACI (Spearman's  $\rho$  -0.07, p=0.01), and a very weak positive correlation with the ICL (Spearman's  $\rho$  0.05, p=0.034). The proportion of high-grade CFAE was 420/1,549 (27%). High-grade CFAE points had a statistically significant slightly higher CF than non-high-grade CFAE points: high-grade 16.7[10.2-26.2]g, non-high-grade 15.3[9.3-24]g, p=0.034.

The effect of changing the CF at a location on CFAE scores was assessed in 2,262 pairs of points, Table 3.3. There was a significant (though small) increase in the ICL score at points where the starting CF was <10g and the change in CF was >8g. If the change in CF was  $\leq$ 8g, there was no significant difference. Conversely, if the starting CF was  $\geq$ 10g, then there was no significant change in the ICL score, even if the change in CF was >8g. There was no significant change in the ACI or SCI between pairs of measurements regardless of the initial CF or change in CF between pairs of measurements.

### **3.4.3 Contact Force and Dominant Frequency**

Across all the AF points, the dominant frequency was 5.9[5.4-6.6] Hz. There was a significant correlation between the dominant frequency and ICL (Spearman's  $\rho$  0.14, p<0.0005), and weaker correlations with the SCI and ACI (Spearman's  $\rho$  -0.06, p=0.04, both), as well as between the ICL and OI (Spearman's  $\rho$  0.07, p=0.024), and the OI with the SCI and ACI (Spearman's  $\rho$  0.12 (SCI), 0.21 (ACI), p<0.0005, both). Compared with non-high-grade CFAE points, high-grade ones had a significantly higher DF, though the difference was negligible (high-grade CFAE: 6.1[5.6-6.8]Hz, non-high-grade: 5.9[5.2-6.6]Hz, p<0.0005), but there was no difference in the OI between CFAE grades (p=0.08). 44 points in 10 patients qualified as high-DF points. The median DF for these points was 8.9[7.8-10.5]Hz. High-DF points were not more likely to be high-grade CFAE points (24% high-DF points were high-grade CFAE while

27% low-DF points were high-grade CFAE points,  $p=0.7$ ). There was no significant difference in the CF of high-DF points compared to low-DF points (high-DF 16.4[11.7-27.4]g, low-DF 16.8[10.2-24.8]g,  $p=0.6$ ).

There was no correlation between the dominant frequency or OI and the contact force (Spearman's  $\rho$   $p>0.05$  for each). A change in the CF between pairs of measurements at a location in the 2,120 AF point pairs assessed did not correlate with a change in the dominant frequency or OI, even where the initial CF was  $<10$ g and change in CF was  $>8$ g, Table 3.3.

**Table 3.4 The change in electrogram properties with a change in catheter orientation between measurements taken at the same location.**

Group	Measure	Catheter Orientation		Median Change	p
		Perpendicular	Parallel		
Electrogram (70 pairs)*	Mean Electrogram Size (mV)	0.026 [0.019-0.03]	0.023 [0.017-0.027]	-13.4%	0.001
	Proportion of signal $>0.05$ mV noise window (%)	37.2 [24.4-42.8]	32.6 [19.4-39.8]	-12.5%	0.001
	Median Complex Size, (mV)	0.144 [0.111-0.206]	0.137 [0.095-0.19]	-5.1%	0.029
	Number of Complexes	36 [15-45]	24 [17-38]	-32.4%	0.039
	Polarity ratio	0.48 [0.4-0.59]	0.57 [0.45-0.63]	17.3%	0.001
	Dominant Deflection Angle (°)	12.5 [8.4-15.6]	14.1 [11.3-15.7]	13.2%	0.022
CFAE (98 Pairs)*	SCI	75 [71-84]	74 [71-79]		0.13
	ACI	93 [87-98]	91 [85-96]		0.16
	ICL	5.5 [4-7]	5 [3-7]		0.24
Spectral Analysis (140 Pairs)	DF (Hz)	5.7[5.2-6.3]	5.9[5.1-6.5]		0.58
	OI	0.18[0.16-0.2]	0.18[0.16-0.21]		0.09

### **3.4.4 Catheter Orientation**

The effect of catheter orientation was assessed by observing the difference in the electrogram, CFAE and spectral analysis parameters on changing the catheter from a perpendicular to parallel orientation in a subset of AF points (Table 3.4). In the case of the electrogram and CFAE pairs, only those where the difference in CF between orientations was  $<8g$  were used to minimize differences secondary to CF for the electrogram and CFAE analysis due to the influence of CF on these measurements. On changing orientation, complexes became smaller and more positive but without any change in CFAE or spectral measures.

## **3.5 Discussion**

This study examined the relationship between CF and catheter orientation with electrogram parameters. The main findings were:

- 1) An increase in CF at a location was associated with an increase in the complex size in both AF and SR, but this difference was only apparent if the initial CF was  $<10g$  and for changes in CF  $>4.5g$  in SR and  $>8g$  in AF.
- 2) Increasing CF at a location was associated with a small increase in ICL scores, though only if the initial CF was  $<10g$  and change in CF was  $>8g$ .
- 3) Changing the CF at a location did not affect spectral measurements.
- 4) Changing from a perpendicular to parallel orientation was associated with a reduction in the electrogram complex size and more positive complexes but no change in CFAE or spectral measures.

### **3.5.1 Catheter contact and the electrogram**

A previous study used manual assessment of the SR electrogram around the PV antra, averaging five complexes per location and found a modest relationship between

CF and electrogram amplitude<sup>187</sup>. In another study, a very weak relationship was found between these parameters throughout the LA in PAF patients, around half of whom were in AF, though the authors did not give details of how the electrogram parameters were measured<sup>205</sup>. The current study examined this relationship in both AF and SR throughout the LA and used automated analysis of 8s of electrogram data at each location. No relationship between the electrogram complex size and CF was observed, likely due to the much larger effect of LA location on complex size.

One would expect that the thickness of the tissue under the catheter and its compliance affect the size of the electrogram: a larger mass of tissue produces a larger electrogram, and a more compliant area would deform around the catheter tip to contact the bipoles more effectively. The thickness of the tissue around the LA<sup>209</sup> and the compliance of different parts of the LA<sup>45,210</sup> are known to differ. During an ablation procedure, the whole of the atrium is potentially mapped and ablated and therefore the current data are in keeping with previous work<sup>187,205</sup> suggesting electrogram size cannot be used as a reliable surrogate for real-time CF measurement in either AF or SR.

The morphology of the bipolar electrogram was also affected by CF, with complexes becoming more negative at higher CF. This may be a function of the proximal bipole having increased contact with the tissue at higher CF (study points were generally taken in a perpendicular orientation). Interestingly, when the catheter was changed from a perpendicular to parallel orientation (whereby the proximal pole would have a similar degree of contact to the distal), the complexes became more positive: at the same time, there was also a reduction in the electrogram complex size (including when changes in CF between measurements were minimized to address any confounding from this). This suggests that for a bipole, it is not just the degree of

contact that affects both the size and morphology of the observed complexes but also its orientation.

The influence of changes in CF on the electrogram is an important consideration, especially where mapping studies are conducted with electrodes at a stable position for a prolonged period of time within the LA, such as recent work with rotor mapping where electrograms are collected for over 10 minutes<sup>211</sup>. Moreover, the effect of a change in CF and catheter orientation on the electrogram is also an important consideration when comparing pre and post-ablation electrograms to judge ablation efficacy based on electrogram attenuation<sup>190</sup> and morphology changes<sup>141</sup> (criteria which have been used to guide clinical ablation<sup>187,191</sup>). The data from the current study suggest that mapping with a CF  $\geq 10$ g of force would minimize CF related changes in the electrogram, as would ensuring the difference in the CF between appraisals of the electrogram are  $\leq 4.5$ g in SR and  $\leq 8$ g in AF. The higher threshold in the case of AF signals is likely secondary to the higher intrinsic variance in the AF electrogram making CF-related changes more difficult to appreciate.

The observation of increased atrial ectopy in SR at higher CF is consistent with findings of increased excitability of atrial tissue from global atrial stretch in animal models<sup>212</sup> and humans<sup>122</sup>, as well as the observation of stretch-induced depolarisations of human myocytes<sup>130</sup>. It is also consistent with the increased susceptibility to AF in those with hypertension<sup>213</sup>. The differential locational vulnerability to stretch induced ectopy suggested by the current study is interesting and may reflect the electromechanical sensitivity of the tissues themselves: the inferior wall demonstrated the strongest correlations between CF and ectopic incidence. It may also be that nearby structures are being affected by the stretch stimulus from the catheter, for example the inferior right and left ganglionated plexi are in proximity to the inferior wall<sup>214</sup>. One

would expect that points taken within the PVs would demonstrate an even higher stretch-related ectopic vulnerability in view of these being common trigger sites for PAF (in the current study, points were taken at the PV antra rather than deep within the PVs, hence this was not assessed).

Interestingly, at the 10g CF level, there was a change in the behaviour of the tissue – ectopics were more frequently observed above 10g of CF than below this threshold. This also appears to be a threshold for observing an effect on the electrogram from a change in CF and may be related to the electrical or compliance properties of the tissue changing above this threshold. At a CF below 10g, the tissue may not be particularly stretched and therefore exhibits less ectopics and incompletely envelops the catheter bipole. The tissue has capacity for stretching and therefore if from this point the CF is increased, more stretch-related activations manifest and the tissue becomes more closely apposed to the bipole. If the starting CF is  $\geq 10$ g the tissue is likely already enveloping the bipole to an extent that further increases in CF make little difference to this and so the electrogram. Moreover, the excitability threshold for stretch-related activations has already been exceeded so further increases in CF have little effect on further increasing the frequency of ectopy.

### **3.5.2 Catheter contact and CFAE parameters**

There was a weak relationship between automated CFAE scores and CF, with the scores suggesting higher CF was associated with greater fractionation. Increasing the CF at a location may be associated with an increase in the detection of low amplitude deflections by the automated CFAE algorithms – an increase in CF was associated with an increase in mean electrogram waveform size with more of the electrogram outside of the noise window, meaning a greater possibility of farfield signals being identified as true activations. Alternatively, it may be that increasing CF



is associated with increasing tissue stretch and is directly causing an increase in activations and therefore influencing CFAE measurements in this manner. Importantly, while the effect of CF on CFAE scores was small, the relationship was no longer apparent if the starting CF was  $\geq 10$ g. It is therefore possible that a proportion of the variation previously observed in CFAE maps<sup>88,90</sup> is contributed to by changes in catheter CF during mapping.

### **3.5.3 Catheter contact and Spectral Analysis Parameters**

A relationship between DF measurements and CFAE scores has previously been observed<sup>105</sup>. Regions harbouring CFAE have also previously been noted to be more extensive than those with high DF<sup>105</sup>, as was the case in the current study. Previous investigators have also noted that fractionated electrograms tend to occur adjacent to high DF areas rather than directly superimposed on them<sup>96</sup>. The latter is the likely explanation for high DF points not being significantly more likely to be high-grade CFAE points in the current study.

Spectral analysis parameters were not affected by CF or catheter orientation. The changes in complex morphology and size secondary to changes in CF would not be expected to affect a frequency-based analysis. An increase in the number of activations observed in a time period as observed here with increasing CF (and having a small effect on CFAE measurements) evidently does not affect spectral analysis parameters. This may be because such extra activations are not consistent enough to have a significant effect in the frequency domain. This also suggests the changes in CFAE scores with changes in CF may be more related to changes in the measurement of the electrogram rather than changes in the electrical properties of the substrate. Therefore, the temporal instability observed in dominant frequency maps is not explained by differences in mapping CF<sup>215</sup>.

### **3.6 Conclusions**

Changes in catheter contact force and orientation affect electrogram complex size and morphology, and this most likely reflects changes in the physical relationship between the catheter bipoles and atrial tissue. Complex size is not affected by increases in CF if the starting CF is  $\geq 10\text{g}$  or if the change in CF is  $\leq 4.5\text{g}$  in SR and  $\leq 8\text{g}$  in AF. Higher CF is also associated with atrial ectopy, likely through stretch-sensitive depolarisations, and this has a greater effect for CF  $\geq 10\text{g}$ . CFAE parameters are affected by CF (again, if the initial CF is  $< 10\text{g}$ ), while spectral analysis parameters are unaffected by this or catheter orientation. This suggests that in AF, the measurement of the electrogram is predominantly being affected by CF, through greater contact between the bipole and the tissue, without greatly affecting the underlying substrate (based on the lack of impact on spectral parameters). Therefore, during mapping of the LA (and electrogram-guided ablation), it is important to be aware of the effects of CF and catheter orientation as these influence the results: conversely, substrate-based ablation targeting spectral parameters is unaffected by catheter contact and orientation. Based on these results, an optimal CF during mapping of  $\geq 10\text{g}$  is suggested, as below this value the CF has a significant influence on the electrogram and CFAE scores.

## 4. Target indices for clinical ablation in atrial fibrillation: insights from contact force, electrogram and biophysical parameter analysis

### 4.1 Abstract

**Background:** In animal studies of radiofrequency ablation, lesion sizes plateau as the maximum lesion size is reached for an ablation. Lesion parameters are not available in clinical ablations, but preclinical work suggests that these correlate with impedance drop and electrogram attenuation. Characterisation of the relationship between catheter CF, ablation duration and these surrogate markers of lesion formation may allow us to define targets for effective ablation.

**Methods and Results:** Fifteen patients undergoing first-time radiofrequency ablation for persistent AF were studied. All were in atrial fibrillation at the time of the procedure. Ablations were performed with an irrigated-tip CF-sensing catheter in temperature-controlled mode (temperature limited to 48°C, power to 30W). Included were 285 left atrial static ablations, 247 with additional impedance data. The ablation FTI correlated with the attenuation of the electrogram with ablation ( $p=0.02$ , Spearman's  $\rho$  -0.14), the relationship plateauing from 500g.s, a reduction in the electrogram amplitude of 20%. The FTI also correlated with the impedance drop during ablation ( $p<0.0005$ , Spearman's  $\rho$  0.79): the relationship was logarithmic, the reduction in the impedance with an increasing FTI also plateauing from 500g.s, an impedance drop of 7.5%. The ablation duration impacted on the impedance drop at an FTI if the duration was less than 10 seconds. Beyond this time point, the FTI achieved rather than the ablation duration or mean CF applied determined the impedance drop.

**Conclusions:** During ablation for persistent AF, an FTI of 500g.s should be targeted with ablation duration of at least 10 seconds.

## **4.2 Introduction**

The aim of ablation for AF is the generation of a transmural lesion. In animal studies, a plateau is observed between lesion size and delivered ablation energy, with no significant change in lesion size at a fixed ablation power for ablation beyond 20 seconds<sup>216</sup>. The relationship between catheter CF and lesion depth<sup>166</sup> also plateaus at higher values in studies of temperature-controlled ablation. These plateaus therefore represent the maximum lesion size that can be attained for a particular set of ablation parameters. During clinical ablation, one would also expect lesion parameters to plateau as this maximum is reached for an ablation, but in clinical procedures lesion parameters are not known.

In animal studies, a correlation has been observed between lesion dimensions and impedance drop during ablation<sup>164,166,168</sup>. Such studies also demonstrate that electrogram amplitude reduction is significantly greater in transmural than non-transmural lesions<sup>141,190</sup>. Therefore, these measures can be used as surrogates of lesion parameters.

Detailed measurements of tissue CF during clinical ablation have now become possible using CF-sensing catheters. The impact of this controllable factor can therefore be assessed on indicators of the effect of ablation on tissue: electrogram amplitude and impedance change. In animal studies, the tissue CF has been found to correlate with both lesion depth<sup>161,166,168</sup> and impedance drop<sup>166,168</sup>. Examination of the interrelationships between these factors may allow us to optimise our ablations, in

particular the identification of a plateau point in man beyond which further ablation has no or minimal effect on the tissue would be especially useful.

The aim of this study was therefore to establish, based on the biophysical and electrogram changes, target indices for radiofrequency ablation.

### **4.3 Methods**

All participants gave informed consent to participate in the study, which was approved by the UK National Research Ethics Service. Consecutive patients undergoing their first ablation procedure for persistent AF were enrolled in the study. All patients were in AF at the start of the procedure and all procedures were performed with the patients under conscious sedation. The majority of the procedures were performed by a single operator. A Thermocool SmartTouch catheter (Biosense Webster, Inc., CA, USA) was used to measure tissue CFs, at a sampling rate of 20Hz. Remote robotic navigation (Sensei Robotic Catheter System, Hansen Medical Inc., CA, USA) was used in a majority of procedures, though this was at the discretion of the operator. Tissue CF and electrogram characteristics were recorded using the Carto3 electro-anatomic mapping system (Biosense Webster, Inc.) and LabSystem Pro electrophysiological recording system (Bard Electrophysiology Division, MA, USA) respectively.

During WACA of the ipsilateral pulmonary veins in pairs and CFAE ablation, thirty second static study ablations were performed, with the ablation catheter in a stable position at least 2.5 seconds prior to the onset of ablation, and for at least 8 seconds after ablation. In all cases, ablations were performed in temperature-controlled mode with temperature limited to 48°C, and power to 30W. The irrigation flow rate was set to 2ml/minute during mapping and 17ml/minute during ablation. All ablations were

performed at a CF of between 5g and 40g. During ablation, the pulmonary vein catheter was kept in either a pulmonary vein or the left atrial appendage. Ablations where there was visually evident macro-displacement of the ablation catheter were excluded from the analysis. All study ablations were non-overlapping so that previously ablated tissue was not included in the analysis and, once they were completed within a lesion set, further ablation was at the operator's discretion, and generally performed as continuous "drag" ablations.

Pre-ablation electrograms were collected on the electrophysiological recording system for 2.5 to 8 seconds - the former for points in the WACA and the latter for the CFAE ablation points. The longer period for the CFAE points was used due to the potential greater complexity of the electrogram at these locations. Post-ablation electrograms were collected for 8 seconds and the first 0.5s discarded to reduce the effects of post-ablation noise. Synchronicity between the mapping and electrogram recording system was ensured by either manually acquiring points simultaneously or, in the last eight patients, through the use of the LabLink data interface (Bard Electrophysiology Division). In a subset of ten patients, impedance during ablation was also recorded. This was measured using a 50kHz current between the tip of the ablation catheter and the ground patch (positioned on the patient's left thigh) and was sampled at 10Hz. The ablation power was also recorded at this sampling rate. The electrogram data was exported from LabSystem Pro, while the CF, location, and ablation biophysics data were exported from Carto3. The data were processed and analysed using custom written Matlab (MathWorks, MA, USA) scripts as described in Chapter 2.7.

Stability during radiofrequency ablation was assessed by comparing the average position of the ablation catheter tip relative to the averaged location of the poles of the

pulmonary vein catheter in three dimensional space over 2.5 seconds (location data recorded at 60Hz). The pulmonary vein catheter was chosen as a reference to allow for movement secondary to respiration to be taken into account. If the average distance between the ablation catheter and pulmonary vein catheter changed by more than 3.5mm (the length of the ablation electrode) between the pre- and post-ablation points taken on Carto3, the catheter was deemed to have been excessively unstable and the ablation excluded from the analysis.

The electrograms analysed in this study were bipolar electrograms (set up between the distal adjacent electrodes on the ablation catheter). Signals in the electrogram recording system were recorded at a low cut-off of 30Hz and a high cut-off of 250Hz. Electrograms which on inspection suffered from excess noise were discarded. After export, the signals were filtered with a 10<sup>th</sup> order 100Hz Butterworth low pass filter. The peaks and troughs in the signal were identified using a 70ms cut off as used in previous published work to prevent double counting of complexes<sup>98</sup>. Complexes less than 0.05mV (peak to trough) were assigned as noise<sup>201</sup>, and a 1mV upper cut-off for the atrial electrogram size adopted based on review of the signals and previous work<sup>217</sup>. The angles of the rising and falling signal were determined for the dominant peak or trough in a complex, from a point at one-third of the complex size from the peak or trough of the signal. A correction factor of 1000 (500 if the electrogram was sampled at 2Khz) for angle measurements was used to make the signal equivalent to that displayed on LabSystem Pro at a sweep speed of 100mm/s and a 32x scale. A rising or falling angle of over 45° meant the complex was discarded as farfield<sup>98</sup>. The complex size was measured from the dominant peak to trough of a complex. The electrogram amplitude was then defined as the mean amplitude of these complexes.

If a pre-ablation electrogram had less than 2 complexes identified or a post-ablation electrogram had only 1 complex identified, it was not included in the analysis (as an isolated complex could be spurious). In a previous study of ablation in paroxysmal AF patients, an increase in the electrogram with ablation was taken to represent micromovement<sup>150</sup>: in the case of patients in AF, the inherent variability of the electrogram was felt to render this criterion less reliable and therefore in the current study, the electrogram more than doubling in size with ablation was felt to be a reasonable indicator of micro-displacement.

The FTI and impedance data were analysed as described in Chapter 2.7. In the case of the former, in order to examine the dynamic relationship between the FTI and impedance drop, all of the ablations were divided into consecutive, cumulative, 10g.s FTI intervals. The maximum impedance drop was then compared with the initial impedance at the start of ablation. The maximum percentage impedance drop during an ablation was determined from the waveform after a Savitzky-Golay filter had been used to remove noise: the initial impedance was compared to the maximum drop recorded during ablation (or portion of ablation in the case of the incremental FTI).

In order to develop a clinically useful parameter that predicted an adequate lesion, we sought a point of ablation where continuing energy application had minimal effect on the lesion parameters, using the impedance drop as a surrogate for the latter. Qualitatively, this would be represented by the point at which a plateau develops in the relationship between the FTI and impedance drop. Quantitatively, we defined this as the point in the fitted curve for this relationship where the impedance drop was 0.5% per 100g.s of FTI. The first derivative of the fitted curve formula was used to determine where the instantaneous gradient of the curve fell to this value.



### 4.3.1 Statistics

Statistical analysis was performed using SPSS (IBM SPSS Statistics, Version 20 IBM Corp Armonk, USA) and Matlab V7.12 with the Statistics Toolbox V7.5. A p-value of <0.05 was regarded as significant. Non-normally distributed data, as assessed by a Jarque-Bera test, were analysed using a Mann-Whitney U test or, if correlated samples, a Wilcoxon Signed Ranks test. Correlation was assessed for non-linear relationships by Spearman's rank correlation.

## 4.4 Results

The baseline characteristics of the study patients are presented in Table 4.1. In

**Table 4.1 Study Population Baseline Characteristics**

Number of Patients	15
Age, mean±SD	62±8 years
Gender	12 male (80%)
CHA <sub>2</sub> DS <sub>2</sub> -VAsc Score, mean±SD	1.6±1
Left Atrial Diameter, mean±SD	4.5±0.6cm
Duration of Non-Paroxysmal Atrial Fibrillation	20±12 months
Severe Left Ventricular Impairment (Ejection Fraction<35%)	2 (13%)
Remote Robotic Navigated Ablation	11 (73%)

the fifteen patients there were 420 study ablations (ablations performed after the study ablations were completed in a region were not included in the analysis). After exclusion of ablations based on the displacement and electrogram criteria, there remained 285 pairs of pre-and post-ablation electrograms.

In the ten patients with biophysical parameters recorded, 247 static ablations were included in the analysis. On average it took 9±2 seconds for the ablations to first reach the power limit of 30W with no relationship between the time taken and the mean ablation CF (p=0.9). At thirty seconds of ablation, there was a significant correlation

between the ablation mean CF and the absolute and filtered percentage (comparing the minimum to initial impedance of the filtered impedance waveform) impedance drop

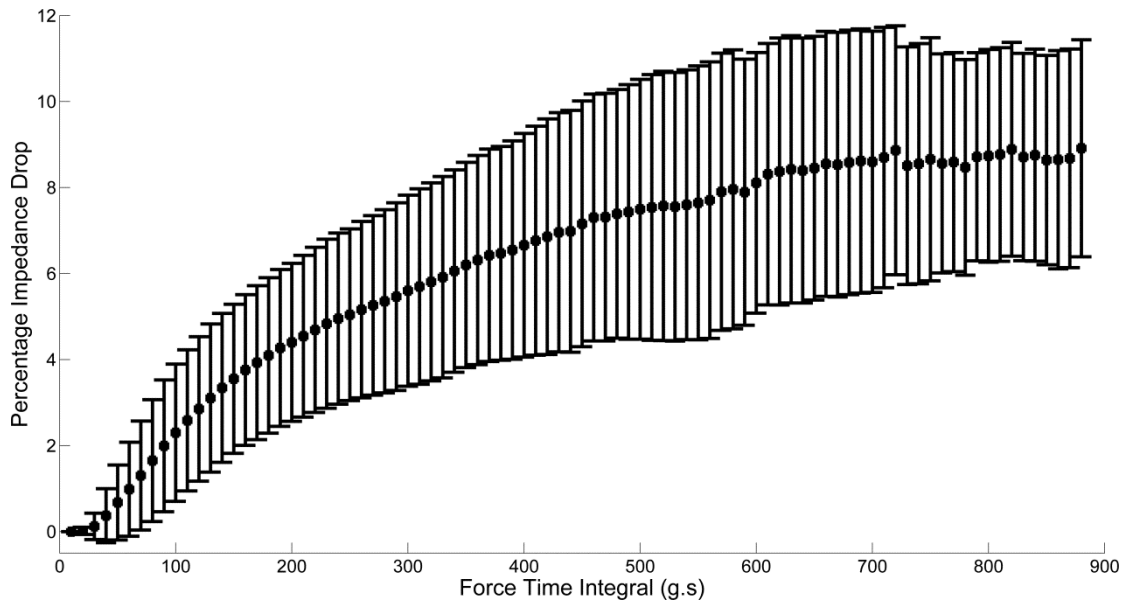


**Figure 4.1 Maximum Percentage Impedance Drop versus Incremental Force Time Integral.** Black squares are mean values for at least 20 readings. Error bars represent one standard deviation. 11,441 measurements represented in the chart.

( $p < 0.0005$  for both, Spearman's  $\rho$  0.38 and 0.51 respectively).

The incremental FTI analysis generated 11,502 separate measurements for all of the study ablations combined. There was a strong correlation between both the absolute maximum impedance drop and filtered percentage maximum impedance drop and the incremental FTI:  $p < 0.0005$  for both, Spearman's  $\rho$  0.66 and 0.79 respectively. As the relationship was stronger with the percentage filtered impedance drop, this was used for the subsequent analysis. Figure 4.1 presents the relationship between the percentage impedance drop and the incremental FTI. There was an initial plateau until 20g.s and then following this there was an increase in the impedance drop with an increasing FTI until a plateau starting from 500g.s, corresponding to a mean impedance drop of around 7.5%.

In order to determine quantitatively the FTI at which the rate of change in the impedance drop engendered by an increasing FTI becomes significantly reduced, a logarithmic curve of best fit was fitted to the dataset ( $y=2.57*\ln(x)-8.89$ , adjusted  $R^2$  0.56): from this curve, the relative plateau was found to develop from an FTI of 514g.s. At this point, the impedance drop determined from the formula of the fitted curve was 7.2%.

The FTI is a function of tissue CF during ablation and the duration of the ablation. The relative importance of mean tissue CF and ablation duration on lesion formation as assessed by impedance drop was investigated.

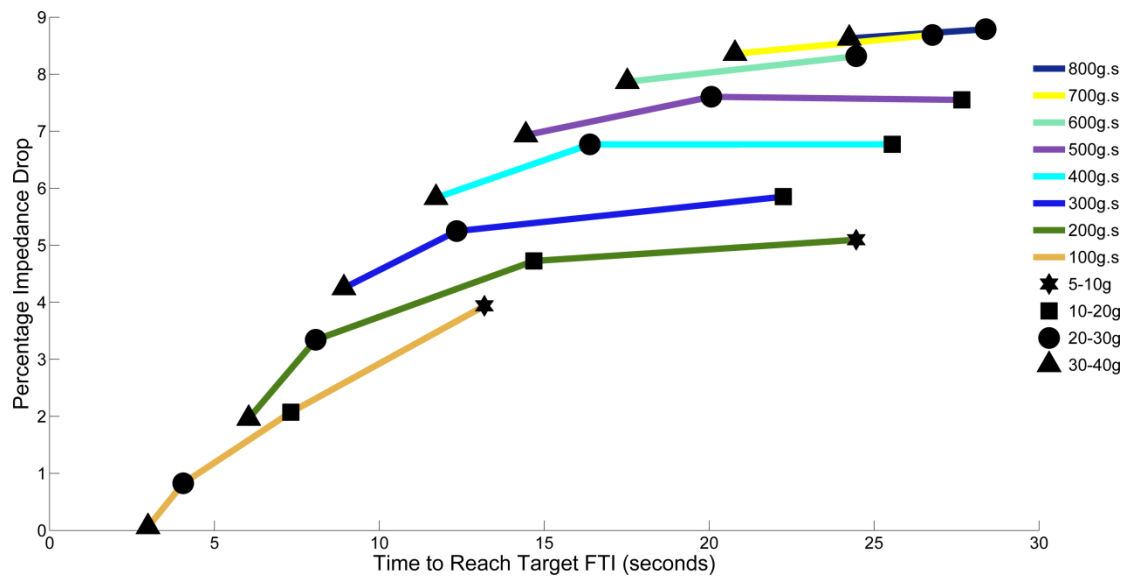


**Figure 4.2 Influence of Mean Contact Force and Ablation Duration on Impedance Drop at a Target Force Time Integral.**

Each point is the average of at least ten ablations.

Figure 4.2 is a plot demonstrating the influence of the components of the FTI on the impedance drop where each line is an FTI target and each point on the line is the (grouped) mean CF to get to that target FTI. As the mean CF during an ablation increased, the time taken to reach the target FTI reduced. Looking firstly at the 100g.s curve, the longer it took to reach the FTI target, and so the lower the mean CF, the greater the impedance drop. In fact, for each curve until the 400g.s curve, there was a

significant heterogeneity in the impedance drop based on the CF group ( $p < 0.025$ ).

Beyond ablation durations of 10 seconds, the curves relatively flattened, suggesting the influence of the ablation duration (and so mean CF) on the impedance drop at an FTI was no longer evident. If ablations less than 10 seconds long were excluded, there were no longer any significant differences in the impedance drop at each FTI secondary to the mean CF group.

#### 4.4.1 The electrogram and ablation

There was a significant difference between the pre and post ablation mean complex sizes ( $p < 0.0005$ , pre-ablation median 0.12mV (range 0.05 to 0.59mV), post-ablation 0.09mV (range 0 to 0.43mV), median decrease of 21% (range 100% decrease to 72% increase).

There was a significant correlation between both the FTI and mean CF and the change in the electrogram complex size ( $p = 0.02$ , Spearman's  $\rho = -0.14$  for both). The

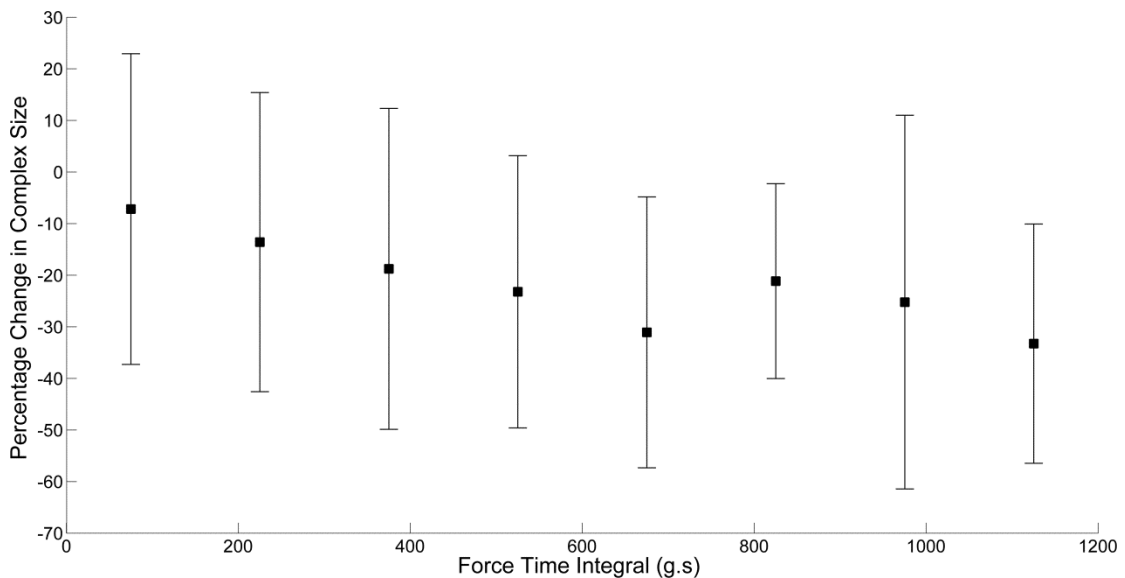


**Figure 4.3 Force Time Integral versus Percentage Change in Electrogram Complex Size.** Black squares are mean value. Error bars represent one standard deviation.

percentage impedance drop during ablation also correlated with the latter ( $p < 0.0005$ , Spearman's  $\rho = -0.33$ ).

There was a linear increase in the amount of electrogram attenuation with an increasing FTI until around 500g.s after which a plateau occurred, at around a 20% reduction in the complex size (Figure 4.3).

A quantitative assessment of the plateau was not performed as the fitted logarithmic curve was only weakly predictive of the decrease in the complex size (adjusted  $R^2$  0.03). This was reflective of the high degree of variability in the attenuation of the electrogram observed. To allow for a quantitative comparison, the electrogram attenuation above and below the point from which there was a qualitative plateau suggested by the data was compared. The percentage reduction in the complex size was significantly lower for FTIs under 490g.s than equal to or above this value ( $p = 0.03$ :  $< 490\text{g.s}$  median -18% (-70 to 72%);  $\geq 490\text{g.s}$  median -23% (-100 to 31%)).

## **4.5 Discussion**

This study prospectively assessed the relationship between catheter CF and biophysical and electrogram parameters in patients undergoing NPAF ablation. An increasing FTI was associated with a greater impedance drop with this relationship plateauing from 500g.s. There was also a relationship between the FTI and the attenuation of the fibrillating electrogram, with a relative plateau again from around 500g.s. The amplitude of the fibrillating electrogram had a more variable response to ablation than the impedance drop and so may not be as useful as a surrogate for lesion formation as the percentage impedance drop, particularly at the level of the individual ablation. The ablation duration impacted on the impedance drop at an FTI if the

duration was less than 10 seconds. Beyond this time point, the FTI achieved rather than the ablation duration or mean CF applied determined the impedance drop.

During temperature-controlled radiofrequency ablation, the maximum temperature reached within the tissue correlates linearly with lesion volume<sup>218</sup>. Catheter tip temperature is less reflective of this maximum temperature with irrigation as this cools the catheter tip<sup>218</sup>. The maximal tissue temperatures can therefore reach higher levels in irrigated than non-irrigated temperature-controlled radiofrequency ablation, though in both types of ablation a plateau occurs in the tissue temperature over the course of the ablation<sup>218</sup>. A linearly increasing fall in impedance with an increasing catheter tip temperature has been described for non-irrigated ablation<sup>164,167,219</sup>. This has been suggested to be due to increased conductivity of cardiac tissue with heating<sup>166</sup>. Therefore, we have assumed that during irrigated radiofrequency ablation, the occurrence of a plateau in the impedance drop reflects a plateau in the size of the lesion.

In this study, the CF during ablation correlated with impedance drop. This has been described previously in animal studies (using non-irrigated ablation<sup>166</sup>), and recently during clinical ablation in paroxysmal atrial fibrillation (PAF) and atrial flutter patients<sup>220</sup>, and in another study of almost exclusively PAF patients<sup>169</sup>, with both clinical studies using temperature-controlled, power limited irrigated ablation. The current study and previous work<sup>166,169,220</sup> have demonstrated that for a given ablation duration, the CF during ablation significantly affects the impedance drop. This is not unexpected as greater contact for the same ablation duration would result in more efficient energy delivery to the myocardium, an increase in the tissue temperature and therefore a greater impedance drop. The FTI is a measure that incorporates both ablation duration and mean CF and therefore includes two important factors impacting on impedance drop.

Previous work has demonstrated a weaker relationship between the impedance drop and FTI<sup>220</sup> than the current study. The current study was conducted in a different patient cohort (NPAF rather than PAF or atrial flutter patients). Also, in the current study, the impedance data were sampled at a higher frequency (10Hz rather than 0.2 Hz during ablation) and the resulting waveform filtered, which would have contributed to the stronger relationship, as well as the use of the percentage rather than absolute impedance drop. Regardless of the improved strength of the relationship observed in the current study, we would concur with previous work<sup>220</sup> that impedance drop cannot be used reliably in place of real time CF measurement to judge contact during ablation due to the point by point variability. This was even more so the case for electrogram attenuation. The focus of the current study though was the dynamics of the relationships between the CF and these surrogates of lesion dimension to establish targets for ablation, rather than using these surrogates as an alternative to measuring the CF during ablation.

Another recent study has investigated the dynamics of the relationship between the impedance and the overall ablation mean CF rather than FTI<sup>169</sup>. The sampling rate of the impedance in that study was every 10 seconds. For ablations at a mean CF of  $\leq 5g$ , there was no real impedance drop after the initial 10 second measurement during ablation and the group therefore recommended a minimum of 5g of contact for ablation. The lower CF cut off in the current study was 5g and so we have not studied the dynamics of the relationships below this level.

This study is the first to correlate catheter CF with electrogram attenuation and impedance parameters during NPAF ablation. In this case, there was a plateau in the degree of electrogram attenuation related to the FTI at around a 20% reduction. This is less than the 62% reduction secondary to the production of transmural lesions seen in a

pacing induced AF sheep model<sup>190</sup>, and the 48-65%<sup>150,152</sup> reduction seen in sinus rhythm patients undergoing ablation. With regard to the paced sheep model, it may be that there is greater ablation sensitivity to CF in that model than in man. The chaotic nature of AF makes changes in the electrogram amplitude less consistent. This would suggest that electrogram attenuation is an unreliable surrogate for lesion size at the individual ablation level in AF.

The relationship between the FTI and electrogram attenuation plateaued at around 500g.s: this was consistent with the impedance data, though the relationship was stronger in the latter case. The identification of a plateau in the relationships between the FTI, electrogram attenuation and impedance drop is the key finding of this study as it represents the lesion approaching the maximum possible size at those ablation settings. The observation that these two surrogates of lesion size, despite the variability in their response to ablation at a single lesion level, are in agreement regarding the existence of this plateau and where this occurs provides internal validation for this finding. Beyond this 500g.s plateau, continued ablation is likely to yield minimal further gains. Such diminishing returns need to be weighed against the potential for complications from continued application of radiofrequency energy at a point such as perforation, steam pops and damage to extra-cardiac structures such as the oesophagus.

The current study demonstrates that for a given FTI, the efficacy of ablation as judged by the impedance drop is affected by the former's constituents: the mean CF and the ablation time. Ablation for less than 10 seconds appears suboptimal regardless of the CF applied or FTI, whereas beyond 10 seconds the FTI (rather than its constituents) becomes the overriding determinant of the impedance drop. This time dependence may be secondary to the progressive ramping up of the power in the temperature-controlled, power limited ablations performed in this study: on average it took around this time



frame for the ablation power to first reach the maximum power cut off. This finding is clinically important, as, if one uses an FTI target for ablation without accounting for the ablation duration, suboptimal lesions could be delivered if the duration is less than 10 seconds, regardless of the FTI achieved. This is especially important with the advent of newer iterations of three dimensional mapping systems (for example the Carto3 Visitag module, Biosense Webster, Inc.) which are able to place lesion markers in an automated manner based solely on reaching an FTI threshold at a point.

Previous work to establish CF targets for ablation has focussed on comparing CF parameters retrospectively based on reconnections in the pulmonary vein isolation lines. A mean segment CF during ablation of at least 19.6g was less frequently observed to be associated with acute reconnection<sup>177</sup>, and at 3 months follow up, segments within a WACA ablated with a minimum FTI below 400g.s had a greater chance of being reconnected<sup>178</sup>. These previous studies subdivided the ipsilateral pulmonary vein ablation lines into seven<sup>177</sup> or eight<sup>178</sup> segments and judged the adequacy of the multiple ablations in these segments based on whether the whole segment reconnected. The current study differs in approach as we investigated at the level of the individual lesion, using biophysical and electrogram parameters, rather than against the wider segment outcome. In so doing, we were able to explore the parameters for the successful creation of an ablation lesion. Based on segment reconnection data, a recommendation has been made that the optimal mean CF during ablation should be 20g<sup>178</sup>: the current study suggests that the duration of ablation and FTI reached are more important determinants of the efficacy of ablation. Within the limits of the contact force and duration parameters investigated, radiofrequency energy applied for a longer period with CF below 20g appears to have the same impact in terms of lesion formation as long as the same FTI is attained and ten seconds of ablation

exceeded. This study therefore suggests that it is more clinically relevant to focus on FTI and ablation duration targets to generate adequate lesions.

#### **4.5.1 Limitations**

The gold standard for establishing the effectiveness of an ablation is the histological assessment of the lesion produced. This is not available in humans and therefore the current study utilised parameters previously shown to correlate with histological lesion parameters. Conclusions are therefore necessarily based on these surrogate markers of lesion formation. Electrode orientation is known to affect lesion size<sup>162,163</sup>. In this study, the catheter orientation was not included in the analysis and may have contributed to some of the variance observed. The majority of patients in this study had ablations performed using remote robotic navigation. This may also have influenced the results of this study. All of the ablations were performed with the same power setting, and the irrigation flow rates were those recommended by the ablation catheter's manufacturer for the power setting used in the study. In preclinical studies, irrigation flow rates have been demonstrated to affect the size of lesions produced<sup>159,221</sup>. It is likely that the use of different power or irrigation settings would alter the energy delivered during ablation and affect lesion formation.

#### **4.6 Conclusions**

The results of this study suggest that during NPAF ablation, impedance drop may be a more accurate surrogate of adequate lesion formation than fibrillatory electrogram attenuation. End points in terms of biophysical parameters for optimal lesion formation include an impedance drop of 7.5% and electrogram attenuation of 20%. However, there was considerable variation in these biophysical parameters on a point by point

basis. A more pragmatic primary target for ablation lesions is therefore an FTI of 500g.s, beyond which there appears to be minimal incremental benefit from further ablation. Additionally, ablations should be at least 10 seconds in duration, regardless of CF or FTI. The clinical impact of adopting such targets for ablation requires further prospective evaluation.

## 5. Catheter contact characteristics and ablation efficacy in the human left atrium

### 5.1 Abstract

**Introduction:** Pre-clinical work suggests factors including catheter orientation and contact consistency during individual radiofrequency ablations influence lesion size.

Our aim was to investigate factors affecting catheter contact in LA and their effects on ablation.

**Methods and Results:** 2,298 eight second static LA mapping points were studied in 30 patients undergoing ablation for AF (16 in AF, 14 SR, 18 RRN procedures) using a CF sensing catheter. Contact force variability (CFV: difference between 20Hz-sampled CF waveform mean peak and trough) increased with mean CF, Spearman's  $\rho$  0.6,  $p < 0.005$ . Catheter drift correlated weakly with CF (Pearson's Correlation -0.06,  $p = 0.005$ ). CFV was higher in SR than AF and with RRN ( $p < 0.001$ ). In AF there was less catheter drift for RRN than manual navigation points but the converse was true in SR. In 747 static 30s LA ablations the influence of contact parameters on ablation efficacy was compared by multivariate analysis of impedance drop during ablation: a lesser drop suggesting reduced efficacy. For FTI, increased CFV ( $> 5g$ ) and locational drift ( $> 3.5mm$ ), perpendicular contact, SR and RRN usage were associated with a lesser impedance drop with ablation ( $p < 0.005$  for each), suggesting reduced efficacy.

**Conclusions:** Beyond the FTI, the quality of catheter contact influences ablation efficacy, and clinical catheter contact is affected by multiple factors, including the atrial rhythm and catheter navigation mode. Maximal efficacy is provided by parallel contact with CFV  $\leq 5g$ , catheter drift  $\leq 3.5mm$  and manual navigation.

## **5.2 Introduction**

In preclinical studies, the degree of contact between the ablation catheter and myocardium influences the size of the subsequent lesion produced by a radiofrequency energy application<sup>166</sup>. The consistency of this contact also affects this<sup>171</sup> as does catheter orientation<sup>222</sup>. The importance of catheter CF to clinical ablation has been investigated in studies looking at the reconnection of segments in the WACA line during AF ablation<sup>177,178</sup>. A limitation of this approach is that rather than assessing the efficacy of ablation by examining the response to individual radiofrequency applications, conclusions are drawn based on the response of regions subjected to multiple applications.

In clinical ablation, an approach to assess individual ablations is challenging due to a lack of access to histological lesion parameters. Impedance drop with ablation correlates with the latter<sup>164,166</sup>, and the nature of the impedance drop relationship with the FTI during clinical ablation has been used to draw conclusions about ablation efficacy<sup>169,206</sup>. Electrogram attenuation<sup>190</sup> or morphology change<sup>141</sup> can also be used similarly<sup>187</sup>. As discussed above, the quality of the contact, such as its consistency and orientation, not just the FTI achieved may impact on ablation efficacy. An understanding of these factors may therefore help further optimize ablations, especially in concert with automated lesion annotation software<sup>223</sup>.

In the current study, we examined factors affecting catheter contact in the LA, investigating the locational and catheter CF stability, contact orientation, anatomical location, and manual versus robotic catheter navigation. Furthermore, as a corollary to preclinical studies assessing individual radiofrequency applications, we examined how these factors affected the impedance drop and electrogram with ablation to determine contact parameters to optimize clinical ablations.

### **5.3 Methods**

All participants gave informed consent to participate in the study. The study had ethical approval from the UK National Research Ethics Service. Consecutive patients with AF undergoing their first ablation were enrolled. Procedures were performed with patients under moderate conscious sedation. CF was measured using a Thermocool SmartTouch catheter (Biosense Webster Inc., Diamond Bar, CA, USA). In a subset of cases, at the discretion of the operator RRN (Sensei Robotic Catheter System, Hansen Medical Inc., Mount View, CA, USA) was used, in which case, the trans-septal sheath used for the ablation catheter was an Artisan sheath (Hansen Medical Inc.), otherwise a Mullins sheath (Medtronic, Minneapolis, MN, USA) was used. Carto3 (Biosense Webster Inc.) was used to record CF, location and biophysical data and LabSystem Pro (Bard Electrophysiology Division, MA, USA) was used to record electrogram data.

Using the ablation catheter, mapping points were taken at evenly spaced locations throughout the LA prior to any ablation. At each location, three to four 8s CF readings (sampled at 20Hz) were taken with the catheter not moved by the operator. At alternate locations, CF was deliberately changed for the second two readings. Location data for the catheters were recorded for each point over a 60Hz sampled 2.5s window.

In the ablation phase, study ablations were performed during WACA and, for patients with persistent AF, complex fractionated atrial electrogram ablation. All study ablations were 30s in duration, with the catheter in a stable position for at least 2.5s prior to radiofrequency energy delivery, and at least 8s after cessation. Ablations were performed in temperature-controlled mode with the temperature limited to 48°C, and power to 30W. The irrigation flow rate was 2ml/minute during mapping and 17ml/minute during ablation (manufacturer's recommendations). All ablations were performed at a CF of 5-40g. Locations where there was macro-displacement were

discarded. Location markers were manually applied pre and post-ablation on Carto3, as well as lesion markers during ablation. All study ablations were non-overlapping and, once completed within a lesion set, further ablation was at the operator's discretion.

Respiratory gating was not used as data during the whole sampling period were analysed for each point. Impedance during ablation was measured between the tip of the ablation catheter and the ground patch (on the patient's left thigh), using a 50 kHz current, and recorded at 10Hz.

All data were processed and analysed using custom-written Matlab (MathWorks, Natick, MA, USA) scripts as described in Chapter 2.7.

Electrogram, impedance and FTI data were processed using previously described methods (Chapter 2.7)<sup>206</sup>. Impedance data were processed to remove noise using a Savitzky-Golay filter. The percentage impedance drop during ablation was determined using the filtered impedance waveform, comparing initial impedance to the minimum recorded during an ablation. FTI was determined by the area under the CF curve derived using trapezoidal integration. To investigate the relationship between FTI and impedance drop, all ablations were divided into consecutive, cumulative, 10g.s FTI intervals. The maximum impedance drop was then compared with the initial impedance at the ablation's start.

Electrogram attenuation was assessed by comparing the median complex size (each complex in the signal being identified by a custom-written script, Chapter 2.7<sup>206</sup>). The electrograms analysed in this part of the study were bipolar electrograms (set up between the distal adjacent electrodes on the ablation catheter). Signals in the electrogram recording system were recorded at a low cut-off of 30Hz and a high cut-off of 250Hz. The peaks and troughs in the signal were identified using a 70ms cut off as used in previous published work to prevent double counting of complexes<sup>98</sup>.

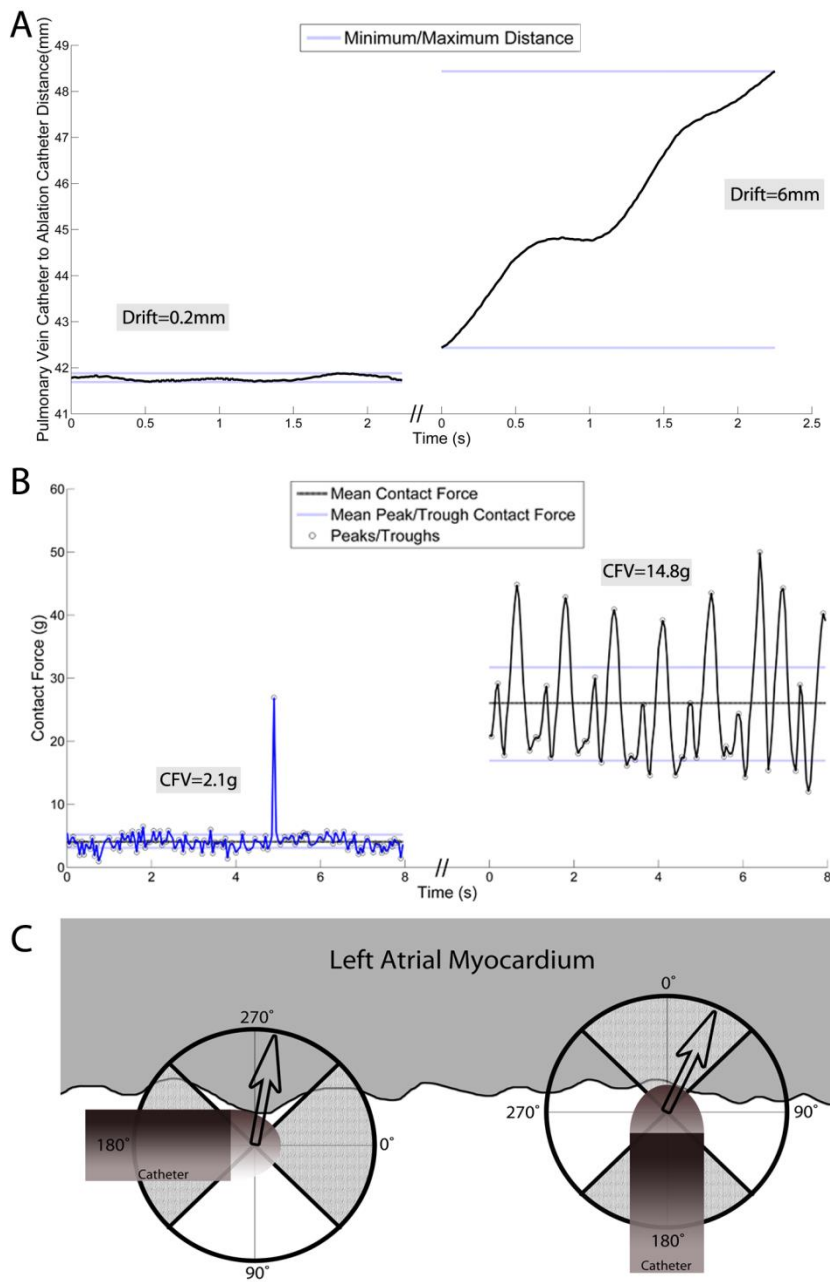


**Figure 5.1 Catheter stability and orientation analysis.** (A) Change in distance between the ablation catheter and pulmonary vein catheter location over time at two locations. Catheter drift is the difference between the minimum and maximum distance between these catheters. (B) Contact force (CF) waveform over time at two mean contact forces – the contact force variability (CFV) is the difference between the mean trough and peak CF. The mean CF is indicated by the solid line while the mean peak and trough CFs are indicated by the dotted lines. On the left of the image is a waveform at low mean CF with low CFV, while on the right is a waveform at higher CF with higher CV. (C) The angle of catheter contact with myocardium. The shaded parts of the circle were considered perpendicular contact zones, the unshaded portions parallel contact. Arrows represent vector of contact. Left is an example of parallel contact, right perpendicular contact.

Complexes less than 0.05mV (peak to trough) were assigned as noise<sup>201</sup> based on



review of the signals and previous work<sup>217</sup>. The angles of the rising and falling signal were determined for the dominant peak or trough in a complex, from a point at one-third of the complex size from the peak or trough of the signal. A correction factor of 1000 (500 if the electrogram was sampled at 2Khz) for angle measurements was used to make the signal equivalent to that displayed on LabSystem Pro at a sweep speed of 100mm/s and a 32x scale. A rising or falling angle of over 45° meant the complex was discarded as farfield<sup>98</sup>. The complex size was measured from the dominant peak to trough of a complex.

Electrogram morphology change<sup>141</sup> was assessed manually using bipolar and unipolar (referenced to an indifferent electrode in the inferior vena cava) electrograms. Unipolar signals were analysed in preference for this analysis but bipolar signals were used where the unipolar signals were poor quality or where the unipolar morphology did not conform to the morphology scheme. The electrogram analysis was conducted only for the SR points in view of the unreliability of assessing electrogram attenuation in the fibrillatory signal<sup>206</sup>, and as electrogram morphology criteria have been histologically validated only in SR<sup>141</sup>.

The circular PV catheter was kept in a stable position in a pulmonary vein during acquisition of mapping or ablation data. The drift of the ablation catheter was determined by referencing the displacement of the sensor to an averaged PV electrode to correct for respiratory motion. The averaged electrode was derived by averaging the location of all 20 PV electrodes. The drift was taken as the range of the distance to this averaged electrode over the recording window (Figure 2. 5). To increase the accuracy of the drift measurement for an ablation, this was taken as the average of the displacements for the pre-ablation, ablation and post-ablation marker points.

The absolute CF range would be influenced by outlier values, therefore, to quantify the peak to trough variation in the CF waveform, (the contact force stability) an averaged measure, the CF variability (CFV), was used (Figure 5.1). This was determined by first identifying all the peaks and troughs in the waveform using an automated script. The peaks were averaged to give an average peak value and the same done for the troughs. The difference between these averaged values gave the CFV.

To define parallel and perpendicular catheter contact, the direction of the CF vector was considered relative to the catheter's axial plane. The contact angle was sampled at 20Hz and recorded as 0-360°, with 0° as the direction the catheter was pointing. Contact was assigned as perpendicular by an automated script if 315° to 45° or 135° to 225°: otherwise it was assigned as parallel (Figure 2.5).

### **5.3.1 Statistics**

Statistical analysis was performed using SPSS (IBM SPSS Statistics, Version 20 IBM Corp, Armonk, NY, USA) and Matlab V7.12 (Statistics Toolbox V7.5). A p-value of <0.05 was taken to indicate statistical significance. Correlations were assessed using a Pearson's correlation where the relationship was linear and a Spearman's rank correlation otherwise. Point-Biserial correlation was used where a continuous variable was compared with a binary one. Normally-distributed data were analysed using a t-test or ANOVA and non-normally-distributed data using a Mann-Whitney U test or Kruskal-Wallis test. Data are presented as mean±standard deviation or median(range). Multivariate regression analysis was used to assess the influence of different factors on the CFV and impedance drop. In the case of impedance drop, the observation that the relationship between the FTI and impedance drop is logarithmic<sup>206</sup> was used to perform linear regression.

## 5.4 Results

**Table 5.1 Study Population Baseline Characteristics**

Number of Patients	30
Age, mean±SD	61±8 years
Gender	21male (70%)
Persistent Atrial Fibrillation	15 (50%)
Duration of Persistent Atrial Fibrillation	20±12 months
CHA <sub>2</sub> DS <sub>2</sub> -VASc Score, mean±SD	1.4±1.0
Left Atrial Diameter, mean±SD	4.4±0.6cm
Severe Left Ventricular Impairment (Ejection Fraction<35%)	2 (7%)
Manual Navigation	12 (40%)

Baseline characteristics of the study patients are presented in Table 5.1.

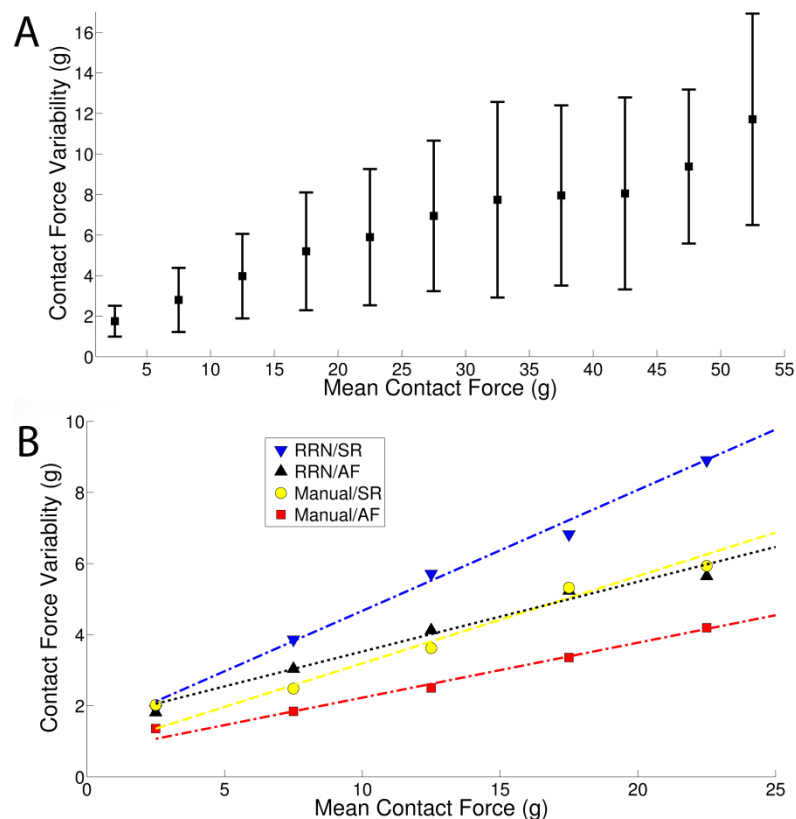


**Figure 5.2 Contact Force Versus Contact Force Variability.** (A) Comparison of mean contact force with contact force variability. Points are mean values for at least 5 measurements (2897 measurements represented in chart). Error bars represent standard deviation. (B) Factors affecting contact force variability. Points are mean values for at least 30 measurements. The linear portions of the curves are shown with lines of best fit. The significance of each factor is displayed in Table 5.2.

All persistent AF patients were in AF at the time of the procedure, as was one of the paroxysmal AF (PAF) patients.

### 5.4.1 Mapping Results

The mean CF was compared to the contact force variability (CFV: the difference between the mean peak and trough CFs in the CF waveform) for 2,298 points (1714 AF; 631 manual, 77±41 points per patient). As the former increased, there was an increase in the CFV (Figure 5.2A, p<0.0005, Spearman’s *rho* 0.6). The relationship was linear until 25g of mean CF, above which the rate of increase levelled off before a further rise from 45g.

**Table 5.2 Multivariate analysis of factors affecting contact force variability**

Co-factor	Unstandardized $\beta$ (95% Confidence Interval)	Number of points	p-value
Mean contact force (g)	0.05 (0.05 to 0.06)		<0.0005
Perpendicular Contact	-0.03 (-0.07 to 0.02)	835	0.2
Remote Robotic Navigation	0.45 (0.41 to 0.5)	1288	<0.0005
Sinus Rhythm	0.29 (0.24 to 0.34)	497	<0.0005
Left pulmonary vein antrum	0.17 (0.09 to 0.25)	287	<0.0005
Left atrial appendage ridge	0.21 (0.13 to 0.29)	260	<0.0005
Postero-inferior wall	0.17 (0.09 to 0.25)	259	<0.0005
Antero-septal wall	0.2 (0.13 to 0.27)	338	<0.0005
Posterior wall	0.24 (0.15 to 0.33)	178	<0.0005
Roof	0.35 (0.26 to 0.44)	150	<0.0005
Left lateral wall	0.36 (0.23 to 0.5)	56	<0.0005

Dependent Variable: Ln(Contact force variability)

Reference location: Right Pulmonary Vein Antrum (277 points)

Adjusted R<sup>2</sup>: 0.45

A positive  $\beta$  value for a co-factor means that if all the other co-factors are unchanged, the contact force variability will be higher as it increases or is present (and *vice versa*)

To explore factors influencing the relationship between the mean CF and CFV, multivariate regression analysis was performed where the mean CF was <25g (1,805 points), allowing comparison of the linear portions of the curves (Table 5.2). The use of RRN and being in SR rather than AF was associated with greater CFV (Figure 5.2B).

Location had a significant influence on the CFV: the right PV antrum had the lowest CFV, the roof and left lateral wall the highest.

There was a weak correlation between the catheter drift and mean CF (Spearman's  $\rho$  -0.07,  $p=0.001$ ) but not CFV and drift (Spearman's  $\rho$ ,  $p=0.9$ ). No difference in locational stability was afforded by perpendicular or parallel contact ( $p=0.34$ ). There was no difference in the drift by atrial rhythm for manual navigation, but with RRN, drift was higher in SR than AF; drift was lower in SR for manual rather than RRN points, with the converse true in AF (Figure 5.3).

### 5.4.2 Ablation Results

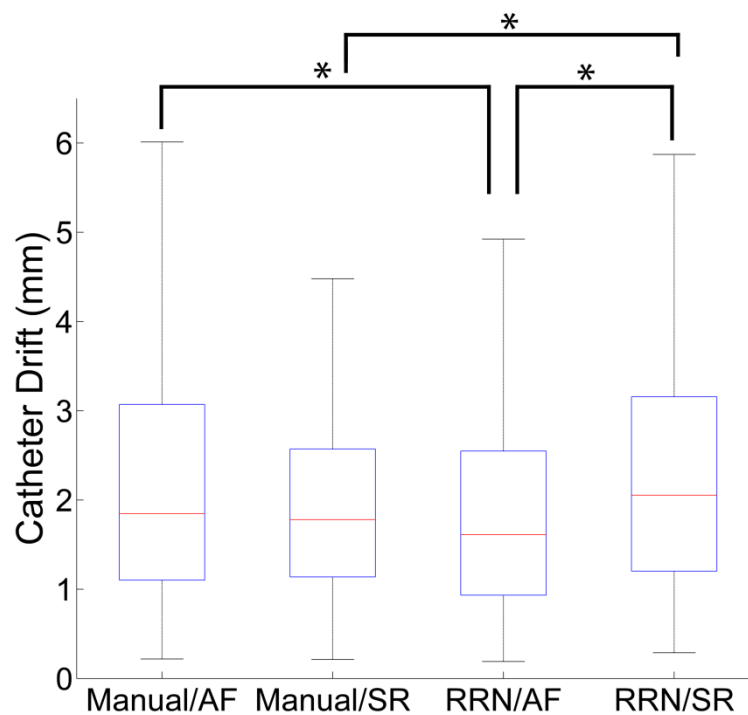
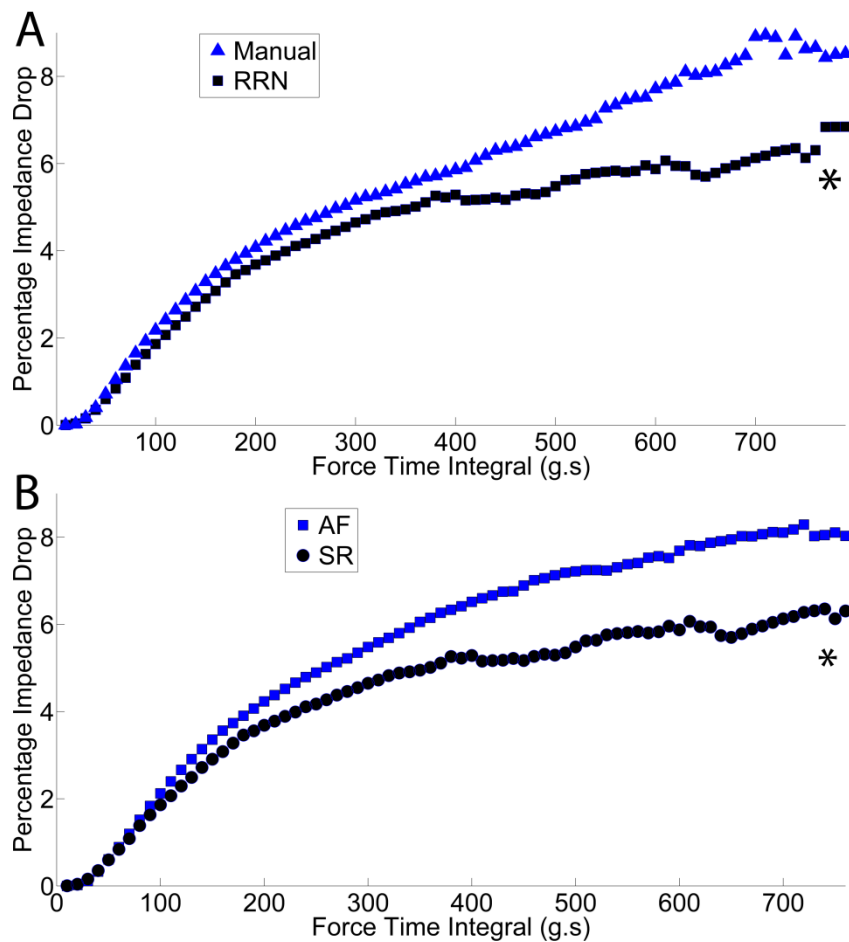
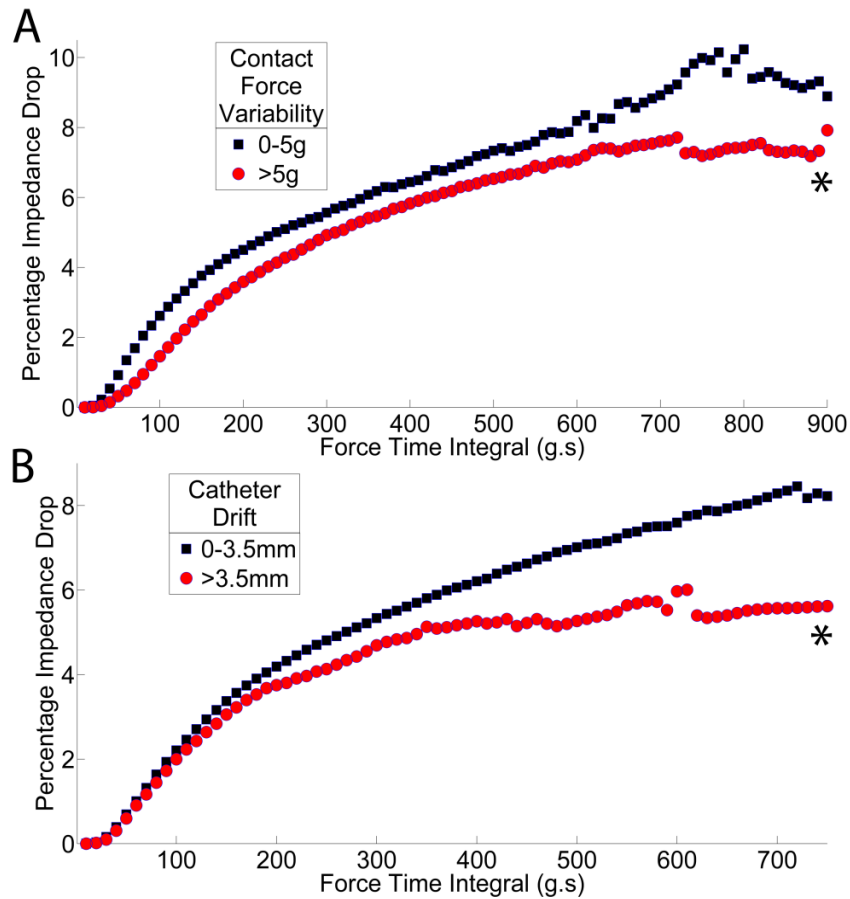


Figure 5.3 Catheter drift by navigation mode and atrial rhythm.



**Figure 5.4 Factors affecting impedance drop during ablation.** (A) Navigation mode (SR ablations) and (B) Atrial Rhythm (RRN ablations). Each point is the mean of at least 10 ablations. \* $p < 0.0005$  from Table 5.3

The impact of catheter contact orientation, CFV, catheter drift, atrial rhythm and location on impedance drop was assessed. 747 ablations were analysed (395 RRN, 352 manual) - ablations performed after the study ablations were completed in a region were not included in the analysis. . The FTI was higher for RRN ablations (440( 85-1362)g.s, manual: 329(117-1024)g.s  $p < 0.005$ ), parallel contact (412(85-1179)g.s, perpendicular: 365(121-1362)g.s  $p = 0.005$ ) and ablations in AF (395(86-1362)g.s, SR: 374(85-1123)g.s,  $p = 0.036$ ). The incremental FTI analysis generated 32,826 measurements.



**Figure 5.5 Factors affecting impedance drop during ablation.** (A) CFV and (B) Catheter drift. Each point is the mean of at least 10 ablations. \* $p < 0.0005$  from Table 5.3

Increasing catheter drift (especially  $>3.5\text{mm}$ ), CFV (especially  $>5\text{g}$ ), SR and RRN rather than manual navigation were associated with shallower logarithmic relationships between the impedance drop and FTI (Figures 5.4 and 5.5). As each ablation was subject to a combination of factors, and to elucidate the importance of these factors to the efficacy of ablation, multivariate regression analysis was performed (Table 5.3). A locational drift  $>3.5\text{mm}$ , CFV  $>5\text{g}$ , perpendicular rather than parallel contact and RRN were associated with a lesser impedance drop per FTI as was being in SR rather than AF.

412 SR ablations were included in the electrogram analysis. Of these, 100 were excluded based on the automated analysis: 3 as there were no identifiable complexes at the start of ablation and 97 as the post-ablation electrogram was larger than the pre-ablation electrogram (suggesting micro-displacement). Of these, for the morphology analysis, 113 ablations were excluded as the pre-ablation morphology did not conform to the three validated pre-ablation morphologies<sup>141</sup> – generally either as the signal was fractionated or an RS bipolar morphology. Of the remaining ablations, 65% were transmural based on electrogram morphology criteria. On binary logistic regression, including the FTI, CFV, contact orientation, catheter drift and navigation mode, only the catheter drift (in mm) was found to be predictive of transmural lesion based on these criteria:  $p=0.01$ , odds ratio of transmural lesion 0.71 (95% confidence interval 0.55 to 0.92). The Nagelkerke  $R^2$  for the model was only 0.06 suggesting it was poorly predictive. FTI was not significantly predictive of transmural lesion ( $p=0.6$ ) in this model, and there was no correlation between the FTI and transmural lesion by these criteria when analysed separately ( $p=0.86$ , Point-Biserial correlation), or comparing an

**Table 5.3 Multivariate analysis of factors affecting the impedance drop with ablation**

Co-factor	Unstandardized $\beta$ (95% Confidence Interval)	p-value
Ln(Force Time Integral) g.s	0.78 (0.77 to 0.78)	<0.005
Remote Robotic Navigation	-0.12 (-0.14 to -0.1)	<0.005
Catheter drift >3.5mm	-0.23 (-0.25 to -0.21)	<0.005
Contact Force Variability >5g (g)	-0.24 (-0.25 to -0.23)	<0.005
Perpendicular Contact Orientation	-0.02 (-0.03 to -0.004)	0.006
Sinus Rhythm	-0.16 (-0.17 to -0.14)	<0.005

Dependent Variable: Square root of percentage impedance drop

Adjusted  $R^2$ : 0.7

A positive  $\beta$  value for a co-factor means that if all the other co-factors are unchanged, the impedance drop will be higher if the co-factor is present or increases (and *vice versa*)



FTI  $\leq 500$ g.s to  $>500$ g.s ( $p=0.5$ ). The post ablation electrograms were significantly attenuated compared with pre-ablation ( $p<0.0005$ ), with a median attenuation of 45(0-100)%, but the degree of attenuation did not correlate with the FTI ( $p=0.74$ ), with no significant difference in attenuation for ablations above or below 500g.s ( $p=0.6$ ). Similarly, there was no correlation with the CFV, catheter drift or mean CF ( $p>0.05$  for each). There was no significant difference in electrogram attenuation by contact orientation or navigation mode ( $p>0.05$  for both).

## **5.5 Discussion**

This study demonstrates that an increase in mean CF is associated with an increased CFV and this relationship varies by LA location. An increasing CF is weakly associated with less catheter drift. The use of RRN is associated with increased CFV as is being in SR. The atrial rhythm does not affect catheter drift with manual navigation but being in SR is associated with increased drift with RRN, and in SR the use of RRN is associated with increased drift compared with manual navigation (while the converse is true in AF). Catheter contact orientation does not affect CFV or catheter drift. The impedance drop/FTI relationship is steeper for RF applications with less drift, lower CFV, parallel rather than perpendicular contact, and when manual navigation is used.

CFV at a point is likely predominantly secondary to respiratory and cardiac motion. Previous work assessing variability of CF using a Force Variability Index found that apnoea was associated with less variability<sup>172</sup>: as none of the cases in the current study were performed with general anaesthetic, this finding could not be explored here. During AF, a major contributor to the CFV is ventricular contraction: in SR, CFV is additionally influenced by global and local (to the catheter) atrial

contraction. This is likely the explanation for the higher CFV observed in SR recordings in the current study.

As mean CF increases, CFV increases. It is hypothesized this is due to a change in the properties of the underlying tissue: at low CF the myocardium has a large capacity for stretching and can buffer sources of variability such as cardiac motion from affecting contact with the catheter; at higher CF, CFV increases, suggesting that less of this variability is buffered by the tissue and more transmitted to the catheter tip. This suggests LA compliance reduces with increasing applied CF.

Contributing to the mean CF/CFV relationship is the stiffness of the ablation catheter and sheath, and this would be influenced by the degree and number of deflections undergone in reaching a location. A stiffer sheath and catheter, as well as a less compliant (stiffer) myocardial region, presumably means more of the variability in the contact secondary to cardiac motion and respiration is transmitted to the catheter tip, leading to a higher CFV for a given CF. Evidence for this is the increased CFV observed for points taken with the stiffer robotic sheath compared with those taken with the softer Mullins sheath.

The relationship between mean CF and CFV levels off at around 25g of CF. In canine LA studies, tissue tenting is visible on intracardiac echocardiography at 25g of CF<sup>137</sup>. The levelling off observed may therefore represent the onset of tenting secondary to catheter contact, with the myocardium adjacent to the catheter having become maximally stretched and the surrounding tissue being recruited to deform by the continued catheter tip pressure. Beyond 45g, there is another rise in the CFV with mean CF, and this may represent the capacity for the adjacent myocardium to buffer changes in CF being exceeded as a precursor to perforation.

In man, the compliance of the LA as a whole has been studied using cardiac catheterization<sup>48</sup> and echocardiography<sup>49</sup>. In canine studies, a regional difference in LA compliance has been observed on comparing the LAA with the LA body, with the former having a higher compliance<sup>45</sup>. In the current study, the steepest relationship between CFV and mean CF was found at the roof, with the right PV antrum having the shallowest relationship. The LAA was between the two regions in terms of the relationship. As stated earlier, we speculate this relationship would not just be related to the characteristics of the myocardium but also the catheter and sheath and the degree of respiratory motion to which an area is subject. In the case of the right PV antrum, the deflection involved in accessing this region through a trans-septal puncture may lead to a reduction of the transmission of the variability in the CF an increased myocardial contact would normally cause. One would predict the roof to be most greatly affected by respiratory motion which would have a major impact on the CFV here.

The catheter drift analysis conducted in this study is novel. By referencing the drift to the pulmonary vein catheter, the aim was to study drift of the catheter relative to the myocardium rather than secondary to respiratory motion (where the contact point with the myocardium may in fact not be altered). As the CF increased there was a minor reduction in the amount of catheter drift observed suggesting an increased stability of the catheter as one would expect. The atrial rhythm did not impact on the catheter drift for manual points. This may relate to the flexibility of the Mullins sheath allowing it to deform with cardiac contraction and so maintain its position. In the case of the RRN points, SR was associated with reduced catheter locational stability. In this case, the stiffer sheath may be less able to deform with cardiac contraction and so maintain its position at a point. Supportive of this hypothesis is that in AF, RRN is associated with increased stability, while for SR points, where cardiac contraction

would have a greater influence, RRN points are less locationally stable than points collected manually. Previous work has suggested an increased locational stability using RRN rather than manual navigation during sinus rhythm<sup>150</sup>, but the methodology there was to compare the location of markers taken 30-60s apart, while the approach in the current study, using a 60Hz sampled 2.5s window around the time of marker placement analyses a higher volume of data.

In preclinical studies, a correlation has been observed between impedance drop<sup>164,166</sup> and FTI<sup>171</sup> during ablation with lesion size. During clinical ablation, impedance drop has been used as a surrogate for lesion dimensions and correlates with CF during ablation<sup>169,206</sup>. The variability of the impedance drop for a single measurement makes it an unreliable marker of the effect of an individual clinical ablation<sup>206</sup>. On the other hand, multiple impedance measurements are taken during an ablation allowing an incremental analysis of the effects of ablation (and by extension, lesion maturation). By combining multiple ablations and analysing them incrementally to produce a large volume of data, the variability in impedance measurements is mitigated to allow the underlying relationships to be explored. Accordingly, the effect of different contact parameters on the impedance drop relationship as a whole was used to assess the effect on ablation efficacy.

Ablations were less effective for patients in SR, even when the CFV and catheter drift were included in the model. This may be due to differences in the underlying atrial tissue itself between patients with persistent AF and PAF, though as all of the former patients in the cohort were in AF and all but one of the latter in SR, it is not possible to rule out that the difference was related to the rhythm itself (and not accounted for completely by differences in catheter drift and CFV).

CFV significantly impacted on the relationship between FTI and impedance drop: a greater CFV led to a shallower relationship, suggesting less effective ablation. The impact of the variability of CF on lesion size has been studied *in vitro*<sup>171</sup>: in that study more variable contact resulted in smaller lesions, but of note, it also resulted in a lower FTI. In the current study, the FTI was controlled for using multivariate analysis and the CFV found to independently affect ablation. It is possible that a high degree of CFV leads to a cooling effect on the tissue through stretching and unstretching, attenuating the tissue heating from radiofrequency energy delivery, and so reducing the effect of ablation. Consequently, it seems advisable to reduce CFV where possible during ablation.

An increased locational drift (>3.5mm) was associated with reduced ablation efficacy. It is unsurprising that locational stability would impact on ablation efficacy—more instability would result in inconsistent RF energy delivery to tissue and over a wider area, leading to less efficient tissue heating and so a smaller lesion. 3.5mm is the length of the ablation element for the catheter used in the study and may be why the impedance drop relationship changes markedly beyond this. During ablation, an observation of greater locational instability should therefore encourage an operator to either ablate to a higher FTI or, preferably, adjust the catheter position.

The impedance drop was higher with parallel contact, though the impact was of a lower magnitude than other parameters. The effect of orientation observed is the opposite of what one might expect as *in vitro* work suggests that with irrigated ablation, lesions are larger with a perpendicular catheter orientation<sup>222</sup>. While the latter work made comparisons based on the orientation of the catheter as a whole, the current study had the benefit of access to the orientation of contact itself, as measured at the catheter tip, and measured the CF directly at the contact point rather than extrapolating this. As

the ablation element is based in the catheter tip, we would suggest assessing contact parameters in this region is more relevant to ablation. Another group examined the effect of contact orientation on impedance drop and also found that impedance drop was lower in a perpendicular orientation: they speculated this might be because less of the catheter tip was in contact with the tissue than when the contact orientation was parallel<sup>169</sup>. A limitation of that study was that CF was lower in the perpendicular orientation ablations. Such confounding was avoided in the current work by factoring in the FTI through multivariate analysis.

RRN was associated with a shallower impedance drop/FTI relationship than manual ablation. This suggests there are factors related to the quality of contact when using RRN rather than manual ablation which means that the impedance drop is lower for the same FTI. This difference is not explained fully by differences in CFV and catheter drift as it remains even when these are present in the model, and suggests FTI targets may need to be adjusted for each navigation mode. The CF for RRN ablation was higher than for manual ablation, and it may be that the ease of attaining a higher CF (and so FTI) with this stiffer sheath outweighs the disadvantages in terms of efficacy when using this.

Previous clinical work has found a very strong relationship between changes in SR electrogram morphology and attenuation and FTI<sup>187</sup>. In the current study, we did not observe this relationship, and in fact none of the other contact parameters other than catheter drift were found to correlate. Part of the explanation for these results is likely the small amount of catheter motion present during the electrogram recording period affecting the electrogram observed, especially in the attenuation analysis where 8s of electrograms were compared. An electrogram-based analysis would be very sensitive to catheter drift, especially as it can only be performed at two time points (pre- and post-

ablation). In the current study it was also found that a reasonable proportion of electrograms observed did not strictly correspond to the morphologies validated histologically as corresponding to transmural or non-transmural lesions which made these criteria more difficult to apply to the data. Based on previous work<sup>164,166,171</sup> it seems unlikely that the lack of correlation with electrogram parameters reflects the FTI and impedance drop having no correlation with lesions size.

### **5.5.1 Limitations**

Contact orientation was treated as a binary rather than continuous variable and assessed in only one plane – the simplifications were used to facilitate analysis. Study ablations were performed with unchanged temperature and power settings: it is not clear how applicable the results would be to other ablation settings.

### **5.6 Conclusions**

This study highlights the complexities of catheter contact within the LA and expands on previous work focusing on the ablation FTI to further explore contact parameters affecting the efficacy of ablation. In this regard, an increased catheter drift and CFV reduce ablation efficacy, as does perpendicular catheter contact and RRN. Therefore, this work suggests the quality of catheter contact, not just its magnitude and duration, affects efficacy. The establishment of target contact parameters is becoming increasingly relevant to clinical ablation with the release of automated lesion marker placement software able to place markers on fulfilment of user-specified contact and ablation parameters<sup>223</sup>, with the current study contributing to establishing optimum values for such parameters. The clinical impact of adopting the targets suggested by the current work requires further prospective evaluation, but by optimizing every delivered

radiofrequency application, one would hypothesize the outcomes from AF ablation procedures would improve.



## 6. Contact Force and Pulmonary Vein Reconnection in Persistent Atrial Fibrillation Ablation: Impact of Steerable Sheaths

### 6.1 Abstract

**Background:** Catheter CF during ablation is predictive of sites of pulmonary(PV) reconnection. The impact of steerable-sheaths on ablation CF and PV reconnection sites was investigated.

**Methods and Results:** 5464 ablations were analysed in 60 patients undergoing first-time persistent AF ablation using a CF-sensing catheter: 19 manual non-steerable sheath (Manual-NSS), 11 manual steerable-sheath and 30 robotic steerable-sheath procedures. Individual WACA lesions were localised using clock-face segmentation and locations of PV reconnections noted acutely and at repeat procedures (26, at a median 8(2-17) months). CFs were higher in the steerable sheath groups ( $p < 0.0005$ ), but less consistent per WACA segment ( $p < 0.005$ ). There were significant differences in the mean CFs around both WACAs by group: in the left WACA, CFs were lower with Manual-NSS other than at the anterior-inferior and posterior-superior regions, and lower in the right WACA, other than the anterior-superior region. CF was significantly lower for ablations in reconnecting segments acutely and at repeat procedures. There was a significant difference in the proportion of segments chronically reconnecting across groups: Manual-NSS 26.5%, manual steerable sheath 4.6%, robot 12%,  $p < 0.0005$ . The left atrial appendage/PV ridge and right posterior wall were common sites of reconnection in all groups.

**Conclusions:** WACA ablation CFs during ablation for persistent AF are predictive of reconnection both acutely and chronically. Steerable-sheaths are associated with increased ablation CF but lower consistency, and there are segments where they fail to increment CF. Certain WACA regions remain prone to reconnection regardless of steerable sheath usage.

## **6.2 Introduction**

Steerable sheath technology aims to improve the AF ablation procedure by providing increased control over catheter manipulation. Such technologies include RRN (Sensei Robotic Catheter System, Hansen Medical Inc., CA, USA) and manual steerable sheaths. Use of steerable sheath technologies may fundamentally affect the quality of contact with the myocardium compared with manual non-steerable sheaths in view of their increased stiffness and potentially greater consistency of contact.

Recent work suggests the adoption of CF-sensing catheters may improve procedural parameters in AF ablation<sup>180,181,224</sup>. Catheter CF during ablation may be important for safety, as excessive contact can lead to myocardial perforation<sup>186</sup>. CF is also important from the viewpoint of efficacy, with higher contact during ablation associated with increased lesion size<sup>153</sup>. From a clinical perspective, reconnecting segments in pulmonary vein isolation lines are more likely to have been ablated at lower CF<sup>172,177,178</sup>.

In this study, we therefore sought to examine the impact of steerable sheath technology on CF, and its consistency, around the WACA lines. Such a study has now become possible *in vivo* due to the availability of CF information when using CF-sensing catheters. The WACA lines were analysed using a segmental model in order to

facilitate detailed regional comparisons in accordance with previous work<sup>172,177,178</sup>. The patterns of immediate and late WACA-segment reconnection were also between technologies: as chronic reconnection was investigated at clinically indicated redo-procedures, a persistent AF population was studied (since these patients are more likely than PAF patients to require repeat ablation<sup>86</sup>).

Our hypothesis was that the technology used to deliver the catheter to the left atrium would impact on the contact forces exerted during ablation and this in turn would directly affect the pattern of WACA reconnection.

### **6.3 Methods**

The study conforms to the guiding principles of the Declaration of Helsinki and all procedures were performed with the patients' informed consent in accordance with local institutional guidelines. Consecutive patients with persistent AF having their first ablation for persistent AF were included in the study. A Thermocool SmartTouch catheter (Biosense Webster Inc., Diamond Bar, CA, USA) was used for ablation guided by the Carto3 electroanatomical mapping system (Biosense Webster Inc.). Patients were divided into 3 groups:

1. Manual-NSS group – using a non-steerable trans-septal sheath (Mullins sheath, Medtronic, MN, USA).
2. Agilis group – using the Agilis NxT steerable trans-septal sheath (St Jude Medical, MN, USA).
3. RRN group

Patients who had crossed over between groups during ablation were excluded.

Procedures were performed in the post-absorptive state under intravenous moderate sedation. Percutaneous access for all catheters was through the right femoral vein. A catheter was placed in the coronary sinus. In the non-RRN groups, two sheaths were positioned in the left atrium, for the SmartTouch (Agilis or Mullins

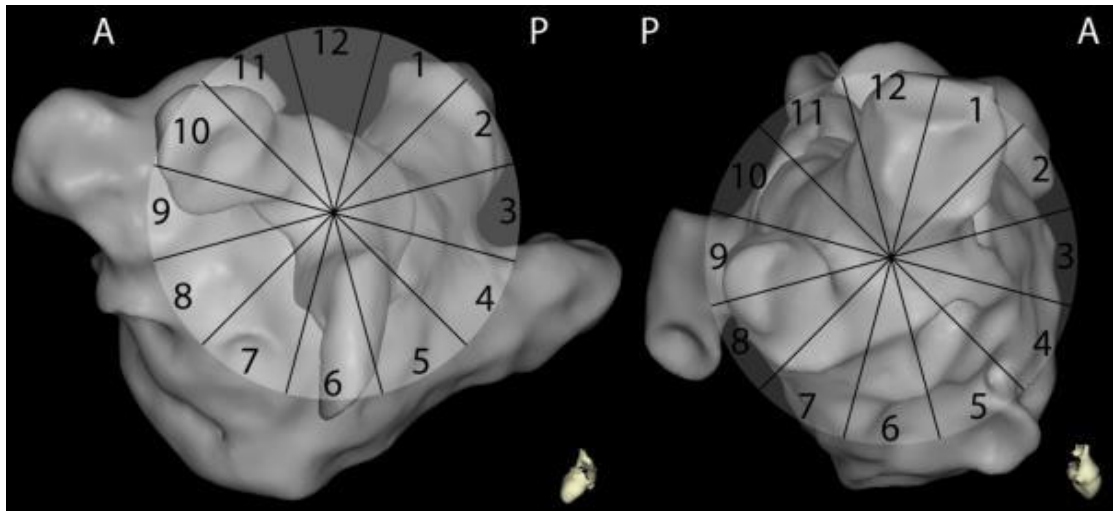


**Figure 6.1 Clock face scheme for assigning ablation location in wide area circumferential ablation lines.**

*Left Side – Left Pulmonary Veins; Right Side – Right Pulmonary Veins*

*A=Anterior; P=Posterior*

sheath) and circular PV catheters (Mullins sheath). For the robotic group, the SmartTouch catheter was passed through an Artisan sheath (Hansen Medical Inc.) and the circular PV catheter through a Mullins sheath.

Ablations were performed with ablation settings at the discretion of the operator, generally in temperature-controlled mode with the temperature limited to 48°C, and power to 30W. WACA was performed to encircle the left- and right-sided PVs as a pair, aiming for entrance block with the initial encirclement, and with exit block confirmed subsequently when the patient was in sinus rhythm (generally through ablation or cardioversion). The ablation of lines of block beyond pulmonary vein isolation and the targeting of fractionated activity subsequent to WACA was at the discretion of the operator. If arrhythmia persisted as an organized atrial tachycardia,

this was mapped and ablated. If arrhythmia could not be terminated, external cardioversion was performed.

Throughout the procedure, operators had access to the CF data. While the force used was at the discretion of the operator, a target 5-40g force range was used.

The location of each ablation was determined from the ablation points recorded on Carto3. Each ablation was assigned a clock face location within a WACA. To do this, the PV pair was viewed in a lateral orientation (left lateral for the left veins and right lateral for the right side). The orientation was then tilted in the cranial-caudal plane so that the intervenous ridge was in the centre of the view. The circumference of the PV pair (along which the WACA lesions were placed) was then divided by a clock-face (Figure 6.1). This meant that 6 o'clock and 12 o'clock were the floor and roof of the left atrium respectively. For the left WACA, 9 o'clock was anterior, while on the right side, 3 o'clock was anterior.

A minimum waiting time of 30 minutes was used in order to judge whether a vein had acutely reconnected<sup>225,226</sup>. Where veins were assessed prior to this time-point, they were excluded from the acute reconnection analysis. Where reconnection occurred acutely, the sites of reconnection were noted using the clock-face method discussed above, based on the signal on the PV catheter and response to ablation.

CF was sampled at 20Hz and the data exported from Carto3 analysed using custom written scripts in Matlab (MathWorks, MA, USA). Where the mean CFs for a WACA or for the procedure were required, CF measurements for the relevant ablations were combined into one long ablation and the average taken of the combined value (to prevent shorter ablations from being given equal weight to the mean as longer ablations). Where drag lesions were performed during WACA, a single ablation would commonly have multiple ablation lesion markers on Carto3 which crossed multiple

WACA segments. To obtain regional CF data, the ablation was subdivided between these marker points. Accordingly, the ablation was temporally subdivided from when the lesion marker point in question was applied to when the next location point was collected on the system. From these subdivided data, the mean CF was established for each point and the mean for a segment of the WACA then derived from the mean of these points in a segment. The ablation FTI was determined by trapezoidal integration of the CF waveform (Figure 2.5).

The consistency of the achieved CF within a WACA was quantified by examining the variability of the mean CFs per segment during the initial encirclement. This was established by assessing the standard deviation (SD) of the ablation mean CFs achieved in a segment for each patient individually. These values were then compared between segments and groups.

The patients' follow up after the procedure was according to the normal practices of the operator. In the case of patients from the cohort who went on to have repeat procedures for recurrent arrhythmia, the sites of reconnection were noted using the clock-face method discussed above.

### **6.3.1 Statistical Methods**

The groups were compared using parametric or non-parametric testing based on the distribution of the data. Normality of this distribution was assessed using a Jarque-Bera test, and appropriate transformations carried out to normalize the data. Parametric (ANOVA, t-test) or non-parametric tests (Mann Whitney U, Kruskal-Wallis) were used to compare the data. Categorical variables were compared using a Chi-squared or Fisher's exact test. A p-value <0.05 was considered statistically significant. Data is presented as mean±SD or median (range). Statistical analysis was performed using

SPSS (IBM SPSS Statistics, Version 20 IBM Corp Armonk, USA) and Matlab V7.12 with the Statistics Toolbox V7.5.

## 6.4 Results

Sixty patients were included in the study. The baseline demographics are presented in Table 6.1.

**Table 6.1 Study Population Characteristics**

	Total	Group			p-value comparing groups
		Manual-NSS	Agilis	RRN	
Number	60	19	11	30	
Age (years±SD)	60±10	62±10	60±16	59±7	0.9
Male Gender	52 (87%)	16 (84%)	9 (82%)	27 (90%)	0.7
LA diameter in cm, (range)	4.0 (4-6)	4.0 (4-6)	4.0 (4-5)	4.0 (4-6)	0.6
Ischemic heart disease	11 (18%)	1 (5%)	3 (27%)	7 (24%)	0.19
Diabetes	6 (10%)	3 (16%)	1(9%)	2 (7%)	0.6
Hypertension	20 (33%)	8 (42%)	3 (27%)	9 (30%)	0.6
Cerebrovascular disease	3 (5%)	1 (5%)	0	2 (7%)	0.7
Severe left ventricular impairment (Ejection Fraction<35%)	3 (5%)	1 (5%)	0	2 (7%)	0.6
CHA <sub>2</sub> DS <sub>2</sub> -VASc Score	1.3±1.2	1.5±1.5	1.3±1.2	1.1±0.9	0.4

There were no significant differences across the three groups. In terms of procedural complications these were all in the RRN group: one pseudoaneurysm and two minor (based on guideline criteria<sup>1</sup>) pericardial effusions, the latter diagnosed on routine post-procedure transthoracic echocardiography. The success rates at 12 months (off anti-arrhythmic drugs, as per guideline definitions<sup>1</sup>) were: Manual-NSS 9/19 (47%); Agilis 2/11 (18%), RRN 16/30 (53%) - p>0.05 for all comparisons.

### 6.4.1 Procedural Mean Contact Forces

There were 5464 individual radiofrequency applications in the study. Mean total CF in the Manual-NSS group was significantly lower than in other groups ( $p < 0.0005$ ), but there was no difference between the steerable sheath groups ( $p = 0.5$ ), Figure 6.2. The

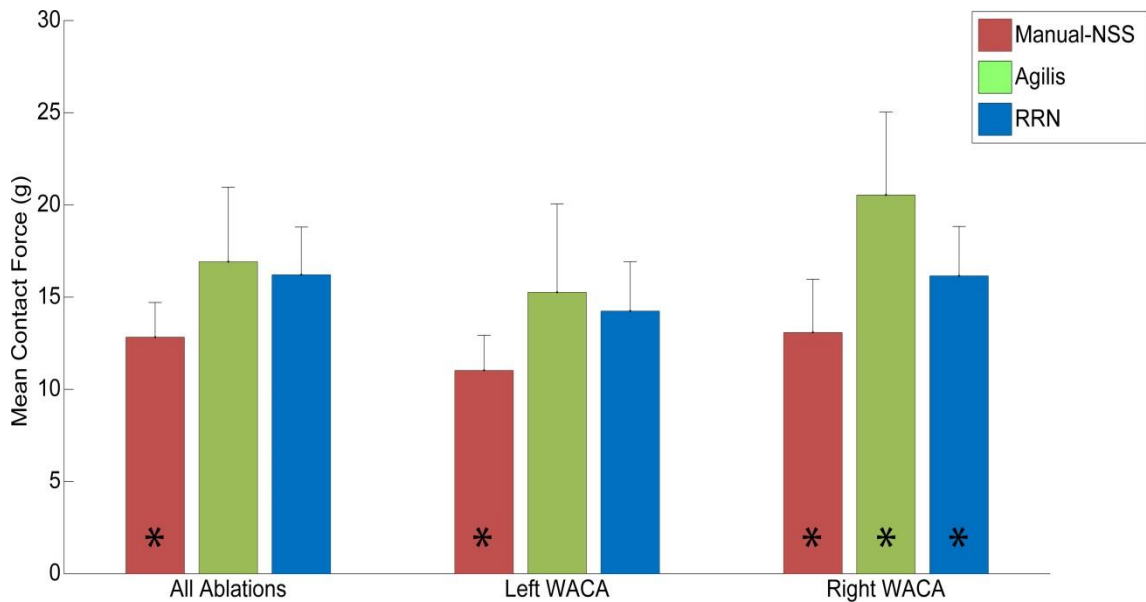


**Figure 6.2 Mean contact force during ablation.**

Error bars are standard deviation.  $* = p < 0.006$  compared with other groups

CFs in the left WACA were significantly lower than the right WACA for the whole cohort ( $p < 0.0005$ ) and also for each group individually ( $p = 0.01$  Manual-NSS,  $p = 0.03$  Agilis,  $p < 0.0005$  RRN).

### 6.4.2 WACA Segmental Contact Forces

There were 2,970 radiofrequency applications in the WACAs in the study, with 5,534 ablation points taken in Carto3. There was a variation in the locations of the peak and trough CFs in the WACAs in each group (Figure 6.3). Within each of the three groups, for each WACA, there was a significant heterogeneity of CFs between segments ( $p < 0.0005$ ).



In the left WACA, the CF was highest for all three groups at the superior-posterior segment. The lowest CF was at the left atrial appendage (LAA)/PV ridge in the Manual-NSS group, and the anterior-inferior region (7-8 o'clock) in both the Agilis and RRN groups. While the use of the RRN or the Agilis sheath led to a significant

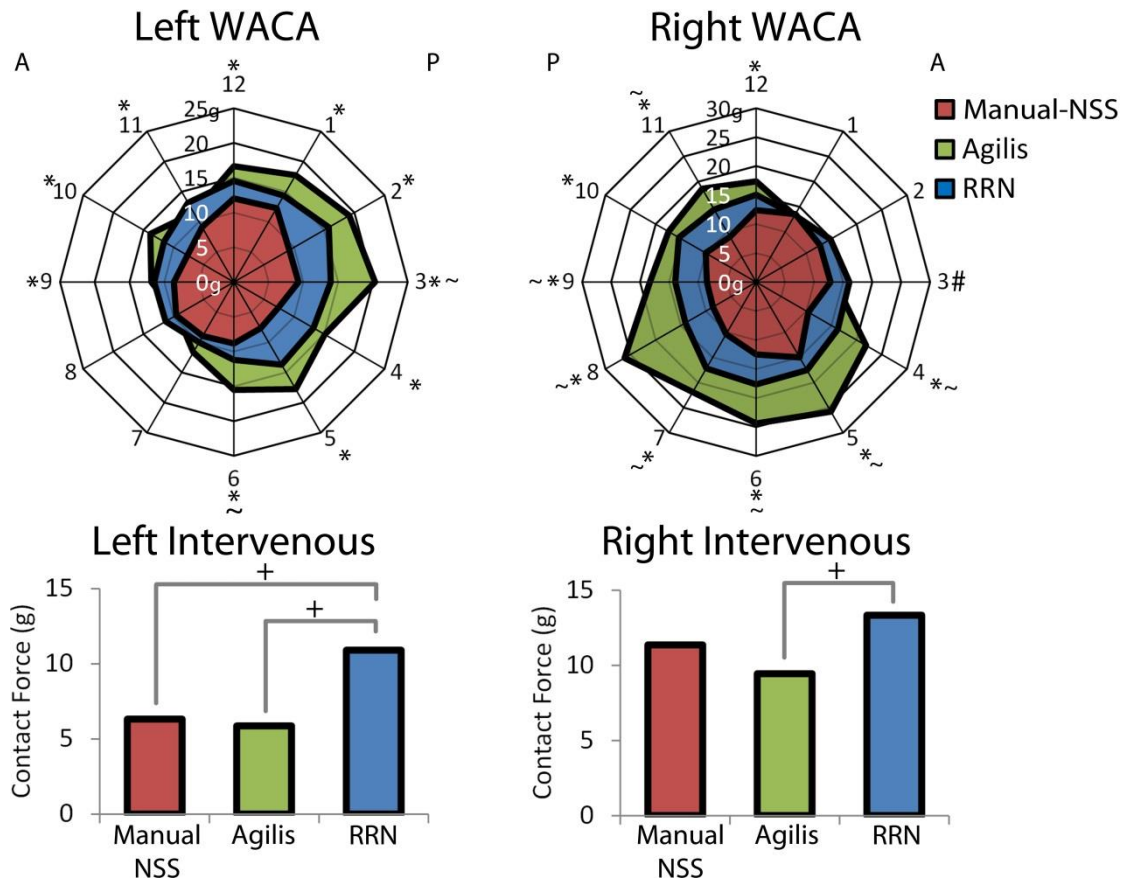


**Figure 6.3 Distribution of contact force in the right and left WACA.**

*Upper half:* Radar plots demonstrating the distribution of contact forces during initial pulmonary vein encirclement. The outer edge represents the clock face segment. The further from the centre of the plots, the higher the median contact force in grams. *Lower half:* Comparison of median contact forces during intervenous ridge ablation  
 \*=Significant difference between Manual-NSS and steerable sheath groups ( $p < 0.05$ );  
 #=Significant difference between RRN and Manual-NSS groups ( $p = 0.009$ ); ~ = Significant difference between RRN and Agilis group ( $p < 0.05$ ); +=Significant difference between indicated groups ( $p < 0.05$ )

increase in the CFs in most of the left WACA compared with the Manual-NSS group, there was no significant impact on the anterior-inferior (7-8 o'clock) region. The Agilis group had significantly higher CFs than the RRN group at 3 and 6 o'clock ( $p < 0.0005$ ).

In the right WACA, the highest CFs for all modalities were at the inferior quadrant (4-8 o'clock). The use of steerable sheaths was associated with an increased CF during ablation in all regions other than the anterior-superior segment where the 3 groups were approximately equal. Agilis sheath use was associated with significantly

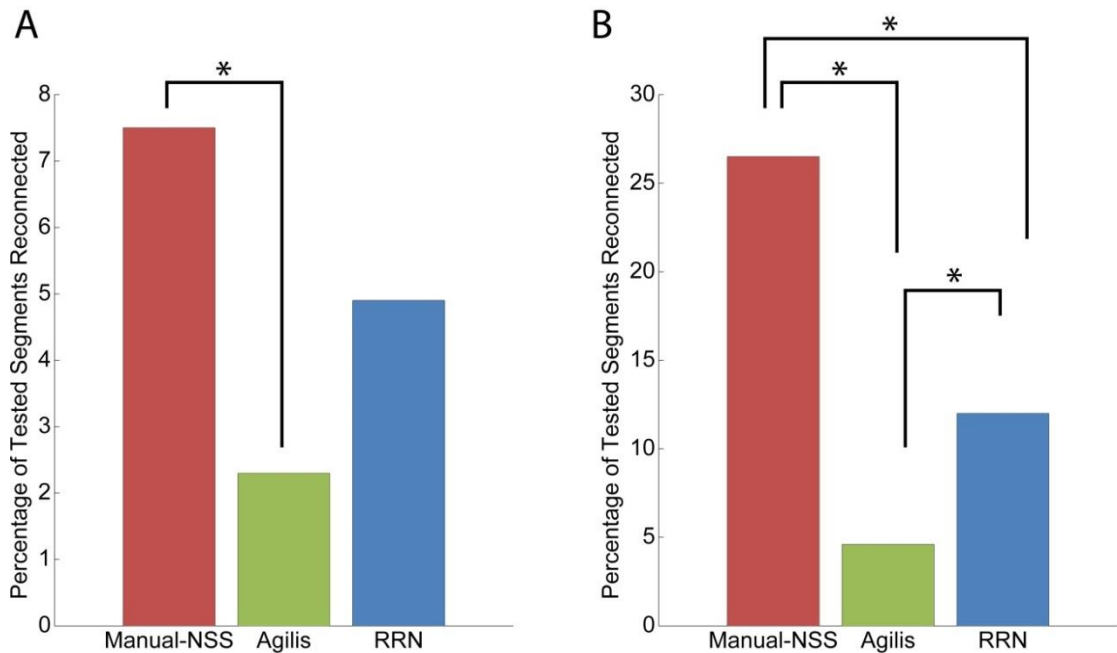


**Figure 6.4 Percentage of wide area circumferential ablation segments reconnecting (A) Acute Reconnection (B) Chronic Reconnection \*= $p < 0.004$**

higher CFs than RRN use from the anterior-inferior to mid posterior segments ( $p < 0.05$ , 4-9 o'clock).

There were significant differences between the consistency of mean ablation CF between the left and right WACA (SD of mean CF per segment per patient: left WACA 3.8(0.02-16.3)g, right WACA 4.7(0-33.3)g,  $p < 0.0005$ ), a lower SD on the left suggesting greater consistency. There was also a significant difference between the groups: Manual-NSS 3.3(0.4-33.3)g, Agilis group 4.4(0.02-26.2)g, RRN 4.6(0-21.7)g, with the Manual-NSS group's ablations having a more consistent mean CF (lower SD of mean CF per segment per patient) than the other two groups' ablations ( $p < 0.005$  for both comparisons), but no difference between the steerable sheath groups ( $p = 0.9$ ).

### 6.4.3 Reconnections

The mean time between completion of the initial WACA isolation and testing for reconnection was 128( $\pm$ 50) minutes for the left WACA and 88 ( $\pm$ 51) minutes on the right side (> 30 minutes in all cases). There were no significant differences in the waiting time in the three groups for either left or right WACA (p=0.4 and p=0.1 respectively).

**Table 6.2 Contact Force and Wide Area Circumferential Ablation Segment Reconnection**

	Acute		Chronic	
	Ablation Mean CF	Ablation FTI	Ablation Mean CF	Ablation FTI
Non-reconnecting segments (median(range))	13.3g (1.1-66.4g)	266g.s (3-3340g.s)	12.5g (1.6-54.4g)	251g.s (4-2552g.s)
Reconnecting segments (median(range))	12.8g (2-45.6g)	291g.s (22-1641g.s)	11.5g (1.1-52.5g)	231g.s (3-1429g.s)
p-value	0.046	0.59	<0.005	0.006

In terms of whole WACA reconnections, excluding for the acute analysis WACAs where the 30 minute waiting time was not fulfilled, 35/112 (31%) PV pairs reconnected acutely (15/59, 25%, left WACAs and 20/53, 38%, right WACAs, p=0.22). There was no significant difference in the rate of acute WACA reconnection between the three groups (Manual-NSS 38%, Agilis 15%, RRN 33% p=0.2). At the time of analysis, 26 patients (9 Manual-NSS, 5 Agilis and 12 RRN) had had a repeat ablation procedure at a median of 8 months (range 2 to 17 months) from the index ablation. In one case, the right PV was electrically silent at the index procedure and had remained so and therefore that vein pair was not included in the analysis. For the left WACA, 16/26 (62%) PV pairs were reconnected, while on the right side, 17/25 (68%) reconnected: there was no significant difference between the two sides in terms of the incidence of

WACA reconnection ( $p=0.78$ ) and no differences between the groups for chronic WACA reconnection (Manual-NSS 78%, Agilis 57%, RRN 63%  $p=0.48$ ).

At the segment level, there was a significant difference in the proportion of segments acutely or chronically reconnecting per group (Figure 6.4). In both cases, the Agilis group had the lowest rate of segment reconnections.

The mean CF for an ablation within a segment was significantly lower in segments that reconnected acutely or chronically (Table 6.2). The FTI was lower for ablations in chronically reconnecting segments than those that did not reconnect.

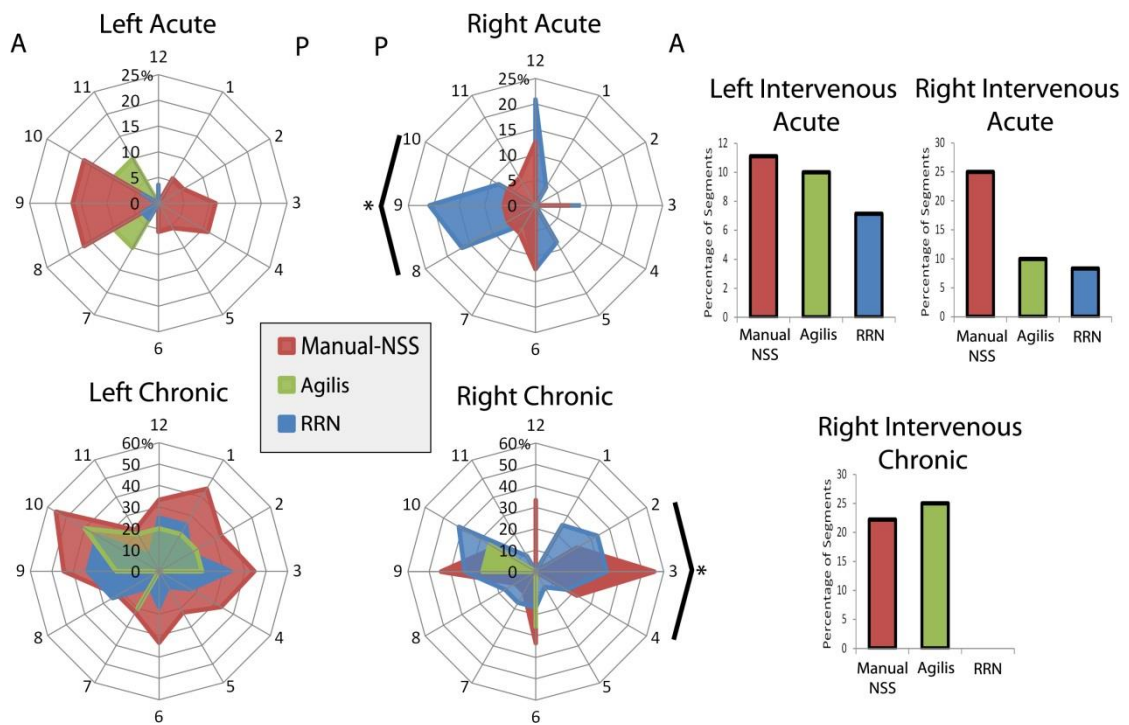


**Figure 6.5 WACA reconnection plots.**

*Radar Plots:* The plot outer edge represents the clock face WACA segment and the further from the centre of the plot, the higher the percentage of that segment reconnecting as a proportion of all assessed segments at that location in that group. *Bar Charts:* Acute and chronic intervenous reconnections. \*=Quadrant where difference in proportions of reconnections between indicated groups is significantly different ( $p<0.05$ ).

The reconnection site data for the WACAs are presented in Figure 6.5. The anterior quadrant of the left WACA (where the ridge with the LAA would be located) was a common site of acute and chronic reconnection across groups. Steerable sheaths

significantly reduced the rate of left posterior quadrant reconnection acutely. They did not significantly affect the rate in other portions of the left WACA acutely or in any Left WACA portion chronically. On the right side, the RRN group had higher acute posterior quadrant reconnections but there was no difference chronically. The use of steerable sheaths significantly reduced the proportion of chronic right anterior quadrant reconnections.

## **6.5 Discussion**

This study demonstrates that the CFs during persistent AF ablation procedures were higher using steerable sheaths than a non-steerable manual sheath. The increase was evident both as a mean across the whole procedure, but was also evident at specific regions around the WACA line. However, there was reduced consistency of the CF achieved in a WACA segment using steerable sheaths compared with the non-steerable sheath procedures. As a corollary to the increased CF with steerable sheaths, there were also fewer segments reconnecting acutely and chronically when these were utilized, though this was not reflected in a significant difference in pulmonary vein reconnections as a whole. CF parameters during WACA ablation were predictive of segment reconnection both acutely and at the time of redo-procedures and the distribution of reconnecting WACA regions varied between the groups.

The use of steerable sheaths led to higher CFs for the ablations as a whole and specifically for the WACAs compared with ablations performed using a non-steerable sheath. This is likely secondary to the increased stiffness of these sheaths compared with manual non-steerable sheaths. The increase in CF observed was not uniform throughout the WACAs but displayed regional variance. While there were areas such as the left PV/LAA ridge and the right posterior wall where steerable sheaths were

associated with a higher CF, there were others such as the left anterior-inferior quadrant and right antero-superior quadrant where the CFs were no higher using steerable sheaths. These latter sites are ones which it is challenging to access using a non-steerable sheath and even with the increased control over catheter manipulation with a steerable sheath, difficulties evidently persist. Another important observation is the increased CF variability when using steerable sheaths. While steerable sheaths facilitate access to different parts of the atrium, and are generally associated with increased CF at those locations, it appears that there is less consistency in the CF attained in a segment when using them. Whether this is a function of the higher CFs achieved or the stiffness of these sheaths compared with the Mullins sheath is unclear.

The finding that ablation CF parameters are predictive of acute and chronic WACA segment reconnection in persistent AF patients is consistent with previous work in acute reconnection in a predominantly persistent AF ablation cohort<sup>177</sup> and chronic WACA reconnection in PAF patients<sup>178</sup>. In the current study, the ablation FTI was not predictive of acute reconnection, suggesting that a sub-optimal FTI may be adequate to cause tissue oedema and acutely isolate a vein, but not to achieve lasting vein isolation. This suggests that adherence to FTI targets might have additional value beyond aiming for the conventional procedural end-point of PV isolation.

Previous studies have examined sites of PV reconnection following WACA both acutely<sup>175,177</sup> and chronically<sup>175,178</sup>. This study expanded on this by examining the impact of steerable sheaths on sites of reconnection. The RRN group was associated with significantly more reconnections at the right posterior wall acutely, despite being associated with higher applied CFs in this region. This may be due to operators curtailing the duration of ablation in this region in response to higher CFs. Chronically,

this region was associated with a relative peak in the incidence of reconnections for all groups (without a disproportionate representation from the RRN group).

There were areas with a predilection for reconnection in all three groups such as the LAA/PV ridge and right inferior wall. This is despite the CFs being significantly increased, on average, in these regions by the use of sheath technology. The reason for this may be that other factors beyond the mean CF attained may be of importance in these regions such as the characteristics of the underlying tissue or catheter stability. Alternatively, it may be the case that the CFs, while being incremented by these technologies in these regions, are not being incremented enough to consistently deliver an effective lesion – in other words, the optimal CF required for effective ablation may be higher in these regions.

It is interesting that the proportion of acutely and chronically reconnecting segments was lowest in the Agilis group, and this was also the group with the highest CFs. At the same time though, steerable sheaths were not associated with a significant difference in the pulmonary vein reconnection rate overall in the current study. These findings suggest that while reconnections rates at the level of the PV pair are overall not affected by the use of steerable sheaths, the burden of reconnection in each reconnecting WACA is lower. The question therefore arises as to why the PV reconnection rate was not significantly reduced by the use of steerable sheaths despite the overall higher CFs. Clearly for a PV pair to not reconnect, all segments of the WACA line isolating it must remain disconnected. From the current data, at a WACA segment level, the increment in CF with the use of steerable sheaths is not uniform. Moreover, the consistency of ablation CF per segment is lower with steerable sheaths. For these two reasons, there is the possibility of delivering suboptimal ablations to WACA segments even with steerable sheaths. Consequently, outcomes in general are likely being affected, which

may be an explanation for the lack of improvement in success rates described with RRN<sup>144,147</sup> or the mixed reports for the Agilis sheath<sup>143,227</sup>. Additionally, there are regions likely more prone to reconnection as discussed above. Certainly the former two potential weaknesses can be overcome by the adoption of strict CF targets for ablation.

In the current study, the success rates for the Agilis group at 12 months were in fact the lowest. The reasons for this likely relate to the factors discussed above but it is also important to bear in mind that this was a non-randomised comparison with asymmetrically sized groups (the Agilis group also being the smallest). Therefore, it is not reasonable to use the study data as a comparison of clinical efficacy between the different sheath technologies.

The operators in the current study, while ablating within a consensus CF range that was felt to ensure catheter-tissue contact (minimum 5g) and prevent excessive contact (maximum 40g), were not targeting a particular CF or FTI (there were few data available at the time of these ablations regarding CF targets). The lesser stiffness of manual non-steerable sheath (and lower associated CF) may mean that attaining the same CF as that with steerable sheaths in all WACA regions is challenging. This should not be the case for the FTI (as a lower CF could be counteracted by a longer ablation resulting in the same FTI), and there is a suggestion that the FTI of ablation achieved is of greater importance to ablation efficacy<sup>206</sup>. Based on the higher CFs associated with the use of steerable sheaths, attaining FTI targets is likely to be easier and less time consuming with steerable rather than non-steerable sheaths though. If the same FTI targets are used with different technologies then one would expect segmental reconnection rates to become similar between groups. If appropriate targets are used, then it may be the case that outcomes are improved as well. This of course assumes that there is no clinically significant difference in the quality of contact delivered (regardless



of similar FTIs being achieved) between the steerable and non-steerable sheath technology.

### **6.5.1 Limitations**

This was a non-randomized study, the numbers in each group were not equal and ablation beyond WACA was not protocolised. As the aim of the study was to investigate the influence of steerable sheaths on CF parameters and WACA reconnection, rather than compare success rates, these limitations were accepted. The CF-consistency assessment assumes that for a given WACA segment in a patient, an operator would be generally aiming for the same ablation CF with each radiofrequency application. For lesions that were drag lesions, there would be some inaccuracy in assigning CF to a particular point in the WACA (as the CF was measured continuously during ablation and so the measurements would have to be split between locations where a drag ablation was performed).

## **6.6 Conclusions**

Steerable sheaths are associated with an increase in CF during persistent AF ablation. Despite steerable sheath technologies increasing CFs in the WACA, this increase is not uniform, with some WACA segments areas showing no increment in CF with steerable sheaths; additionally, these sheaths are also associated with a lower consistency of achieved CF in a WACA segment. Certain WACA regions retain a predilection for reconnection despite higher applied CF with these sheaths, suggesting regional differences in optimal required ablation parameters. Overall PV reconnection rates are not significantly affected by steerable sheath use (though the burden of

reconnection in a WACA is reduced), likely secondary to the weaknesses of this technology described above. The adoption of CF targets may overcome these weaknesses and improve outcomes. The current study suggests achieving CF targets for ablation may be easier with steerable sheaths due to the potential for attaining higher CFs.

## 7. Conclusions and Future Directions

The aim of this thesis has been to study factors affecting the contact between the catheter and left atrial myocardium in man, and to investigate how this affects the left atrium mechanically, electrically and with respect to radiofrequency ablation. The work gives insight into the mechanical and electrical properties of the *in vivo* human left atrium. It is of direct clinical relevance as the findings shed light on the role of catheter contact in affecting the results of cardiac mapping and ablation efficacy.

The left atrium is not a uniform structure and this affects the behaviour of the catheter within the left atrium. The stability of contact, in terms of the variability of the CF waveform and catheter positional stability, varies by left atrial location, as demonstrated by the experiment in Chapter 5. The former finding gives interesting insight into the nature of the mechanical relationship between the catheter and different parts of the left atrium: not only the compliance properties of the tissue but also the accessibility of the tissue for the catheter. This combination of influences on the mechanical relationship observed cannot be untangled to allow the relative contributions of each to be established. While not an unadulterated reflection of the compliance properties of the tissue, this mixed mechanical relationship is what is observed *in vivo* during catheter ablation, and therefore is of clinical relevance. It would be interesting to directly assess the compliance properties of different left atrial regions in explanted hearts to establish how far the results here agree with those from the *in vivo* assessment.

The quality of contact is also affected by the atrial rhythm as demonstrated in the experiment described in Chapter 5. The increased instability secondary to local atrial contraction during sinus rhythm is not surprising but has been quantified in the current work.

Beyond the mechanical properties of the left atrium, the equipment used to deliver the catheter is also an important determinant of the quality of contact. The influence of the catheter delivery mode on contact force is examined in Chapter 6. The work suggests that stiffer, steerable sheaths are associated with higher contact forces. This is important from the viewpoint of safety during the procedure. It is also important for ablation efficacy, as the correlation between reconnecting areas (suggesting inadequate ablation) and low CF during ablation has been highlighted by this experiment and in previous reports<sup>172,177,178</sup>. Chapter 5 examines further the relationship between the mode of catheter delivery and the effect this has on the quality of contact. Stiffer sheaths are likely associated with a reduction in the stability of the catheter as measured by the variability of the contact force waveform. While there may be advantages for positional stability to the use of such sheaths in AF, the converse appears to be the case in SR. Overall, for the same FTI, the impedance drop is actually lower with the use of a stiffer robotic sheath. These disadvantages highlighted in Chapter 5 are counterbalanced by the increased ease in obtaining higher CF (and so FTI during ablation) using a stiffer sheath, as shown in Chapter 6. Importantly, Chapter 6 also suggests that the CF during ablation may not be the only determinant of an effective ablation, as there are WACA regions that reconnect despite the mean CF being incremented by the use of steerable sheath technology. This suggests factors impacting on ablation efficacy beyond the FTI in Chapter 5, for example the stability of contact, may play a role.

In Chapter 4, the relationship between ablation efficacy and the FTI is explored. This leads to the generation of an FTI target for ablation. Targets have also been suggested in other reports<sup>178,179</sup> but these were based on regions electrically reconnecting and so may not be applicable to individual radiofrequency applications.

While in other work the impedance drop relationship with contact force over time has been examined<sup>169,220</sup>, the incremental analysis performed in this experiment is unique. The advantage of this method is that it effectively makes each ablation into multiple sub-ablations. By increasing the data available, the inherent variability in impedance measurements is compensated to allow the underlying relationships to become more apparent. A fall in impedance is in this case being used as a surrogate for lesion dimensions but, in itself, the fall in impedance is also an outcome of ablation. In that sense, the relationship between the FTI and impedance drop during an ablation is a direct reflection of ablation efficacy *per se*, though in this case biophysical efficacy. Importantly, the work in Chapters 4 and 5 suggests changes in the electrogram correlate poorly with ablation CF parameters compared with impedance drop. This is important as electrogram attenuation is a commonly used surrogate of clinical ablation efficacy clinically<sup>175,191</sup>.

The impedance drop/FTI relationship is further used to compare ablations under different contact conditions in Chapter 5. One could also envision this methodology being used for other types of comparison, such as between ablation power settings or different catheter irrigation technologies. In such an analysis, a steeper relationship between the impedance drop per FTI would suggest a more effective ablation. A comparison of ablation power settings would be an important one: in the current work, for simplicity of analysis, all study ablations were performed at the same temperature and power settings. Power is an important component of radiofrequency applications<sup>216</sup>, and how this influences efficacy clinically would be of great interest. Additionally, this methodology could also be used to compare temperature controlled with power controlled ablation. Ongoing work by the thesis author is investigating the latter, as well as the predictive benefit of incorporating the ablation power into the FTI

and using the impedance drop/FTI relationship to compare the efficacy of surround flow irrigation compared with standard irrigation.

The implication of comparing impedance drops at different FTIs using the above methodology is that depending on its constituents, the same FTI can be associated with different efficacies. In Chapter 4, this was investigated by looking at the components of the FTI (the mean contact force and ablation duration). The findings suggest that once 10 seconds of ablation is exceeded, the mean contact force applied does not affect the impedance drop achieved beyond the FTI. This is important with respect to optimizing ablations and suggests that beyond this time point the FTI achieved determines efficacy rather than the mean contact force applied. In turn this suggests that FTI targets should take precedence for ablations.

The findings of Chapters 4 and 5 suggest that factors beyond the FTI affect the efficacy of ablation. An important future area of study would be the nature of the FTI/impedance relationship in different LA regions. It may be that the plateau point for the curves, as studied for ablation in general in Chapter 4, may vary by location, and so the target FTI would also be different. A regional variation in ablation CF sensitivity may be one explanation for the observation in Chapter 3 of regions reconnecting in wide area circumferential ablation lines even in the face of CFs being incremented in those regions through the use of steerable sheath technology: it may be that these regions require higher CF targets than those achieved using steerable sheaths, for example due to greater wall thickness. It would be very useful for clinical ablation to establish target FTI's for each left atrial region. Similarly, it may also be the case that the FTI targets required for ablation differ between different sheath technologies, as these certainly have a bearing on the nature of contact with the myocardium.

The quality of contact with the myocardium in terms of catheter location and CF waveform stability also had an important influence on the efficacy of ablation, as did the orientation of catheter contact. These, along with the duration of ablation and the achieved FTI are all within the control (or can be adjusted for) by the operator. If these measures are taken into account then every delivered radiofrequency application could be optimised, which one would hope would improve the efficacy of the AF ablation procedure. Such detailed optimisation is now possible with the introduction of automated lesion marker placement software such as the Visitag upgrade for Carto from Biosense Webster. In a study by Anter et al.,<sup>223</sup> such an algorithm was used and found to be associated with lower rates of acute pulmonary vein reconnection but not improved success rates at 6 months. The limitation of that study though was that only catheter displacement and impedance drop were used by the annotation algorithm. The results from this thesis could be used to further refine the targets for ablation to include contact parameters which increase ablation efficacy (though contact force variability is not included in Visitag at present). Based on the findings of the current work, a randomised trial expanding on the work of Anter et al., and incorporating the findings of this thesis could be envisaged – the control group being ablated without the automated lesion placement software being used, and the intervention group with this software being used in conjunction with the proposed contact settings. From Chapter 4, a target FTI of 500g.s and ablation duration of at least 10 seconds would be suggested. Based on the data presented in Chapter 5, in addition to the FTI and ablation duration targets, a catheter drift of <3.5mm, a contact force variability of <5g and a parallel orientation of catheter contact would be recommended. It may be that if the correct optimisation parameters are used for ablation, the single procedure success rates for AF

ablation will improve. Certainly, for clinical ablation at St Bartholomew's Hospital the aim is now for ablations to exceed 10 seconds and target a maximum FTI of 500g.s.

As a precursor to a trial investigating the impact of ablation targets on AF ablation, the thesis author is currently involved with a prospective, multicentre, randomised trial studying the impact of having access to CF data on PAF ablation. This follows on from a multicentre retrospective analysis in this area conducted by the thesis author in patients with persistent AF<sup>149</sup>.

The above work suggests catheter contact affects the efficacy of ablation. During clinical ablation, electrogram parameters are used to guide ablation: whether this is in the identification of targets such as highly fractionated areas or high dominant frequency regions or in the assessment of electrogram attenuation. In Chapter 3, the results suggest that electrogram size is not correlated with CF. This is unexpected but is likely because of the influence of atrial location on the baseline electrogram size. It also means that electrogram size cannot replace real-time contact force measurement for assessing catheter contact clinically. In order to better understand the relationship between CF and the electrogram, a paired analysis was undertaken. This is useful as it mitigated any baseline differences in electrogram parameters and allowed thresholds to be established where these parameters are no longer affected by CF. For the electrogram size and fractionated electrogram scores, this experiment allowed threshold values beyond which the CF no longer has a significant influence on the results to be successfully established: in the case of spectral analysis parameters though, catheter contact was not found to have an effect. As catheter contact affected fractionation scores but not spectral parameters, this experiment offered guidance for the contact forces that should be applied during mapping of the left atrium to reduce any CF-related variability.



With respect to catheter contact affecting atrial electrophysiology, there was some evidence for this. Certainly in sinus rhythm, the incidence of atrial ectopics increased with increasing CF. In the AF cases, no changes in spectral parameters were observed with catheter contact but there was a change in fractionation scores. This could reflect a lower sensitivity of the former to pick up any changes from catheter contact or that the changes in the latter are driven purely by changes in the size of the recorded electrogram leading to more complexes being identified and so a higher automated score (without an actual alteration of the underlying electrophysiology).

One would have expected a more significant role for CF in affecting the clinical fibrillatory electrogram based on the prior animal and cellular work discussed in Chapter 1.9. The important difference here though is principally that previous work has not been performed in fibrillating tissue. In a fibrillatory atrium, the electrogram at a point is subject to signals emanating from a multitude of sources, whether local or farfield. If the contact force is affecting these signals, then it may well be that the effect is too subtle to be appreciated by the tools used to investigate it in the current work. Also, if a site is purely passive to the fibrillatory process then changes in contact force at that point may not have a significant effect regardless.

One reason for the modest effects of CF on electrogram parameters seen *in vivo* in these experiments is that, in the context of the moving heart, the contact force applied is a waveform rather than an absolute value. This is well illustrated by the work on contact force variability in Chapter 5. Therefore, the actual contact force applied at the time when an action potential is generated by a myocyte may vary markedly from the mean contact force. Further complicating matters is that the stretch stimulus is being applied not just to the contact point with the catheter but to a region (especially at higher contact forces when greater amounts of the surface are recruited to deform as the

local myocardium approaches its maximal strain capacity). Therefore, it is possible that CF is affecting the observed signals but that the actual force applied at the time of action potential generation is not reflected by the mean CF during the 8 second recording period.

In order to investigate the relationship between the fibrillatory electrogram and contact force in more detail therefore, one approach would be to focus purely on regions actively driving the arrhythmia. These could be identified using the recently described contact<sup>66,211</sup> or non-contact methodologies<sup>228</sup>. In this context, recent work suggests that CFAE signal grades do not identify stable driver sources (identified by panoramic left atrial contact-based electrogram analysis)<sup>229</sup>. Changing the contact force at driver sites may have a more easily identifiable effect on the electrogram due to their importance to the fibrillatory signal. In both AF and SR cases, the use of electrogram data synchronized to the millisecond with the contact force data, and possibly a higher sampling rate of contact force measurements may allow the actual contact force at the time of (or just prior to) the generation of a complex to be established which may improve the ability to detect changes secondary to this. Certainly, the newer version of the Carto electroanatomical mapping system has the capability of continuous electrogram recording (beyond the 2.5 second window). This would allow for the two types of measurement to be synchronized beyond what is possible using two independent systems.

In conclusion, these data demonstrate that multiple factors, including the catheter delivery technology and atrial location, affect the contact between the catheter and the left atrium and that catheter contact has a significant impact on the efficacy of radiofrequency ablation. Electrogram parameters are not a reliable surrogate for real-time catheter contact force measurement, including catheter contact during ablation.

Catheter contact affects electrogram parameters during sinus rhythm and atrial fibrillation, though it does not affect spectral measurements, and there is a threshold for the observed effects. The data presented in this thesis can therefore be used to improve the efficacy and reliability of clinical left atrial mapping and radiofrequency ablation.

## 8. References

1. Calkins H, Kuck KH, Cappato R, Brugada J, Camm AJ, Chen S-A, Crijns HJG, Damiano RJ, Davies DW, DiMarco J, Edgerton J, Ellenbogen K, Ezekowitz MD, Haines DE, Haissaguerre M, Hindricks G, Iesaka Y, Jackman W, Jalife J, Jais P, Kalman J, Keane D, Kim Y-H, Kirchhof P, Klein G, Kottkamp H, Kumagai K, Lindsay BD, Mansour M, Marchlinski FE, McCarthy PM, Mont JL, Morady F, Nademanee K, Nakagawa H, Natale A, Nattel S, Packer DL, Pappone C, Prystowsky E, Raviele A, Reddy V, Ruskin JN, Shemin RJ, Tsao H-M, Wilber D. 2012 HRS/EHRA/ECAS Expert Consensus Statement on Catheter and Surgical Ablation of Atrial Fibrillation: Recommendations for Patient Selection, Procedural Techniques, Patient Management and Follow-up, Definitions, Endpoints, and Research Trial Design. *Heart Rhythm*. 2012; 9:632–696.e21.
2. Benjamin EJ, Wolf PA, D'Agostino RB, Silbershatz H, Kannel WB, Levy D. Impact of atrial fibrillation on the risk of death: the Framingham Heart Study. *Circulation*. 1998; 98:946.
3. Wolf PA, Abbott RD, Kannel WB. Atrial fibrillation as an independent risk factor for stroke: the Framingham Study. *Stroke*. 1991; 22:983.
4. Stewart S, Hart CL, Hole DJ, McMurray JJV. A population-based study of the long-term risks associated with atrial fibrillation: 20-year follow-up of the Renfrew/Paisley study. *Am. J. Med.* 2002; 113:359–364.
5. Reynolds MR, Ellis E, Zimetbaum P. Quality of Life in Atrial Fibrillation: Measurement Tools and Impact of Interventions. *J. Cardiovasc. Electrophysiol.* 2008; 19:762–768.
6. Dorian P, Jung W, Newman D, Paquette M, Wood K, Ayers GM, Camm J, Akhtar M, Luderitz B. The impairment of health-related quality of life in patients with intermittent atrial fibrillation: implications for the assessment of investigational therapy. *J. Am. Coll. Cardiol.* 2000; 36:1303–1309.
7. Thrall G, Lip GYH, Carroll D, Lane D. Depression, Anxiety, and Quality of Life in Patients With Atrial Fibrillation. *Chest*. 2007; 132:1259–1264.
8. Majeed A. Trends in the prevalence and management of atrial fibrillation in general practice in England and Wales, 1994-1998: analysis of data from the general practice research database. *Heart*. 2001; 86:284–288.
9. Stewart S, Murphy NF, Murphy N, Walker A, McGuire A, McMurray JJV. Cost of an emerging epidemic: an economic analysis of atrial fibrillation in the UK. *Heart Br. Card. Soc.* 2004; 90:286–292.
10. Hart RG, Benavente O, McBride R, Pearce LA. Antithrombotic therapy to prevent stroke in patients with atrial fibrillation: a meta-analysis. *Ann. Intern. Med.* 1999; 131:492–501.
11. Lip GYH, Nieuwlaat R, Pisters R, Lane DA, Crijns HJGM. Refining Clinical Risk Stratification for Predicting Stroke and Thromboembolism in Atrial Fibrillation Using a Novel Risk Factor-Based Approach: The Euro Heart Survey on Atrial Fibrillation. *Chest*. 2009; 137:263–272.
12. Connolly SJ, Ezekowitz MD, Yusuf S, Eikelboom J, Oldgren J, Parekh A, Pogue J, Reilly PA, Themeles E, Varrone J, others. Dabigatran versus warfarin in patients with atrial fibrillation. *N. Engl. J. Med.* 2009; 361:1139–1151.
13. Patel MR, Mahaffey KW, Garg J, Pan G, Singer DE, Hacke W, Breithardt G, Halperin JL, Hankey GJ, Piccini JP, Becker RC, Nessel CC, Paolini JF, Berkowitz SD, Fox KAA, Califf RM, ROCKET AF Investigators. Rivaroxaban versus warfarin in nonvalvular atrial fibrillation. *N. Engl. J. Med.* 2011; 365:883–891.

14. Fountain RB, Holmes DR, Chandrasekaran K, Packer D, Asirvatham S, Van Tassel R, Turi Z. The PROTECT AF (WATCHMAN Left Atrial Appendage System for Embolic PROTECTION in Patients with Atrial Fibrillation) trial. *Am. Heart J.* 2006; 151:956–961.
15. Van Gelder IC, Hagens VE, Bosker HA, Kingma JH, Kamp O, Kingma T, Said SA, Darmanata JI, Timmermans AJM, Tijssen JGP, others. A comparison of rate control and rhythm control in patients with recurrent persistent atrial fibrillation. *N. Engl. J. Med.* 2002; 347:1834–1840.
16. Wyse DG, Waldo AL, DiMarco JP, Domanski MJ, Rosenberg Y, Schron EB, Kellen JC, Greene HL, Mickel MC, Dalquist JE, Corley SD. A comparison of rate control and rhythm control in patients with atrial fibrillation. *N. Engl. J. Med.* 2002; 347:1825–1833.
17. Talajic M, Khairy P, Levesque S, Connolly SJ, Dorian P, Dubuc M, Guerra PG, Hohnloser SH, Lee KL, Macle L, Nattel S, Pedersen OD, Stevenson LW, Thibault B, Waldo AL, Wyse DG, Roy D. Maintenance of sinus rhythm and survival in patients with heart failure and atrial fibrillation. *J. Am. Coll. Cardiol.* 2010; 55:1796–1802.
18. De Denus S, Sanoski CA, Carlsson J, Opolski G, Spinler SA. Rate vs rhythm control in patients with atrial fibrillation: a meta-analysis. *Arch. Intern. Med.* 2005; 165:258.
19. Testa L, Biondi-Zoccai GGL, Russo AD, Bellocchi F, Andreotti F, Crea F. Rate-control vs. rhythm-control in patients with atrial fibrillation: a meta-analysis. *Eur. Heart J.* 2005; 26:2000–2006.
20. Chen S, Dong Y, Fan J, Yin Y. Rate vs. rhythm control in patients with atrial fibrillation - an updated meta-analysis of 10 randomized controlled trials. *Int. J. Cardiol.* 2011; 153:96–98.
21. Jenkins LS, Brodsky M, Schron E, Chung M, Rocco T Jr, Lader E, Constantine M, Sheppard R, Holmes D, Mateski D, Floden L, Prasun M, Greene HL, Shemanski L. Quality of life in atrial fibrillation: the Atrial Fibrillation Follow-up Investigation of Rhythm Management (AFFIRM) study. *Am. Heart J.* 2005; 149:112–120.
22. Corley SD, Epstein AE, DiMarco JP, Domanski MJ, Geller N, Greene HL, Josephson RA, Kellen JC, Klein RC, Krahn AD, Mickel M, Mitchell LB, Nelson JD, Rosenberg Y, Schron E, Shemanski L, Waldo AL, Wyse DG, AFFIRM Investigators. Relationships between sinus rhythm, treatment, and survival in the Atrial Fibrillation Follow-Up Investigation of Rhythm Management (AFFIRM) Study. *Circulation.* 2004; 109:1509–1513.
23. Bunch TJ, Crandall BG, Weiss JP, May HT, Bair TL, Osborn JS, Anderson JL, Muhlestein JB, Horne BD, Lappe DL, Day JD. Patients Treated with Catheter Ablation for Atrial Fibrillation Have Long-Term Rates of Death, Stroke, and Dementia Similar to Patients Without Atrial Fibrillation. *J. Cardiovasc. Electrophysiol.* 2011; 22:839–845.
24. Hunter RJ, McCready J, Diab I, Page SP, Finlay M, Richmond L, French A, Earley MJ, Sporton S, Jones M, Joseph JP, Bashir Y, Betts TR, Thomas G, Staniforth A, Lee G, Kistler P, Rajappan K, Chow A, Schilling RJ. Maintenance of sinus rhythm with an ablation strategy in patients with atrial fibrillation is associated with a lower risk of stroke and death. *Heart.* 2011; 98:48–53.
25. Fichtner S, Deisenhofer I, Kindsmüller S, Dzijan-Horn M, Tzeis S, Reents T, Wu J, Luise Estner H, Jilek C, Ammar S, Kathan S, Hessling G, Ladwig K-H. Prospective Assessment of Short- and Long-Term Quality of Life After Ablation for Atrial Fibrillation. *J. Cardiovasc. Electrophysiol.* 2012; 23:121–127.
26. Cappato R. Worldwide Survey on the Methods, Efficacy, and Safety of Catheter Ablation for Human Atrial Fibrillation. *Circulation.* 2005; 111:1100–1105.
27. Hunter RJ, Schilling RJ. Long-term outcome after catheter ablation for atrial fibrillation: safety, efficacy and impact on prognosis. *Heart.* 2010; 96:1259–1263.

28. Arbelo E, Brugada J, Hindricks G, Maggioni AP, Tavazzi L, Vardas P, Laroche C, Anselme F, Inama G, Jais P, Kalarus Z, Kautzner J, Lewalter T, Mairesse GH, Perez-Villacastin J, Riahi S, Taborsky M, Theodorakis G, Trines SA. The Atrial Fibrillation Ablation Pilot Study: an European Survey on Methodology and Results of Catheter Ablation for Atrial Fibrillation: conducted by the European Heart Rhythm Association. *Eur. Heart J.* 2014; 35:1466–1478.
29. Wijffels MCEF, Kirchhof CJHJ, Dorland R, Allessie MA. Atrial Fibrillation Begets Atrial Fibrillation: A Study in Awake Chronically Instrumented Goats. *Circulation.* 1995; 92:1954–1968.
30. Yue L, Feng J, Gaspo R, Li GR, Wang Z, Nattel S. Ionic remodeling underlying action potential changes in a canine model of atrial fibrillation. *Circ. Res.* 1997; 81:512–525.
31. Gaspo R, Bosch RF, Bou-Abboud E, Nattel S. Tachycardia-induced changes in Na<sup>+</sup> current in a chronic dog model of atrial fibrillation. *Circ. Res.* 1997; 81:1045–1052.
32. Kirchhoff S, Nelles E, Hagendorff A, Krüger O, Traub O, Willecke K. Reduced cardiac conduction velocity and predisposition to arrhythmias in connexin40-deficient mice. *Curr. Biol.* 1998; 8:299–302.
33. Verheule S, van Batenburg CA, Coenjaerts FE, Kirchhoff S, Willecke K, Jongsma HJ. Cardiac conduction abnormalities in mice lacking the gap junction protein connexin40. *J. Cardiovasc. Electrophysiol.* 1999; 10:1380–1389.
34. Van Der Velden HMW, Ausma J, Rook MB, Hellemons AJCGM, Van Veen TAAB, Allessie MA, Jongsma HJ. Gap Junctional Remodeling in Relation to Stabilization of Atrial Fibrillation in the Goat. *Cardiovasc. Res.* 2000; 46:476–486.
35. Igarashi T, Finet JE, Takeuchi A, Fujino Y, Strom M, Greener ID, Rosenbaum DS, Donahue JK. Connexin gene transfer preserves conduction velocity and prevents atrial fibrillation. *Circulation.* 2012; 125:216–225.
36. Kostin S, Klein G, Szalay Z, Hein S, Bauer EP, Schaper J. Structural Correlate of Atrial Fibrillation in Human Patients. *Cardiovasc. Res.* 2002; 54:361–379.
37. Morillo CA, Klein GJ, Jones DL, Guiraudon CM. Chronic Rapid Atrial Pacing: Structural, Functional, and Electrophysiological Characteristics of a New Model of Sustained Atrial Fibrillation. *Circulation.* 1995; 91:1588–1595.
38. Ausma J, Wijffels M, Thoné F, Wouters L, Allessie M, Borgers M. Structural Changes of Atrial Myocardium Due to Sustained Atrial Fibrillation in the Goat. *Circulation.* 1997; 96:3157–3163.
39. Brundel BJJM, Ausma J, Van Gelder IC, Van Der Want JLL, Van Gilst WH, Crijns HJGM, Henning RH. Activation of Proteolysis by Calpains and Structural Changes in Human Paroxysmal and Persistent Atrial Fibrillation. *Cardiovasc. Res.* 2002; 54:380–389.
40. Rucker-Martin C, Pecker F, Godreau D, Hatem SN. Dedifferentiation of Atrial Myocytes During Atrial Fibrillation: Role of Fibroblast Proliferation in Vitro. *Cardiovasc. Res.* 2002; 55:38–52.
41. Xu J, Cui G, Esmailian F, Plunkett M, Marelli D, Ardehali A, Odum J, Laks H, Sen L. Atrial extracellular matrix remodeling and the maintenance of atrial fibrillation. *Circulation.* 2004; 109:363–368.
42. Pagel PS, Kehl F, Gare M, Hettrick DA, Kersten JR, Warltier DC. Mechanical function of the left atrium: new insights based on analysis of pressure-volume relations and Doppler echocardiography. *Anesthesiology.* 2003; 98:975–994.
43. Mitchell JH, Gupta DN, Payne RM. Influence of Atrial Systole on Effective Ventricular Stroke Volume. *Circ. Res.* 1965; 17:11–18.

44. Ricksten SE, Yao T, Ljung B, Thorén P. Distensibility of the left atrial wall in spontaneously hypertensive rats compared with that in normotensive Wistar-Kyoto rats. *Clin. Sci. Lond. Engl.* 1979; 59 Suppl 6:361s–363s.
45. Hoit BD, Walsh RA. Regional atrial distensibility. *Am. J. Physiol.* 1992; 262:H1356–H1360.
46. Davis CA, Rembert JC, Greenfield JC. Compliance of left atrium with and without left atrium appendage. *Am. J. Physiol.* 1990; 259:H1006–H1008.
47. Hoit BD, Shao Y, Tsai LM, Patel R, Gabel M, Walsh RA. Altered left atrial compliance after atrial appendectomy. Influence on left atrial and ventricular filling. *Circ. Res.* 1993; 72:167–175.
48. Ko Y-G, Ha J-W, Chung N, Shim W-H, Kang S-M, Rim S-J, Jang Y, Cho S-Y, Kim S-S. Effects of left atrial compliance on left atrial pressure in pure mitral stenosis. *Catheter. Cardiovasc. Interv.* 2001; 52:328–333.
49. Stefanadis C, Dernellis J, Stratos C, Tsiamis E, Vlachopoulos C, Toutouzas K, Lambrou S, Pitsavos C, Toutouzas P. Effects of balloon mitral valvuloplasty on left atrial function in mitral stenosis as assessed by pressure–area relation. *J. Am. Coll. Cardiol.* 1998; 32:159–168.
50. Flachskampf FA, Weyman AE, Guerrero JL, Thomas JD. Calculation of atrioventricular compliance from the mitral flow profile: analytic and in vitro study. *J. Am. Coll. Cardiol.* 1992; 19:998–1004.
51. Güray Y, Demirkan B, Karan A, Güray Ü, Boyacı A, Korkmaz Ş. Left Atrial Compliance and Pulmonary Venous Flow Velocities Are Related to Functional Status in Patients with Moderate-to-Severe Mitral Stenosis. *Echocardiography.* 2009; 26:1173–1178.
52. Masugata H, Mizushige K, Senda S, Lu X, Kinoshita A, Sakamoto H, Nozaki S, Sakamoto S, Matsuo H. Evaluation of Left Atrial Wall Elasticity Using Acoustic Microscopy. *Angiology.* 1999; 50:583–590.
53. White CW, Kerber RE, Weiss HR, Marcus ML. The effects of atrial fibrillation on atrial pressure-volume and flow relationships. *Circ. Res.* 1982; 51:205–215.
54. Leistad E, Christensen G, Ilebekk A. Effects of atrial fibrillation on left and right atrial dimensions, pressures, and compliances. *Am. J. Physiol.* 1993; 264:H1093–H1097.
55. Stefanadis C, Dernellis J, Stratos C, Tsiamis E, Tsioufis C, Toutouzas K, Vlachopoulos C, Pitsavos C, Toutouzas P. Assessment of Left Atrial Pressure–Area Relation in Humans by Means of Retrograde Left Atrial Catheterization and Echocardiographic Automatic Boundary Detection: Effects of Dobutamine. *J. Am. Coll. Cardiol.* 1998; 31:426–436.
56. White CW, Holida MD, Marcus ML. Effects of acute atrial fibrillation on the vasodilator reserve of the canine atrium. *Cardiovasc. Res.* 1986; 20:683–689.
57. Scherf D, Romano FJ, Terranova R. Experimental studies on auricular flutter and auricular fibrillation. *Am. Heart J.* 1948; 36:241–251.
58. Scherf D. Studies on auricular tachycardia caused by aconitine administration. *Proc. Soc. Exp. Biol. Med. Soc. Exp. Biol. Med. N. Y. N.* 1947; 64:233–239.
59. Berenfeld O, Zaitsev AV, Mironov SF, Pertsov AM, Jalife J. Frequency-Dependent Breakdown of Wave Propagation Into Fibrillatory Conduction Across the Pectinate Muscle Network in the Isolated Sheep Right Atrium. *Circ. Res.* 2002; 90:1173–1180.

60. Haissaguerre M, Jais P, Shah DC, Takahashi A, Hocini M, Quiniou G, Garrigue S, Le Mouroux A, Le Metayer P, Clémenty J. Spontaneous initiation of atrial fibrillation by ectopic beats originating in the pulmonary veins. *N. Engl. J. Med.* 1998; 339:659.
61. Moe GK, Abildskov JA. Atrial fibrillation as a self-sustaining arrhythmia independent of focal discharge. *Am. Heart J.* 1959; 58:59–70.
62. Moe GK, Rheinboldt WC, Abildskov JA. A Computer Model of Atrial Fibrillation. *Am. Heart J.* 1964; 67:200–220.
63. Konings KT, Kirchhof CJ, Smeets JR, Wellens HJ, Penn OC, Allessie MA. High-density mapping of electrically induced atrial fibrillation in humans. *Circulation.* 1994; 89:1665.
64. Schuessler RB, Grayson TM, Bromberg BI, Cox JL, Boineau JP. Cholinergically Mediated Tachyarrhythmias Induced by a Single Extrastimulus in the Isolated Canine Right Atrium. *Circ. Res.* 1992; 71:1254–1267.
65. Skanes AC, Mandapati R, Berenfeld O, Davidenko JM, Jalife J. Spatiotemporal Periodicity During Atrial Fibrillation in the Isolated Sheep Heart. *Circulation.* 1998; 98:1236–1248.
66. Narayan SM, Krummen DE, Rappel W-J. Clinical Mapping Approach To Diagnose Electrical Rotors and Focal Impulse Sources for Human Atrial Fibrillation. *J. Cardiovasc. Electrophysiol.* 2012; 23:447–454.
67. Oral H, Knight BP, Tada H, Özaydın M, Chugh A, Hassan S, Scharf C, Lai SWK, Greenstein R, Pelosi F, Strickberger SA, Morady F. Pulmonary Vein Isolation for Paroxysmal and Persistent Atrial Fibrillation. *Circulation.* 2002; 105:1077–1081.
68. Elayi CS, Verma A, Di Biase L, Ching CK, Patel D, Barrett C, Martin D, Rong B, Fahmy TS, Khaykin Y, Hongo R, Hao S, Pelargonio G, Dello Russo A, Casella M, Santarelli P, Potenza D, Fanelli R, Massaro R, Arruda M, Schweikert RA, Natale A. Ablation for longstanding permanent atrial fibrillation: results from a randomized study comparing three different strategies. *Heart Rhythm.* 2008; 5:1658–1664.
69. Nademanee K, Schwab MC, Kosar EM, Karwecki M, Moran MD, Visessook N, Michael AD, Ngarmukos T. Clinical Outcomes of Catheter Substrate Ablation for High-Risk Patients With Atrial Fibrillation. *J. Am. Coll. Cardiol.* 2008; 51:843–849.
70. O'Neill MD, Wright M, Knecht S, Jais P, Hocini M, Takahashi Y, Jönsson A, Sacher F, Matsuo S, Lim KT, Arantes L, Derval N, Lellouche N, Nault I, Bordachar P, Clémenty J, Haïssaguerre M. Long-term follow-up of persistent atrial fibrillation ablation using termination as a procedural endpoint. *Eur. Heart J.* 2009; 30:1105–1112.
71. Konings KTS, Smeets JLRM, Penn OC, Wellens HJJ, Allessie MA. Configuration of Unipolar Atrial Electrograms During Electrically Induced Atrial Fibrillation in Humans. *Circulation.* 1997; 95:1231–1241.
72. Gerstenfeld EP, Lavi N, Bazan V, Gojraty S, Kim SJ, Michele J. Mechanism of Complex Fractionated Electrograms Recorded During Atrial Fibrillation in a Canine Model. *Pacing Clin. Electrophysiol.* 2011; 34:844–857.
73. Umapathy K, Masse S, Kolodziejaska K, Veenhuyzen GD, Chauhan VS, Husain M, Farid T, Downar E, Sevaptisidis E, Nanthakumar K. Electrogram fractionation in murine HL-1 atrial monolayer model. *Heart Rhythm.* 2008; 5:1029–1035.
74. Atienza F, Calvo D, Almendral J, Zlochiver S, Grzeda KR, Martinez-Alzamora N, Gonzalez-Torrecilla E, Arenal A, Fernandez-Aviles F, Berenfeld O. Mechanisms of fractionated electrograms formation in the posterior left atrium during paroxysmal atrial fibrillation in humans. *J. Am. Coll. Cardiol.* 2011; 57:1081.



75. Rostock T, Rotter M, Sanders P, Takahashi Y, Jaïs P, Hocini M, Hsu L-F, Sacher F, Clémenty J, Haïssaguerre M. High-density activation mapping of fractionated electrograms in the atria of patients with paroxysmal atrial fibrillation. *Heart Rhythm*. 2006; 3:27–34.
76. Kalifa J. Mechanisms of Wave Fractionation at Boundaries of High-Frequency Excitation in the Posterior Left Atrium of the Isolated Sheep Heart During Atrial Fibrillation. *Circulation*. 2006; 113:626–633.
77. Yamabe H, Morihisa K, Tanaka Y, Uemura T, Enomoto K, Kawano H, Ogawa H. Mechanisms of the maintenance of atrial fibrillation: role of the complex fractionated atrial electrogram assessed by noncontact mapping. *Heart Rhythm*. 2009; 6:1120–1128.
78. Yamabe H, Morihisa K, Koyama J, Enomoto K, Kanazawa H, Ogawa H. Analysis of the mechanisms initiating random wave propagation at the onset of atrial fibrillation using noncontact mapping: role of complex fractionated electrogram region. *Heart Rhythm*. 2011; 8:1228–1236.
79. Nademanee K, McKenzie J, Kosar E, Schwab M, Sunsaneewitayakul B, Vasavakul T, Khunnawat C, Ngarmukos T. A new approach for catheter ablation of atrial fibrillation: mapping of the electrophysiologic substrate. *J. Am. Coll. Cardiol*. 2004; 43:2044–2053.
80. Oral H, Chugh A, Good E, Wimmer A, Dey S, Gadeela N, Sankaran S, Crawford T, Sarrazin JF, Kuhne M, Chalfoun N, Wells D, Frederick M, Fortino J, Benloucif-Moore S, Jongnarangsin K, Pelosi F, Bogun F, Morady F. Radiofrequency Catheter Ablation of Chronic Atrial Fibrillation Guided by Complex Electrograms. *Circulation*. 2007; 115:2606–2612.
81. Estner HL, Hessling G, Ndrepepa G, Wu J, Reents T, Fichtner S, Schmitt C, Bary CV, Kolb C, Karch M, Zrenner B, Deisenhofer I. Electrogram-guided substrate ablation with or without pulmonary vein isolation in patients with persistent atrial fibrillation. *Europace*. 2008; 10:1281–1287.
82. Verma A, Mantovan R, Macle L, De Martino G, Chen J, Morillo CA, Novak P, Calzolari V, Guerra PG, Nair G, others. Substrate and Trigger Ablation for Reduction of Atrial Fibrillation (STAR AF): a randomized, multicentre, international trial. *Eur. Heart J*. 2010;
83. Lin Y-J, Tai C-T, Chang S-L, Lo L-W, Tuan T-C, Wongcharoen W, Udyavar AR, Hu Y-F, Chang C-J, Tsai W-C, Kao T, Higa S, Chen S-A. Efficacy of Additional Ablation of Complex Fractionated Atrial Electrograms for Catheter Ablation of Nonparoxysmal Atrial Fibrillation. *J. Cardiovasc. Electrophysiol*. 2009; 20:607–615.
84. Deisenhofer I, Estner H, Reents T, Fichtner S, Bauer A, Wu J, Kolb C, Zrenner B, Schmitt C, Hessling G. Does Electrogram Guided Substrate Ablation Add to the Success of Pulmonary Vein Isolation in Patients with Paroxysmal Atrial Fibrillation? A Prospective, Randomized Study. *J. Cardiovasc. Electrophysiol*. 2009; 20:514–521.
85. Oral H, Chugh A, Yoshida K, Sarrazin JF, Kuhne M, Crawford T, Chalfoun N, Wells D, Boonyapisit W, Veerareddy S, others. A randomized assessment of the incremental role of ablation of complex fractionated atrial electrograms after antral pulmonary vein isolation for long-lasting persistent atrial fibrillation. *J. Am. Coll. Cardiol*. 2009; 53:782.
86. Hunter RJ, Berriman TJ, Diab I, Baker V, Finlay M, Richmond L, Duncan E, Kamdar R, Thomas G, Abrams D, Dhinoja M, Sporton S, Earley MJ, Schilling RJ. Long-term efficacy of catheter ablation for atrial fibrillation: impact of additional targeting of fractionated electrograms. *Heart*. 2010; 96:1372–1378.
87. Hayward RM, Upadhyay GA, Mela T, Ellinor PT, Barrett CD, Heist EK, Verma A, Choudhry NK, Singh JP. Pulmonary vein isolation with complex fractionated atrial electrogram ablation for paroxysmal and nonparoxysmal atrial fibrillation: A meta-analysis. *Heart Rhythm*. 2011; 8:994–1000.

88. Roux J-F, Gojraty S, Bala R, Liu CF, Hutchinson MD, Dixit S, Callans DJ, Marchlinski F, Gerstenfeld EP. Complex fractionated electrogram distribution and temporal stability in patients undergoing atrial fibrillation ablation. *J. Cardiovasc. Electrophysiol.* 2008; 19:815–820.
89. Verma A, Wulffhart Z, Beardsall M, Whaley B, Hill C, Khaykin Y. Spatial and temporal stability of complex fractionated electrograms in patients with persistent atrial fibrillation over longer time periods: relationship to local electrogram cycle length. *Heart Rhythm.* 2008; 5:1127–1133.
90. Redfearn DP, Simpson CS, Abdollah H, Baranchuk AM. Temporo-spatial stability of complex fractionated atrial electrograms in two distinct and separate episodes of paroxysmal atrial fibrillation. *Europace.* 2009; 11:1440–1444.
91. Lo L-W, Higa S, Lin Y-J, Chang S-L, Tuan T-C, Hu Y-F, Tsai W-C, Tsao H-M, Tai C-T, Ishigaki S, Oyakawa A, Maeda M, Suenari K, Chen S-A. The Novel Electrophysiology of Complex Fractionated Atrial Electrograms: Insight from Noncontact Unipolar Electrograms. *J. Cardiovasc. Electrophysiol.* 2009; 21:640–648.
92. Roux J-F, Gojraty S, Bala R, Liu CF, Dixit S, Hutchinson MD, Garcia F, Lin D, Callans DJ, Riley M, Marchlinski F, Gerstenfeld EP. Effect of pulmonary vein isolation on the distribution of complex fractionated electrograms in humans. *Heart Rhythm.* 2009; 6:156–160.
93. Matsuo S, Yamane T, Date T, Tokutake K-I, Hioki M, Narui R, Ito K, Tanigawa S-I, Yamashita S, Tokuda M, Inada K, Arase S, Yagi H, Sugimoto K-I, Yoshimura M. Substrate Modification by Pulmonary Vein Isolation and Left Atrial Linear Ablation in Patients with Persistent Atrial Fibrillation: Its Impact on Complex-Fractionated Atrial Electrograms. *J. Cardiovasc. Electrophysiol.* 2012; 23:962–970.
94. De Bakker JMT, Wittkampf FHM. The Pathophysiologic Basis of Fractionated and Complex Electrograms and the Impact of Recording Techniques on Their Detection and Interpretation. *Circ. Arrhythm. Electrophysiol.* 2010; 3:204–213.
95. Narayan SM, Wright M, Derval N, Jadidi A, Forclaz A, Nault I, Miyazaki S, Sacher F, Bordachar P, Clémenty J. Classifying fractionated electrograms in human atrial fibrillation using monophasic action potentials and activation mapping: Evidence for localized drivers, rate acceleration, and nonlocal signal etiologies. *Heart Rhythm.* 2011; 8:244–253.
96. Lee G, Roberts-Thomson K, Madry A, Spence S, Teh A, Heck PM, Kumar S, Kistler PM, Morton JB, Sanders P, Kalman JM. Relationship among complex signals, short cycle length activity, and dominant frequency in patients with long-lasting persistent AF: a high-density epicardial mapping study in humans. *Heart Rhythm.* 2011; 8:1714–1719.
97. Takahashi Y, O'Neill MD, Hocini M, Dubois R, Matsuo S, Knecht S, Mahapatra S, Lim KT, Jaïs P, Jonsson A, others. Characterization of electrograms associated with termination of chronic atrial fibrillation by catheter ablation. *J. Am. Coll. Cardiol.* 2008; 51:1003–1010.
98. Hunter RJ, Diab I, Thomas G, Duncan E, Abrams D, Dhinoja M, Sporton S, Earley MJ, Schilling RJ. Validation of a classification system to grade fractionation in atrial fibrillation and correlation with automated detection systems. *Europace.* 2009; 11:1587–1596.
99. Hunter RJ, Diab I, Tayebjee M, Richmond L, Sporton S, Earley MJ, Schilling RJ. Characterization of Fractionated Atrial Electrograms Critical for Maintenance of Atrial Fibrillation: A Randomized, Controlled Trial of Ablation Strategies (The CFAE AF Trial). *Circ. Arrhythm. Electrophysiol.* 2011; 4:622–629.
100. Lazar S, Dixit S, Callans DJ, Lin D, Marchlinski FE, Gerstenfeld EP. Effect of pulmonary vein isolation on the left-to-right atrial dominant frequency gradient in human atrial fibrillation. *Heart Rhythm.* 2006; 3:889–895.

101. Sanders P, Berenfeld O, Hocini M, Jais P, Vaidyanathan R, Hsu L-F, Garrigue S, Takahashi Y, Rotter M, Sacher F, Scavee C, Ploutz-Snyder R, Jalife J, Haissaguerre M. Spectral Analysis Identifies Sites of High-Frequency Activity Maintaining Atrial Fibrillation in Humans. *Circulation*. 2005; 112:789–797.
102. Lemola K, Ting M, Gupta P, Anker JN, Chugh A, Good E, Reich S, Tschopp D, Igic P, Elmouchi D, Jongnarangsin K, Bogun F, Pelosi F Jr, Morady F, Oral H. Effects of two different catheter ablation techniques on spectral characteristics of atrial fibrillation. *J. Am. Coll. Cardiol*. 2006; 48:340–348.
103. Lin Y-J, Kao T, Tai C-T, Chang S-L, Lo L-W, Tuan T-C, Udyavar AR, Hu Y-F, Tso H-W, Higa S, Chen S-A. Spectral analysis during sinus rhythm predicts an abnormal atrial substrate in patients with paroxysmal atrial fibrillation. *Heart Rhythm*. 2008; 5:968–974.
104. Lin Y-J, Tsao H-M, Chang S-L, Lo L-W, Hu Y-F, Chang C-J, Tsai W-C, Suenari K, Huang S-Y, Chang H-Y, Wu T-J, Chen S-A. Role of high dominant frequency sites in nonparoxysmal atrial fibrillation patients: insights from high-density frequency and fractionation mapping. *Heart Rhythm*. 2010; 7:1255–1262.
105. Verma A, Lakkireddy D, Wulffhart Z, Pillarisetti J, Farina D, Beardsall M, Whaley B, Giewercer D, Tsang B, Khaykin Y. Relationship Between Complex Fractionated Electrograms (CFE) and Dominant Frequency (DF) Sites and Prospective Assessment of Adding DF-Guided Ablation to Pulmonary Vein Isolation in Persistent Atrial Fibrillation (AF). *J. Cardiovasc. Electrophysiol*. 2011; 22:1309–1316.
106. Stiles MK, Brooks AG, Kuklik P, John B, Dimitri H, Lau DH, Wilson L, Dhar S, Roberts\_Thomson RL, Mackenzie L, Young GD, Sanders P. High\_Density Mapping of Atrial Fibrillation in Humans: Relationship Between High\_Frequency Activation and Electrogram Fractionation. *J. Cardiovasc. Electrophysiol*. 2008; 19:1245–1253.
107. Levine JH, Guarnieri T, Kadish AH, White RI, Calkins H, Kan JS. Changes in myocardial repolarization in patients undergoing balloon valvuloplasty for congenital pulmonary stenosis: evidence for contraction-excitation feedback in humans. *Circulation*. 1988; 77:70–77.
108. Taggart P, Sutton PM, Treasure T, Lab M, O'Brien W, Runnalls M, Swanton RH, Emanuel RW. Monophasic action potentials at discontinuation of cardiopulmonary bypass: evidence for contraction-excitation feedback in man. *Circulation*. 1988; 77:1266–1275.
109. Franz MR, Burkhoff D, Yue DT, Sagawa K. Mechanically induced action potential changes and arrhythmia in isolated and in situ canine hearts. *Cardiovasc. Res*. 1989; 23:213–223.
110. Calkins H, Levine JH, Kass DA. Electrophysiological effect of varied rate and extent of acute in vivo left ventricular load increase. *Cardiovasc. Res*. 1991; 25:637–644.
111. Takagi S, Miyazaki T, Moritani K, Miyoshi S, Furukawa Y, Ito S, Ogawa S. Gadolinium suppresses stretch-induced increases in the differences in epicardial and endocardial monophasic action potential durations and ventricular arrhythmias in dogs. *Jpn. Circ. J*. 1999; 63:296–302.
112. Franz MR, Cima R, Wang D, Proffitt D, Kurz R. Electrophysiological effects of myocardial stretch and mechanical determinants of stretch-activated arrhythmias. *Circulation*. 1992; 86:968–978.
113. Ravelli F, Allesie M. Effects of Atrial Dilatation on Refractory Period and Vulnerability to Atrial Fibrillation in the Isolated Langendorff-Perfused Rabbit Heart. *Circulation*. 1997; 96:1686–1695.
114. Nazir SA, Lab MJ. Mechanoelectric feedback in the atrium of the isolated guinea-pig heart. *Cardiovasc. Res*. 1996; 32:112–119.

115. Tavi P, Laine M, Weckström M. Effect of gadolinium on stretch-induced changes in contraction and intracellularly recorded action- and afterpotentials of rat isolated atrium. *Br. J. Pharmacol.* 1996; 118:407–413.
116. Eijsbouts SCM, Majidi M, van Zandvoort M, Allessie MA. Effects of acute atrial dilation on heterogeneity in conduction in the isolated rabbit heart. *J. Cardiovasc. Electrophysiol.* 2003; 14:269–278.
117. Satoh T, Zipes DP. Unequal atrial stretch in dogs increases dispersion of refractoriness conducive to developing atrial fibrillation. *J. Cardiovasc. Electrophysiol.* 1996; 7:833–842.
118. Tse HF, Pelosi F, Oral H, Knight BP, Strickberger SA, Morady F. Effects of simultaneous atrioventricular pacing on atrial refractoriness and atrial fibrillation inducibility: role of atrial mechano-electrical feedback. *J. Cardiovasc. Electrophysiol.* 2001; 12:43–50.
119. Kaseda S, Zipes DP. Contraction-excitation feedback in the atria: a cause of changes in refractoriness. *J. Am. Coll. Cardiol.* 1988; 11:1327–1336.
120. Bode F, Katchman A, Woosley RL, Franz MR. Gadolinium Decreases Stretch-Induced Vulnerability to Atrial Fibrillation. *Circulation.* 2000; 101:2200–2205.
121. Franz MR, Bode F. Mechano-electrical feedback underlying arrhythmias: the atrial fibrillation case. *Prog. Biophys. Mol. Biol.* 2003; 82:163–174.
122. Ravelli F, Masè M, del Greco M, Marini M, Disertori M. Acute atrial dilatation slows conduction and increases AF vulnerability in the human atrium. *J. Cardiovasc. Electrophysiol.* 2011; 22:394–401.
123. Kalifa J, Jalife J, Zaitsev AV, Bagwe S, Warren M, Moreno J, Berenfeld O, Nattel S. Intra-Atrial Pressure Increases Rate and Organization of Waves Emanating From the Superior Pulmonary Veins During Atrial Fibrillation. *Circulation.* 2003; 108:668–671.
124. Yoshida K, Ulfarsson M, Oral H, Crawford T, Good E, Jongnarangsin K, Bogun F, Pelosi F, Jalife J, Morady F, Chugh A. Left atrial pressure and dominant frequency of atrial fibrillation in humans. *Heart Rhythm.* 2011; 8:181–187.
125. Chang S-L, Chen Y-C, Chen Y-J, Wangcharoen W, Lee S-H, Lin C-I, Chen S-A. Mechano-electrical feedback regulates the arrhythmogenic activity of pulmonary veins. *Heart Br. Card. Soc.* 2007; 93:82–88.
126. Nazir SA, Lab MJ. Mechano-electric feedback and atrial arrhythmias. *Cardiovasc. Res.* 1996; 32:52–61.
127. Kamkin A, Kiseleva I, Wagner KD, Leiterer KP, Theres H, Scholz H, Günther J, Lab MJ. Mechano-electric feedback in right atrium after left ventricular infarction in rats. *J. Mol. Cell. Cardiol.* 2000; 32:465–477.
128. Isenberg G, Kondratev D, Dyachenko V, Kazanski V, Gallitelli MF. Isolated Cardiomyocytes: Mechanosensitivity of Action Potential, Membrane Current and Ion Concentration [Internet]. In: Kamkin A, Kiseleva, I, editors. *Mechanosensitivity in Cells and Tissues.* Academia; 2005. Available from: <http://www.ncbi.nlm.nih.gov/books/NBK7511/>
129. Zeng T, Bett GCL, Sachs F. Stretch-Activated Whole Cell Currents in Adult Rat Cardiac Myocytes. *Am. J. Physiol. - Heart Circ. Physiol.* 2000; 278:H548–H557.
130. Kamkin A, Kiseleva I, Isenberg G. Stretch-Activated Currents in Ventricular Myocytes: Amplitude and Arrhythmogenic Effects Increase with Hypertrophy. *Cardiovasc. Res.* 2000; 48:409–420.
131. Riemer TL, Tung L. Stretch-induced excitation and action potential changes of single cardiac cells. *Prog. Biophys. Mol. Biol.* 2003; 82:97–110.

132. Kamkin A, Kiseleva I, Wagner K-D, Scholz H. Mechano-Electric Feedback in the Heart: Evidence from Intracellular Microelectrode Recordings on Multicellular Preparations and Single Cells from Healthy and Diseased Tissue [Internet]. In: Kamkin A, Kiseleva I, editors. *Mechanosensitivity in Cells and Tissues*. Academia; 2005. Available from: <http://www.ncbi.nlm.nih.gov/books/NBK7511/>
133. Kamkin A, Kiseleva I, Isenberg G. Activation and Inactivation of a Non-Selective Cation Conductance by Local Mechanical Deformation of Acutely Isolated Cardiac Fibroblasts. *Cardiovasc. Res.* 2003; 57:793–803.
134. Kohl P, Kamkin AG, Kiseleva IS, Noble D. Mechanosensitive fibroblasts in the sino-atrial node region of rat heart: interaction with cardiomyocytes and possible role. *Exp. Physiol.* 1994; 79:943–956.
135. Goshima K. Formation of nexuses and electrotonic transmission between myocardial and FL cells in monolayer culture. *Exp. Cell Res.* 1970; 63:124–130.
136. Gaudesius G, Miragoli M, Thomas SP, Rohr S. Coupling of Cardiac Electrical Activity Over Extended Distances by Fibroblasts of Cardiac Origin. *Circ. Res.* 2003; 93:421–428.
137. Okumura Y, Johnson SB, Bunch TJ, Henz BD, O'Brien CJ, Packer DL. A Systematical Analysis of In Vivo Contact Forces on Virtual Catheter Tip/Tissue Surface Contact during Cardiac Mapping and Intervention. *J. Cardiovasc. Electrophysiol.* 2008; 19:632–640.
138. Nakagawa H, Ikeda A, Govari A, Ephrath Y, Ariel G, Pitha J, Sharma T, Lazzara R, Jackman W. Electrogram Amplitude and Impedance are Poor Predictors of Electrode-Tissue Contact Force for Radiofrequency Ablation. *Heart Rhythm.* 2009;AB06–2, Abstract.
139. Ikeda A, Nakagawa H, Shah D, Lambert H, Vanenkov Y, Aeby N, Pitha J, Jackman W. Electrogram parameters (injury current, amplitude and dv/dt) and impedance are poor predictors of electrode-tissue contact force for radiofrequency ablation. *Heart Rhythm.* 2008;S322–S323. Abstract.
140. Mizuno H, Vergara P, Maccabelli G, Trevisi N, Eng SC, Brombin C, Mazzone P, Della Bella P. Contact Force Monitoring for Cardiac Mapping in Patients with Ventricular Tachycardia. *J. Cardiovasc. Electrophysiol.* 2013; 24:519–524.
141. Otomo K, Uno K, Fujiwara H, Isobe M, Iesaka Y. Local unipolar and bipolar electrogram criteria for evaluating the transmuralty of atrial ablation lesions at different catheter orientations relative to the endocardial surface. *Heart Rhythm.* 2010; 7:1291–1300.
142. Piorkowski C, Kottkamp H, Gerdts-Li J-H, Arya A, Sommer P, Dagues N, Esato M, Riahi S, Weiss S, Kircher S, Hindricks G. Steerable Sheath Catheter Navigation for Ablation of Atrial Fibrillation: A Case-Control Study. *Pacing Clin. Electrophysiol.* 2008; 31:863–873.
143. Piorkowski C, Eitel C, Rolf S, Bode K, Sommer P, Gaspar T, Kircher S, Wetzel U, Parwani AS, Boldt L-H, Mende M, Bollmann A, Husser D, Dagues N, Esato M, Arya A, Haverkamp W, Hindricks G. Steerable Versus Nonsteerable Sheath Technology in Atrial Fibrillation Ablation A Prospective, Randomized Study. *Circ. Arrhythm. Electrophysiol.* 2011; 4:157–165.
144. Steven D, Servatius H, Rostock T, Hoffmann B, Drewitz I, Müllerleile K, Sultan A, Aydin MA, Meinertz T, Willems S. Reduced Fluoroscopy During Atrial Fibrillation Ablation: Benefits of Robotic Guided Navigation. *J. Cardiovasc. Electrophysiol.* 2010; 21:6–12.
145. Ullah W, McLean A, Hunter RJ, Baker V, Richmond L, Cantor EJ, Dhinoja MB, Sporton S, Earley MJ, Schilling RJ. Randomized Trial Comparing Robotic to Manual Ablation for Atrial Fibrillation. *Heart Rhythm.* 2014; 11:1862–1869.

146. Thomas D, Scholz EP, Schweizer PA, Katus HA, Becker R. Initial experience with robotic navigation for catheter ablation of paroxysmal and persistent atrial fibrillation. *J. Electrocardiol.* 2012; 45:95–101.
147. DiBiase L, Wang Y, Horton R, Gallinghouse GJ, Mohanty P, Sanchez J, Patel D, Dare M, Canby R, Price LD, Zagrodzky JD, Bailey S, Burkhardt JD, Natale A. Ablation of Atrial Fibrillation Utilizing Robotic Catheter Navigation in Comparison to Manual Navigation and Ablation: Single-Center Experience. *J. Cardiovasc. Electrophysiol.* 2009; 20:1328–1335.
148. Kautzner J, Peichl P, Čihák R, Wichterle D, Mlěochová H. Early Experience with Robotic Navigation for Catheter Ablation of Paroxysmal Atrial Fibrillation. *Pacing Clin. Electrophysiol.* 2009; 32:S163–S166.
149. Ullah W, Hunter RJ, Haldar S, Mclean A, Dhinoja M, Sporton S, Earley MJ, Lorgat F, Wong T, Schilling RJ. Comparison of Robotic and Manual Persistent AF Ablation Using Catheter Contact Force Sensing: An International Multicenter Registry Study. *Pacing Clin. Electrophysiol.* 2014; 37:1427–1435.
150. Malcolm-Lawes LC, Lim PB, Koa-Wing M, Whinnett ZI, Jamil-Copley S, Hayat S, Francis DP, Kojodjojo P, Davies DW, Peters NS, Kanagaratnam P. Robotic assistance and general anaesthesia improve catheter stability and increase signal attenuation during atrial fibrillation ablation. *Europace.* 2013; 15:41–47.
151. Koa-Wing M, Kojodjojo P, Malcolm-Lawes LC, Salukhe TV, Linton NWF, Grogan AP, Bergman D, Lim PB, Whinnett ZI, McCarthy K, Ho SY, O'Neill MD, Peters NS, Davies DW, Kanagaratnam P. Robotically Assisted Ablation Produces More Rapid and Greater Signal Attenuation Than Manual Ablation. *J. Cardiovasc. Electrophysiol.* 2009; 20:1398–1404.
152. Duncan ER, Finlay M, Page SP, Hunter R, Goromonzi F, Richmond L, Baker V, Ginks M, Ezzat V, Dhinoja M, Earley MJ, Sporton S, Schilling RJ. Improved Electrogram Attenuation during Ablation of Paroxysmal Atrial Fibrillation with the Hansen Robotic System. *Pacing Clin. Electrophysiol.* 2012; 35:730–738.
153. Yokoyama K, Nakagawa H, Shah DC, Lambert H, Leo G, Aeby N, Ikeda A, Pitha JV, Sharma T, Lazzara R, Jackman WM. Novel contact force sensor incorporated in irrigated radiofrequency ablation catheter predicts lesion size and incidence of steam pop and thrombus. *Circ. Arrhythm. Electrophysiol.* 2008; 1:354–362.
154. Haines DE, Watson DD. Tissue heating during radiofrequency catheter ablation: A thermodynamic model and observations in isolated perfused and superfused canine right ventricular free wall. *Pacing Clin. Electrophysiol.* 1989; 12:962–976.
155. Haverkamp W, Hindricks G, Gulker H, Rissel U, Pfennings W, Borggrefe M, Breithardt G. Coagulation of ventricular myocardium using radiofrequency alternating current: bio-physical aspects and experimental findings. *Pacing Clin. Electrophysiol.* 1989; 12:187–195.
156. Haines DE, Watson DD, Verow AF. Electrode radius predicts lesion radius during radiofrequency energy heating. Validation of a proposed thermodynamic model. *Circ. Res.* 1990; 67:124–129.
157. Haines D, Verow A. Observations on electrode-tissue interface temperature and effect on electrical impedance during radiofrequency ablation of ventricular myocardium. *Circulation.* 1990; 82:1034–1038.
158. Nakagawa H, Yamanashi WS, Pitha JV, Arruda M, Wang X, Ohtomo K, Beckman KJ, McClelland JH, Lazzara R, Jackman WM. Comparison of In Vivo Tissue Temperature Profile and Lesion Geometry for Radiofrequency Ablation With a Saline-Irrigated Electrode Versus Temperature Control in a Canine Thigh Muscle Preparation. *Circulation.* 1995; 91:2264–2273.
159. Weiss C, Antz M, Eick O, Eshagzaiy K, Meinertz T, Willems S. Radiofrequency catheter ablation using cooled electrodes: impact of irrigation flow rate and catheter contact pressure on lesion dimensions. *Pacing Clin. Electrophysiol.* 2002; 25:463–469.

160. Nakagawa H, Wittkamp FH, Yamanashi WS, Pitha JV, Imai S, Campbell B, Arruda M, Lazzara R, Jackman WM. Inverse relationship between electrode size and lesion size during radiofrequency ablation with active electrode cooling. *Circulation*. 1998; 98:458–465.
161. Haines DE. Determinants of lesion size during radiofrequency catheter ablation: The role of electrode-tissue contact pressure and duration of energy delivery. *J. Cardiovasc. Electrophysiol*. 1991; 2:509–515.
162. Petersen HH, Chen X, Pietersen A, Svendsen JH, Haunso S. Temperature-controlled radiofrequency ablation of cardiac tissue: an in vitro study of the impact of electrode orientation, electrode tissue contact pressure and external convective cooling. *J. Interv. Card. Electrophysiol*. 1999; 3:257–262.
163. Wood MA, Goldberg SM, Parvez B, Pathak V, Holland K, Ellenbogen AL, Han FT, Alexander D, Lau M, Reshko L, Goel A. Effect of electrode orientation on lesion sizes produced by irrigated radiofrequency ablation catheters. *J. Cardiovasc. Electrophysiol*. 2009; 20:1262–1268.
164. Avital B, Mughal K, Hare J, Helms R, Krum D. The Effects of Electrode-Tissue Contact on Radiofrequency Lesion Generation. *Pacing Clin. Electrophysiol*. 1997; 20:2899–2910.
165. Stagegaard N, Petersen HH, Chen X, Svendsen JH. Indication of the radiofrequency induced lesion size by pre-ablation measurements. *Europace*. 2005; 7:525–534.
166. Eick OJ, Gerritse B, Schumacher B. Popping Phenomena in Temperature-Controlled Radiofrequency Ablation: When and Why Do They Occur? *Pacing Clin. Electrophysiol*. 2000; 23:253–258.
167. Reithmann C, Remp T, Hoffmann E, Matis T, Wakili R, Steinbeck G. Different Patterns of the Fall of Impedance as the Result of Heating During Ostial Pulmonary Vein Ablation: Implications for Power Titration. *Pacing Clin. Electrophysiol*. 2005; 28:1282–1291.
168. Thiagalingam A, D'Avila A, Foley L, Guerrero JL, Lambert H, Leo G, Ruskin JN, Reddy VY. Importance of catheter contact force during irrigated radiofrequency ablation: evaluation in a porcine ex vivo model using a force-sensing catheter. *J. Cardiovasc. Electrophysiol*. 2010; 21:806–811.
169. DeBortoli A, Sun L-Z, Solheim E, Hoff PI, Schuster P, Ohm O-J, Chen J. Ablation Effect Indicated by Impedance Fall is Correlated with Contact Force Level During Ablation for Atrial Fibrillation. *J. Cardiovasc. Electrophysiol*. 2013; 24:1210–1215.
170. Di Biase L, Natale A, Barrett C, Tan C, Elayi CS, Ching CK, Wang P, Al-Ahmad A, Arruda M, Burkhardt JD, Wisnoskey BJ, Chowdhury P, De Marco S, Armaganijan L, Litwak KN, Schweikert RA, Cummings JE. Relationship Between Catheter Forces, Lesion Characteristics, “Popping,” and Char Formation: Experience with Robotic Navigation System. *J. Cardiovasc. Electrophysiol*. 2009; 20:436–440.
171. Shah DC, Lambert H, Nakagawa H, Langenkamp A, Aeby N, Leo G. Area Under the Real-Time Contact Force Curve (Force-Time Integral) Predicts Radiofrequency Lesion Size in an In Vitro Contractile Model. *J. Cardiovasc. Electrophysiol*. 2010; 21:1038–1043.
172. Kumar S, Morton JB, Halloran K, Spence SJ, Lee G, Wong MCG, Kistler PM, Kalman JM. Effect of respiration on catheter-tissue contact force during ablation of atrial arrhythmias. *Heart Rhythm*. 2012; 9:1041–1047.
173. Ho SY, McCarthy KP. Anatomy of the Left Atrium for Interventional Electrophysiologists. *Pacing Clin. Electrophysiol*. 2009; 33:620–627.

174. Kistler PM, Ho SY, Rajappan K, Morper M, Harris S, Abrams D, Sporton SC, Schilling RJ. Electrophysiologic and anatomic characterization of sites resistant to electrical isolation during circumferential pulmonary vein ablation for atrial fibrillation: a prospective study. *J. Cardiovasc. Electrophysiol.* 2007; 18:1282–1288.
175. Rajappan K, Kistler PM, Earley MJ, Thomas G, Izquierdo M, Sporton SC, Schilling RJ. Acute and chronic pulmonary vein reconnection after atrial fibrillation ablation: a prospective characterization of anatomical sites. *Pacing Clin. Electrophysiol.* 2008; 31:1598–1605.
176. Kuck K-H, Reddy VY, Schmidt B, Natale A, Neuzil P, Saoudi N, Kautzner J, Herrera C, Hindricks G, Jaïs P, Nakagawa H, Lambert H, Shah DC. A novel radiofrequency ablation catheter using contact force sensing: Toccata study. *Heart Rhythm.* 2012; 9:18–23.
177. Haldar S, Jarman JWE, Panikker S, Jones DG, Salukhe T, Gupta D, Wynn G, Hussain W, Markides V, Wong T. Contact force sensing technology identifies sites of inadequate contact and reduces acute pulmonary vein reconnection: A prospective case control study. *Int. J. Cardiol.* 2013; 168:1160–1166.
178. Neuzil P, Reddy VY, Kautzner J, Petru J, Wichterle D, Shah D, Lambert H, Yulzari A, Wissner E, Kuck K-H. Electrical Reconnection Following PVI is Contingent on Contact Force during Initial Treatment - Results From the EFFICAS I Study. *Circ. Arrhythm. Electrophysiol.* 2013; 6:327–333.
179. Reddy VY, Shah D, Kautzner J, Schmidt B, Saoudi N, Herrera C, Jaïs P, Hindricks G, Peichl P, Yulzari A, Lambert H, Neuzil P, Natale A, Kuck K-H. The relationship between contact force and clinical outcome during radiofrequency catheter ablation of atrial fibrillation in the TOCCATA study. *Heart Rhythm.* 2012; 9:1789–1795.
180. Marijon E, Faza S, Guy-Moyat B, Bouzeman A, Providencia R, Treguer F, Combes N, Boveda S, Combes S, Albenque J-P. Real-Time Contact Force Sensing for Pulmonary Vein Isolation in the Setting of Paroxysmal Atrial Fibrillation: Procedural and One-Year Results. *J. Cardiovasc. Electrophysiol.* 2013;
181. Wakili R, Clauss S, Schmidt V, Ulbrich M, Hahnefeld A, Schüssler F, Siebermair J, Kääb S, Estner HL. Impact of real-time contact force and impedance measurement in pulmonary vein isolation procedures for treatment of atrial fibrillation. *Clin. Res. Cardiol. Off. J. Ger. Card. Soc.* 2014; 103:97–106.
182. Martinek M, Lemes C, Sigmund E, Derndorfer M, Aichinger J, Winter S, Nesser H-J, Pürerfellner H. Clinical impact of an open-irrigated radiofrequency catheter with direct force measurement on atrial fibrillation ablation. *Pacing Clin. Electrophysiol. PACE.* 2012; 35:1312–1318.
183. Andrade JG, Monir G, Pollak SJ, Khairy P, Dubuc M, Roy D, Talajic M, Deyell M, Rivard L, Thibault B, Guerra PG, Nattel S, Macle L. Pulmonary vein isolation using “contact force” ablation: The effect on dormant conduction and long-term freedom from recurrent atrial fibrillation—A prospective study. *Heart Rhythm.* 2014; 11:1919–1924.
184. Stabile G, Solimene F, Calò L, Anselmino M, Castro A, Pratola C, Golia P, Bottoni N, Grandinetti G, De Simone A, De Ponti R, Dottori S, Bertaglia E. Catheter-tissue contact force for pulmonary veins isolation: a pilot multicentre study on effect on procedure and fluoroscopy time. *Europace.* 2014; 16:335–340.
185. Shah D, Lambert H, Langenkamp A, Vanenkov Y, Leo G, Gentil-Baron P, Walpoth B. Catheter tip force required for mechanical perforation of porcine cardiac chambers. *Europace.* 2011; 13:277–283.
186. Perna F, Heist EK, Danik SB, Barrett CD, Ruskin JN, Mansour M. Assessment of the Catheter Tip Contact Force Resulting in Cardiac Perforation in the Swine Atria Using the Force Sensing Technology. *Circ. Arrhythm. Electrophysiol.* 2011; 4:218–224.



187. Kumar S, Chan M, Lee J, Wong MCG, Yudi M, Morton JB, Spence SJ, Halloran K, Kistler PM, Kalman JM. Catheter-Tissue Contact Force Determines Atrial Electrogram Characteristics Before and Lesion Efficacy After Antral Pulmonary Vein Isolation in Humans. *J. Cardiovasc. Electrophysiol.* 2013;
188. Sohns C, Karim R, Harrison J, Arujuna A, Linton N, Sennett R, Lambert H, Leo G, Williams S, Razavi R, Wright M, Schaeffter T, O'Neill M, Rhode K. Quantitative Magnetic Resonance Imaging Analysis of the Relationship Between Contact Force and Left Atrial Scar Formation After Catheter Ablation of Atrial Fibrillation. *J. Cardiovasc. Electrophysiol.* 2014; 25:138–145.
189. Gepstein L, Hayam G, Shpun S, Cohen D, Ben-Haim SA. Atrial Linear Ablations in Pigs : Chronic Effects on Atrial Electrophysiology and Pathology. *Circulation.* 1999; 100:419–426.
190. Sanchez JE, Kay GN, Benser ME, Hall JA, Walcott GP, Smith WM, Ideker RE. Identification of transmural necrosis along a linear catheter ablation lesion during atrial fibrillation and sinus rhythm. *J. Interv. Card. Electrophysiol.* 2003; 8:9–17.
191. Pappone C, Rosanio S, Oreto G, Tocchi M, Gugliotta F, Vicedomini G, Salvati A, Dicandia C, Mazzone P, Santinelli V, Gulletta S, Chierchia S. Circumferential radiofrequency ablation of pulmonary vein ostia: A new anatomic approach for curing atrial fibrillation. *Circulation.* 2000; 102:2619–2628.
192. Schwartzman D, Michele JJ, Trankiem CT, Ren JF. Electrogram-guided radiofrequency catheter ablation of atrial tissue comparison with thermometry-guide ablation: comparison with thermometry-guide ablation. *J. Interv. Card. Electrophysiol.* 2001; 5:253–266.
193. McGann CJ, Kholmovski EG, Oakes RS, Blauer JJE, Daccarett M, Segerson N, Airey KJ, Akoum N, Fish E, Badger TJ, DiBella EVR, Parker D, MacLeod RS, Marrouche NF. New Magnetic Resonance Imaging-Based Method for Defining the Extent of Left Atrial Wall Injury After the Ablation of Atrial Fibrillation. *J. Am. Coll. Cardiol.* 2008; 52:1263–1271.
194. Badger TJ, Daccarett M, Akoum NW, Adjei-Poku YA, Burgon NS, Haslam TS, Kalvaitis S, Kuppahally S, Vergara G, McMullen L, Anderson PA, Kholmovski E, MacLeod RS, Marrouche NF. Evaluation of Left Atrial Lesions After Initial and Repeat Atrial Fibrillation Ablation Lessons Learned From Delayed-Enhancement MRI in Repeat Ablation Procedures. *Circ. Arrhythm. Electrophysiol.* 2010; 3:249–259.
195. Hunter RJ, Jones DA, Boubertakh R, Malcolm-Lawes LC, Kanagaratnam P, Juli CF, Davies DW, Peters NS, Baker V, Earley MJ, Sporton S, Davies LC, Westwood M, Petersen SE, Schilling RJ. Diagnostic Accuracy of Cardiac Magnetic Resonance Imaging in the Detection and Characterization of Left Atrial Catheter Ablation Lesions: A Multicenter Experience. *J. Cardiovasc. Electrophysiol.* 2013; 24:396–403.
196. Peters DC, Wylie JV, Hauser TH, Kissinger KV, Botnar RM, Essebag V, Josephson ME, Manning WJ. Detection of Pulmonary Vein and Left Atrial Scar after Catheter Ablation with Three-dimensional Navigator-gated Delayed Enhancement MR Imaging: Initial Experience. *Radiology.* 2007; 243:690–695.
197. Harrison JL, Jensen HK, Peel SA, Chiribiri A, Grøndal AK, Bloch LØ, Pedersen SF, Bentzon JF, Kolbitsch C, Karim R, Williams SE, Linton NW, Rhode KS, Gill J, Cooklin M, Rinaldi CA, Wright M, Kim WY, Schaeffter T, Razavi RS, O'Neill MD. Cardiac magnetic resonance and electroanatomical mapping of acute and chronic atrial ablation injury: a histological validation study. *Eur. Heart J.* 2014;eht560.
198. Gepstein L, Hayam G, Ben-Haim SA. A Novel Method for Nonfluoroscopic Catheter-Based Electroanatomical Mapping of the Heart In Vitro and In Vivo Accuracy Results. *Circulation.* 1997; 95:1611–1622.
199. Kabra R, Singh J. Recent trends in imaging for atrial fibrillation ablation. *Indian Pacing Electrophysiol. J.* 2010; 10:215–227.

200. Savitzky A, Golay MJE. Smoothing and Differentiation of Data by Simplified Least Squares Procedures. *Anal. Chem.* 1964; 36:1627–1639.
201. Verma A, Novak P, Macle L, Whaley B, Beardsall M, Wulffhart Z, Khaykin Y. A prospective, multicenter evaluation of ablating complex fractionated electrograms (CFEs) during atrial fibrillation (AF) identified by an automated mapping algorithm: acute effects on AF and efficacy as an adjuvant strategy. *Heart Rhythm.* 2008; 5:198–205.
202. Hunter RJ, Liu Y, Lu Y, Wang W, Schilling RJ. Left Atrial Wall Stress Distribution and Its Relationship to Electrophysiologic Remodeling in Persistent Atrial Fibrillation. *Circ. Arrhythm. Electrophysiol.* 2012; 5:351–360.
203. Verma A, Patel D, Famy T, Martin DO, Burkhardt JD, Elayi SC, Lakkireddy D, Wazni O, Cummings J, Schweikert RA, Saliba W, Tchou PJ, Natale A. Efficacy of Adjuvant Anterior Left Atrial Ablation During Intracardiac Echocardiography-Guided Pulmonary Vein Antrum Isolation for Atrial Fibrillation. *J. Cardiovasc. Electrophysiol.* 2007; 18:151–156.
204. Jarman JWE, Wong T, Kojodjojo P, Spohr H, Davies JER, Roughton M, Francis DP, Kanagaratnam P, O'Neill MD, Markides V, Davies DW, Peters NS. Organizational index mapping to identify focal sources during persistent atrial fibrillation. *J. Cardiovasc. Electrophysiol.* 2014; 25:355–363.
205. Nakagawa H, Kautzner J, Natale A, Peichl P, Cihak R, Wichterle D, Ikeda A, Santangeli P, Di Biase L, Jackman WM. Locations of high contact force during left atrial mapping in atrial fibrillation patients: electrogram amplitude and impedance are poor predictors of electrode-tissue contact force for ablation of atrial fibrillation. *Circ. Arrhythm. Electrophysiol.* 2013; 6:746–753.
206. Ullah W, Hunter RJ, Baker V, Dhinoja M, Sporton S, Earley MJ, Schilling RJ. Target Indices for Clinical Ablation in Atrial Fibrillation: Insights from Contact Force, Electrogram and Biophysical Parameter Analysis. *Circ. Arrhythm. Electrophysiol.* 2014; 7:63–68.
207. Everett TH, Kok L-C, Vaughn RH, Moorman JR, Haines DE. Frequency domain algorithm for quantifying atrial fibrillation organization to increase defibrillation efficacy. *IEEE Trans. Biomed. Eng.* 2001; 48:969–978.
208. Takahashi Y, Sanders P, Jaïs P, Hocini M, Dubois R, Rotter M, Rostock T, Nalliah CJ, Sacher F, Clémenty J, Haïssaguerre M. Organization of Frequency Spectra of Atrial Fibrillation: Relevance to Radiofrequency Catheter Ablation. *J. Cardiovasc. Electrophysiol.* 2006; 17:382–388.
209. Tan H-W, Wang X-H, Shi H-F, Zhou L, Gu J-N, Liu X. Left atrial wall thickness: anatomic aspects relevant to catheter ablation of atrial fibrillation. *Chin. Med. J. (Engl.)*. 2012; 125:12–15.
210. Ullah W, Hunter RJ, Baker V, Dhinoja MB, Sporton S, Earley MJ, Schilling RJ. Factors Affecting Catheter Contact in the Human Left Atrium and their Impact on Ablation Efficacy. *J. Cardiovasc. Electrophysiol.* 2014;
211. Narayan SM, Krummen DE, Shivkumar K, Clopton P, Rappel W-J, Miller JM. Treatment of Atrial Fibrillation by the Ablation of Localized Sources. *J. Am. Coll. Cardiol.* 2012; 60:628–636.
212. Ravelli F, Allessie M. Effects of atrial dilatation on refractory period and vulnerability to atrial fibrillation in the isolated Langendorff-perfused rabbit heart. *Circulation.* 1997; 96:1686–1695.
213. Benjamin EJ, Levy D, Vaziri SM, D'Agostino RB, Belanger AJ, Wolf PA. Independent risk factors for atrial fibrillation in a population-based cohort: The framingham heart study. *JAMA.* 1994; 271:840–844.
214. Po SS, Nakagawa H, Jackman WM. Localization of Left Atrial Ganglionated Plexi in Patients with Atrial Fibrillation. *J. Cardiovasc. Electrophysiol.* 2009; 20:1186–1189.

215. Habel N, Znojkwicz P, Thompson N, Müller JG, Mason B, Calame J, Calame S, Sharma S, Mirchandani G, Janks D, Bates J, Noori A, Karnbach A, Lustgarten DL, Sobel BE, Spector P. The temporal variability of dominant frequency and complex fractionated atrial electrograms constrains the validity of sequential mapping in human atrial fibrillation. *Heart Rhythm*. 2010; 7:586–593.
216. Wittkampf FH, Hauer RN, Robles de Medina EO. Control of radiofrequency lesion size by power regulation. *Circulation*. 1989; 80:962–968.
217. Calò L, De Ruvo E, Sciarra L, Gricia R, Navone G, De Luca L, Nuccio F, Sette A, Pristipino C, Dulio A, Gaita F, Liyo E. Diagnostic Accuracy of a New Software for Complex Fractionated Electrograms Identification in Patients with Persistent and Permanent Atrial Fibrillation. *J. Cardiovasc. Electrophysiol*. 2008; 19:1024–1030.
218. Petersen HH, Chen X, Pietersen A, Svendsen JH, Haunsø S. Tissue Temperatures and Lesion Size During Irrigated Tip Catheter Radiofrequency Ablation: An In Vitro Comparison of Temperature-Controlled Irrigated Tip Ablation, Power-Controlled Irrigated Tip Ablation, and Standard Temperature-Controlled Ablation. *Pacing Clin. Electrophysiol*. 2000; 23:8–17.
219. Nsah E, Berger R, Rosenthal L, Hui R, Ramza B, Jumrussirikul P, Lawrence JH, Tomaselli G, Kass D, Calkins H. Relation between impedance and electrode temperature during radiofrequency catheter ablation of accessory pathways and atrioventricular nodal reentrant tachycardia. *Am. Heart J*. 1998; 136:844–851.
220. Kumar S, Haqqani HM, Chan M, Lee J, Yudi M, Wong MCG, Morton JB, Ling L-H, Robinson T, Heck PM, Kelland NF, Halloran K, Spence SJ, Kistler PM, Kalman JM. Predictive Value Of Impedance Changes For Real-Time Contact Force Measurements During Catheter Ablation Of Atrial Arrhythmias In Humans. *Heart Rhythm*. 2013; 10:962–969.
221. Demazumder D, Mirotznik MS, Schwartzman D. Biophysics of radiofrequency ablation using an irrigated electrode. *J. Interv. Card. Electrophysiol*. 2001; 5:377–389.
222. Wood MA, Goldberg SM, Parvez B, Pathak V, Holland K, Ellenbogen AL, Han FT, Alexander D, Lau M, Reshko L, Goel A. Effect of Electrode Orientation on Lesion Sizes Produced by Irrigated Radiofrequency Ablation Catheters. *J. Cardiovasc. Electrophysiol*. 2009; 20:1262–1268.
223. Anter E, Tschabrunn CM, Contreras-Valdes FM, Buxton AE, Josephson ME. Radiofrequency ablation annotation algorithm reduces the incidence of linear gaps and reconnection after pulmonary vein isolation. *Heart Rhythm*. 2014; 11:783–790.
224. Kimura M, Sasaki S, Owada S, Horiuchi D, Sasaki K, Itoh T, Ishida Y, Kinjo T, Tomita H, Okumura K. Comparison of Lesion Formation between Contact Force-Guided and non-Guided Circumferential Pulmonary Vein Isolation: A Prospective, Randomized Study. *Heart Rhythm*. 2014; 11:984–991.
225. Jiang C-Y, Jiang R-H, Matsuo S, Liu Q, Fan Y-Q, Zhang Z-W, Fu G-S. Early detection of pulmonary vein reconnection after isolation in patients with paroxysmal atrial fibrillation: a comparison of ATP-induction and reassessment at 30 minutes postisolation. *J. Cardiovasc. Electrophysiol*. 2009; 20:1382–1387.
226. Wang X, Liu X, Sun Y, Gu J, Shi H, Zhou L, Hu W. Early identification and treatment of PV re-connections: role of observation time and impact on clinical results of atrial fibrillation ablation. *Europace*. 2007; 9:481–486.
227. Rajappan K, Baker V, Richmond L, Kistler PM, Thomas G, Redpath C, Sporton SC, Earley MJ, Harris S, Schilling RJ. A randomized trial to compare atrial fibrillation ablation using a steerable vs. a non-steerable sheath. *Europace*. 2009; 11:571–575.

228. Haissaguerre M, Hocini M, Shah AJ, Derval N, Sacher F, Jais P, Dubois R. Noninvasive Panoramic Mapping of Human Atrial Fibrillation Mechanisms: A Feasibility Report. *J. Cardiovasc. Electrophysiol.* 2013; 24:711–717.
229. Narayan SM, Shivkumar K, Krummen DE, Miller JM, Rappel W-J. Panoramic Electrophysiological Mapping but not Electrogram Morphology Identifies Stable Sources for Human Atrial Fibrillation Stable Atrial Fibrillation Rotors and Focal Sources Relate Poorly to Fractionated Electrograms. *Circ. Arrhythm. Electrophysiol.* 2013; 6:58–67.